2011

Assymmetry in distribution systems: causes, harmful effects and remedies

Isaac Plummer
Louisiana State University and Agricultural and Mechanical College

ASYMMETRY IN DISTRIBUTION SYSTEMS: CAUSES, HARMFUL EFFECTS AND REMEDIES

A Thesis

Submitted to the Graduate Faculty of the
Louisiana State University and
Agricultural and Mechanical College
in partial fulfillment of the
requirements for the degree of
Master of Science in Electrical Engineering

in

The Department of Electrical and Computer Engineering

by
Isaac Plummer
Diploma, University of Technology-Jamaica, July 1996
B.S., Louisiana State University, May 2003
May 2011

ACKNOWLEDGEMENTS

I would like to first thank God for the health, strength and focus he provided throughout my thesis. He has blessed me with a wonderful family and friends and I give him praise.

I believe personal accomplishments cannot be truly and fully realized without collective achievement and all the persons that have been an integral part of the successful completion of my thesis have accentuated this statement.

Humility, hard work, research, creativity, honesty and integrity, are key principles and tools which are imperative to the successful completion of this thesis. Each of these principles and tools were manifested through my interaction with each person throughout the process of the thesis. Each individual shape each one of these principles and tools in a unique way and this is why I would like to take the time to acknowledge Dr. Leszek S. Czarnecki, Dr. Mendrela, Dr. Mahrene, Michael McAnelly, friends and my family especially my wife Katherine and son Seraiah for the support and inspiration during the process of this thesis.

I appreciate Dr. Leszek S. Czarnecki because he has not only provided technical leadership throughout this thesis but he also provided the right environment for the nurturing and maturing of the complete person. He goes beyond the basics and that is why I thank him for his invaluable contribution to my career growth and accomplishment.

Michael McAnelly, thank you for your support, technical advice and the utilization of your lab. He has also done more than the basics to assist me in successfully completing my thesis and I am appreciative of his support.

Dr. Mendrela, I appreciate your technical advice and the time you spend in ensuring that the technical content of my thesis is correct and of sound motor principles.

Dr. Mahrene I appreciate you for taking the time to invest in the successful completing of my thesis. I am also thankful for the help I got from all my other family and friends.

TABLE OF CONTENTS

LIST OF FIGURES

ABSTRACT

Current and voltage asymmetry denigrates the power system performance. The current asymmetry reduces efficiency, productivity and profits at the generation, transmission and distribution of electric energy. Voltage asymmetry reduces efficiency, productivity and profits at the consumption/utilization level.

There are a lot of conference and journal papers on the subject of voltage and current asymmetry, however, the information is scattered over a large number of journals and conferences and published over several years. Therefore, the thesis provides a comprehensive compilation of all possible published information on current and voltage asymmetry in the electrical power systems.

Published information on sources of asymmetry, its propagation, negative effects upon transmission and customer equipment and possible remedies are compiled, discussed and analyzed in this thesis. This is done with respect to the voltage asymmetry and current asymmetry, as well as their mutual interaction. Some situations related to the voltage and current asymmetry are modeled in this thesis using the Electrical Transient Analyzer Program (ETAP) software.

Due to the economics and efficiency of transmission, distribution and load diversity such as single-phase, two-phase and three-phase utilization, asymmetric current and voltage is an inherent feature in the distribution system. Therefore it has to be mitigated. The thesis discusses methods aimed at reducing the current and voltage asymmetry in the distribution system. Some of the sources of these methods are based on the Current Physical Component (CPC) power theory.

INTRODUCTION

1.1 Negative Effects of Asymmetry

The economic benefits of energy providers and its users are strongly dependent on the supply reliability, security and efficiency of the power system and consequently, on the supply quality and the loading quality. For instance, negative sequence current increases energy loss at delivery. The negative sequence voltage causes temperature increase of the induction motors. Also, there are other negative effects of the voltage and current asymmetries. Since the voltage and current asymmetry causes various negative effects in power systems, these effects are the subject of our concern and investigations.

The three categories of asymmetry that contribute to the negative effect of asymmetry on the power system are: current asymmetry, voltage asymmetry and the simultaneous occurrence of both current and voltage asymmetry.

Voltage asymmetry reduces efficiency, productivity and profits at the consumption/utilization level. It contributes to a reverse magnetic field, increases the temperature of windings, reduces output torque and increases the slip of rotating machinery. According to ref. [17] and [18] the effect of voltage asymmetry on a three-phase induction motor operating at rated load will cause an increase in losses, increase in the temperature of the windings, reduction of life expectancy and reduce efficiency. For example, according to ref. [17], 1% voltage asymmetry increases motor winding temperature from 120^0C to 130^0C with a I^2R loss of 33% of the total losses and an efficiency reduction of 0.5%. Furthermore the life expectancy of the windings is reduced from 20 years to 10 years. However as the percent voltage asymmetry increase so does the temperature of the motor. For instance at 4% voltage asymmetry the winding temperature increase from 120^0C to 160^0C with a I^2R loss of 40% of the total losses and the efficiency reduce by 3-4%. At these values the life expectancy is further reduced to 1.25

years. As a consequence of this, motors should be derated (larger power rating) to compensate for the extra heating. However, this could increase the difficulty of relay coordination and therefore increase the cost of protection.

Three-phase rectifiers and inverters are also affected by voltage asymmetry - negative sequence voltage. There are three main negative impacts of voltage asymmetry on rectifiers. First, the voltage asymmetry produces a supply current asymmetry that increases the temperature of the rectifier's diodes and disturbs protective devices. Second, the asymmetric voltage causes an increase in the magnitude of the zero sequence harmonics ref. [40] and also increase of the voltage ripples on the dc-bus voltage. This increases the electrical demand of the capacity on the dc-bus capacitor and or inductor. Third, it increases the ripple torque in the ASD induction machine thereby increasing mechanical and thermal demand ref. [54] and [55]. According to ref. [53] it is estimated that in the United States of America between 1-2 billion dollars per year is attributed to the reduction of life expectation of motors due to the presence of harmonic and voltage asymmetry.

Current asymmetry means that a negative sequence component occurs in the supply current. Such a component does not contribute to useful energy transmission, but to transmission of energy dissipated in power system equipment in the form of heat. As a result, the current asymmetry reduces efficiency, productivity and profits at generation, transmission and distribution of electric energy. Consequently, the ampacity of cables, transmission and distribution lines have to be selected based on the level of negative sequence current it will be subjected to during operations. Also the capacity of transformers and the efficiency of motors are reduced. In other words the negative sequence current increases losses in the cables, transmission and distribution lines, transformers and equipment on the power system ref. [14]. This is shown in figure 4.6 of the ETAP model where the ampacity of cables, transmission and distribution

lines were overloaded due to negative sequence current flow. Also appendix B shows the data associated with this model.

The negative sequence current causes voltage asymmetry. For instance, the current asymmetry caused by very large single-phase loads such as high speed traction systems and AC arc furnace contribute to dissimilar voltage drops on the balanced three-phases of the supply system and consequently, it produces voltage asymmetry. For example, in ref. [45] a situation is described, where a 350MW steam turbine generator supplies two 60MVA electric arc furnaces (EAF) through a three-mile 230 KV transmission line. The EAF draws asymmetrical current, which causes voltage asymmetry. As a result, the following sequence of events occurred: the generator had a cracked shaft near the turbine-end coupling, then there was two failures of the rotating portion of the brushless exciter and then while operating close to full load the generator's exciter–end retaining ring of the rotor failed. This cost the company a significant amount of money and time to repair the generator.

Other negative effects occur at transient asymmetries, mainly caused by faults in the power systems. Transient current asymmetry occurs due to single-phase - line-to-ground faults and line-to-line faults etc. These are extreme levels of current asymmetry that can last for only a few seconds but can lead to system instability and failure if not eliminated in time. Relays and circuit breakers remove the fault current before it exceeds the $(i^n)^2t$ characteristic of the devices and equipment connected. The operation of re-closers can produce transient asymmetry which can result in nuisance tripping of relays. This is because the negative sequence setting has been exceeded due to the transient asymmetry. Also Single Phase Switching (SPS) scheme are used to improve the reliability of transmission systems and by extension also enhance the reliability of the electrically close generators. However, according to ref. [58] the generators and transformers could be subjected to negative and zero sequence condition for up 60 cycles or longer with SPS.

Since the system will only be operating on two phases in this time period the generator would be subjected to heating due to the negative sequence current while the transformer will be subjected to zero sequence circulating current. However, asymmetry due to faults will not be covered in details in the thesis.

In some situations both the voltage and the current asymmetry have to be taken into account. This increases the complexity of the problem and modeling is usually required. Figure 4.10 shown in the ETAP model used to analyze the condition with 90% voltage magnitude of phase A and lumped7 load in network 6, representing single phase load imbalance. The results show that transmission and distribution lines and transformers were overloaded. Also most of the loads were subjected to currents that have exceeded their rated values. The combination of these two sources of asymmetry created critical operating conditions (appendix B) for the power system and should be avoided.

1.2 Sources of Asymmetry

Voltage asymmetry and current asymmetry are two different kinds of asymmetries in the power system. Also there source and nature of occurrence are different. For instance there are two reasons for the occurrence of voltage asymmetry. The first is due to the structural asymmetry of parameters of generators, transformers transmission and distribution lines. The second is caused by the voltage drop on the system impedance by asymmetrical currents. For example, the generator can contribute to voltage asymmetry if the stator impedances for particular phases are not mutually equal. This can be attributed to some level of mechanical asymmetry of the stator and its windings. For instance, the eccentricity of the rotor causes variation of the air gap which will result in asymmetry of the phase inductances. Another source of voltage asymmetry is the transformer. Transformers can affect the voltage asymmetry in two ways. The first is through the transformer geometry. This asymmetry is mainly due to the difference that exists between the

mutual impedances of the transformer phases. Mutual reactance is directly proportional to the magnetic couplings between ports and the occurrence of stray losses produced in the tank and frames are associated with the mutual resistances ref. [1]. The second is through the configuration such as an open delta connected transformer banks on the distribution system.

The primary source of current asymmetry is load imbalance, which is due to single-phase loads on the distribution system or faults on the load side. Even though load imbalance is usually time-varying, it can be regarded as contributing to permanent current asymmetry. Permanent imbalance occurs under normal operating conditions of the system. The single or double phase loading of the three-phase 3-wire and three-phase 4-wire system and also imbalance three phase loads are the contributors to permanent imbalance. The magnitude of the current asymmetry with respect to traction loads is dependent on the path the train travels or route profile, the loading of the train and on the power supply configuration. AC arc furnace and heavy reactive single phase loads such as welders are some other examples of permanent imbalance on the power system. Also the voltage asymmetry causes asymmetry of the supply current. This is particularly visible in the current of induction motors supplied with asymmetrical voltage, since the motors impedance for the negative sequence is lower than that of the impedance for the positive sequence voltage. For example 1% asymmetry in the supply voltage can cause 6% or more of current asymmetry in induction motors.

1.3 Methods of Asymmetry Mitigation.

There are a few levels and approaches to the reduction of asymmetry in voltages and currents. Asymmetry can be confined or reduced by:

1. Imposing regulation and standards with respect to:
    1. Equipment and transmission line construction.
    2. Adopting standards on acceptable levels of current and voltage asymmetry.

2. Structural modifications of single-phase loads – both on utility and customer sides.

3. Single-phase voltage regulators.

4. Balancing compensators

1.1 Imposing regulation and standards with respect to equipment and transmission line design will provide a systematic and cost effective way of mitigating asymmetry in the power system. This initial stage of asymmetric reduction ensure that generators, transmission lines, transformers, switching equipment and three-phase motors are designed and manufactured to be symmetrical. For example, the impedance in each phase of the generator and motor is equal and symmetrical with respect to each other. Transmission and distribution lines are spaced and transposed to mitigate asymmetry.

1.2 NEMA, IEEE and CIGRE/CIRED JWG C4.103 performed research and analysis to create standards for current and voltage asymmetry in the power system. When these standards are selected as the acceptable level of current and voltage asymmetry, fines can be imposed on the respective entities to reduce asymmetry. For instance, fines can be imposed on utilities and customers to keep asymmetry within the standard levels. Therefore, utilities are required to supply reliable power to customers and they are not allowed to have an asymmetric level beyond the level stipulated by the standards. Similarly, customers are not allowed to create asymmetry beyond the stipulated levels.

2. One of the main objectives of asymmetric reduction is to use the most effective method of reduction in a cost effective way. Structural arrangement is one of those cost effective ways. For instance, the rearranging or redistributing of all single-phase loads equally among all the three phases can mitigate asymmetry. This refers to the distribution of the supply of individual homes or alternating connections in row of houses in residential subdivisions, per floor supply in

commercial buildings or street lights. Also by arranging the connection phases between the distribution transformers and the primary feeder, the level of asymmetry can be reduced ref. [59].

For traction load, the load scheduling of the trains can improve the balance between the phases of the three-phase system. For instance, since this is a large single phase load the scheduling in relation with other traction system can be implemented in such a way that the loading on the three-phase system is balanced.

2.1. Traction system transformer connections schemes.

- V- connection: The schemes have different efficiency levels in asymmetry reduction. However, they can be selected based on the investment, operation and maintenance cost ref. [58]. According to ref. [58] the single-phase connection and the V-connection schemes are the most economical mitigation technique. But the V-connection scheme is more efficient when compared with the single-phase scheme.
- Single – phase connection: In this arrangement the single transformer is fed with two phases. One of the output phases is connected to the catenary that supplies the train while the other is connected to the rails as the return current path. Therefore with this arrangement each of the different phases of the three-phase system can be balance by systematically distributing the phase connection base on the loading.
- The Scott transformer: Is two single phase transformers consisting of special winding ratios, which is connected to the three phase system. The connection is such that the output, which is a two-phase orthogonal voltage system, will provide connection of two single-phase systems [13].
- Leblanc transformer.

  Steinmetz – transformer: According to ref. [14] the Steinmetz transformer is a three-phase transformer that is designed with a power balancing load feature. This consists of a

capacitor and an inductor that is rated in such a way that proportionality to the traction load will produce a balanced system. However, ref. [14] further states that the following condition must be realized if effective balancing is to be achieved: The three-phase rated power of the transformer must be equal to the active power of the single-phase load.

When structural modifications are not sufficient for reduction of asymmetry to a level imposed by standards, some equipment which enables reducing of asymmetry can be used. This includes:

3. Single-phase voltage regulators: Single-phase regulators are used to increase or decrease the voltage in each phase of a three-phase system, in such a way that symmetry is achieved. However, they should be used carefully, to ensure that asymmetry is not elevated.

4. Balancing compensators: This can be built as reactance devices or as switching compensators. There are some situations in which shunt switching compensators and reactance devices are the best mitigation technique to use. For example, if the current asymmetry is caused by an arc furnace then a shunt switching compensator can be used. Shunt switching compensator not only mitigate asymmetry but it also mitigate reactance current, harmonics and any other quantities that degrade supply and loading quality. Also if the current asymmetry is caused in an industrial environment where large single-phase fixed parameter loads cannot be reconfigured to obtain balance then a reactance balancing compensator can be used [chapter 16 – Dr. Czarnecki unpublished data].

1.4 Objective of the Thesis

The thesis objective is to create a database of a variety of aspects of voltage and current asymmetry in the power system for future use. This database will include published information on

- The sources of voltage and current asymmetry.

- The propagation of voltage and current asymmetry.
- The negative effects voltage and current asymmetry has on electrical equipment.
- The level of voltage and current asymmetry that can be expected in various situations.
- Voltage and current asymmetry contribution to harmonic generation.
- Compensation techniques used to mitigate the negative sequence current and voltage that is generated in the power system.

1.5 Approach of the Thesis

The thesis objective will be achieved by compilation, arrangement and discussion of all the possible published information on the current and voltage asymmetry, their sources, propagation, negative effects on transmission and customer equipment and on possible remedies aimed at their reduction in the power system.

Some situations related to the voltage and current asymmetry are analyzed and modeled using ETAP software.

The negative impact of current and voltage asymmetry on the electrical devices and equipment in the power system will be discussed in Chapter 2. Sources and level of current and voltage asymmetry will be discussed in Chapter 3. Propagation of voltage asymmetry in the power system will be analyzed in Chapter 4. Design of reactance compensators for reducing current asymmetry, based on the CPC power theory, will be presented in Chapter 5.

CHAPTER 2

NEGATIVE IMPACT OF CURRENT AND VOLTAGE ASYMMETRY ON SELECTED EQUIPMENT

The economic benefits of energy providers and its users are strongly dependent on the supply reliability, security and efficiency of the power system equipment and consequently, on the supply quality and loading quality. For instance, negative sequence current increases loss throughout the process of energy delivery. The negative sequence voltage increases temperature of induction motors. There are also other negative effects of the voltage and current asymmetries.

The performance of some power equipment is affected by current asymmetry, some by the voltage asymmetry, and some by both. Specifically, current asymmetry affects mainly generating and transmission equipment, and the voltage asymmetry primarily affects customer's loads. This is why they are analyzed and discussed separately below.

2.1 Effects of Voltage Asymmetry

2.1.1 Induction Machine

When asymmetrical voltage is applied to a three-phase induction (asynchronous) motor, its performance will deteriorate and the life expectancy will be reduced refs.[11], [14], [16], [17], [60-65] and [18]. This voltage asymmetry causes current asymmetry. For example, according to NEMA MG-1, 1% voltage asymmetry in an induction motor can contribute to 6-10% increase in current asymmetry. The current asymmetry causes increase losses and by extension increase temperature which leads to reduced life-expectation and reduced efficiency of the induction motor. Furthermore it causes torque pulsation, increased vibration and mechanical stresses. In most of the industry and manufacturing plants, more than 90 % of all motors used for production are induction motors, therefore, voltage asymmetry decreases ref.[17] [53] the profit of these plants. The voltage asymmetry can be more harmful ref. [11] when the motor is operated at full

mechanical load. In other words the degree of impact of the voltage asymmetry varies with the motor loading at the time.

The asymmetry of the supply voltage negatively affects, not only the motor, but also the environment in which the motor is installed. This can be seen by the example given in ref. [11] where a motor with a locked rotor current that is 6 times the normal operating current would increase to 30% asymmetry in the motor line current if the voltage asymmetry is 5%.

The major effects of asymmetry on induction motors are compiled and discussed in more details below.

2.1.1.1 Motor Temperature

According to ref. [17] and [65] the temperature rise, losses, efficiency and life expectancy of a typical three-phase induction motor are dependent on the voltage asymmetry. Furthermore, ref. [17] describes an induction motor at rated load, when supplied with a symmetrical voltage, has winding temperature of 120^0C, I^2R losses of 30% of total losses and life expectancy of approximately 20 years. For such a motor, a voltage asymmetry increase of 1%, increases the temperature to 130^0C, I^2R losses increases to 33%, efficiency is reduced by 0.5% and life expectancy is reduced to 10 years. For the same motor at voltage asymmetry of 5%, the temperature increases to 180^0C, I^2R losses increases to 45%, efficiency is reduced by approx. 5% or more and life expectancy is reduced to 1 year.

The variation of these major effects with the level of voltage asymmetry is shown in figure 2.2 ref. [17] and [11]. According to ref. [59], the power loss increases with increase of the voltage asymmetry, as shown in Fig. 2.1, but the winding temperature increases faster than the power loss. Some increase in power loss is related to increase in the winding resistance R with its temperature increase. This is known as the creeping phenomenon and it accounts for the spread between the heating and loss curves in figure 2.1 and 2.2 ref.[17] and [6].

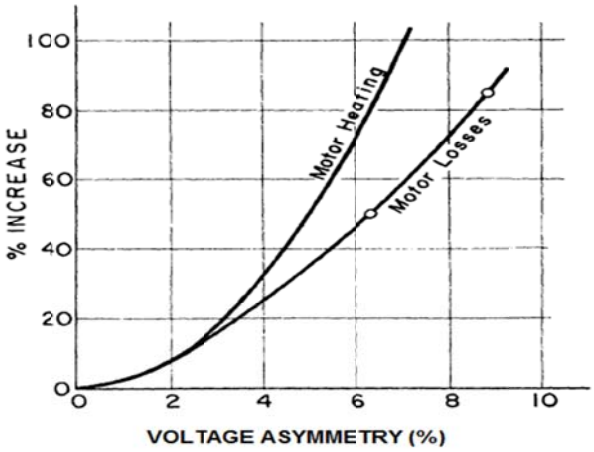

Figure 2.1: Relationship between motor loss and temperature due to % voltage asymmetry increase

A very detailed study on the effect of the voltage asymmetry on induction motors is presented in [60]. It stipulates that when considering the degree of temperature increase you should consider the eight (8) different voltage asymmetry cases. For instance, single phase under voltage asymmetry, two phases under-voltage asymmetry, single phase over-voltage asymmetry etc. all affect the degree of temperature increase. According to ref. [60] the under-voltage asymmetry case causes the worst temperature increase for the same voltage asymmetry factor.

2.1.1.2 Life-time Expectation

According to refs. [17] and [6], the temperature of the motor winding increase with the supply voltage asymmetry can be approximated by the formula:

$$Temp\ increase\ in\ (^{\circ}C)\ \simeq 2 * (\%voltage\ asymmetry)^2,$$

According to ref. [17], 10^0C increase in temperature reduces the insulation life of the windings by a half. It further states that a 3% voltage asymmetry can reduce the life of the motor winding to approximately ¼ its life expectancy. Another important observation stated in ref. [17] [61] is that a 5% voltage asymmetry could reduce the life of the motor winding to less than the typical warranty for a new motor.

2.1.1.3 The Speed of Rotation

The slip *s* is defined as

$$s = \frac{n_s - n_r}{n_s} * 100$$

The positive sequence slip s_p is small when compared with the negative sequence slip s_n. The impedance of induction motors is dependent on the slip. At high slip, such as at motor start or under locked rotor condition, the impedance is low. At low slip the impedance is high. Furthermore, the ratio of the positive sequence impedance to the negative sequence impedance is [11] approximately equal to the ratio of the starting current of the motor to the running current of the motor:

$$\frac{Z_p}{Z_n} \simeq \frac{I_{start}}{I_{running}}$$

Where, n_s denote synchronous speed, n_r denotes rotor speed. The slip for positive sequence is:

$$s_p = \frac{n_s - n_r}{n_s}$$

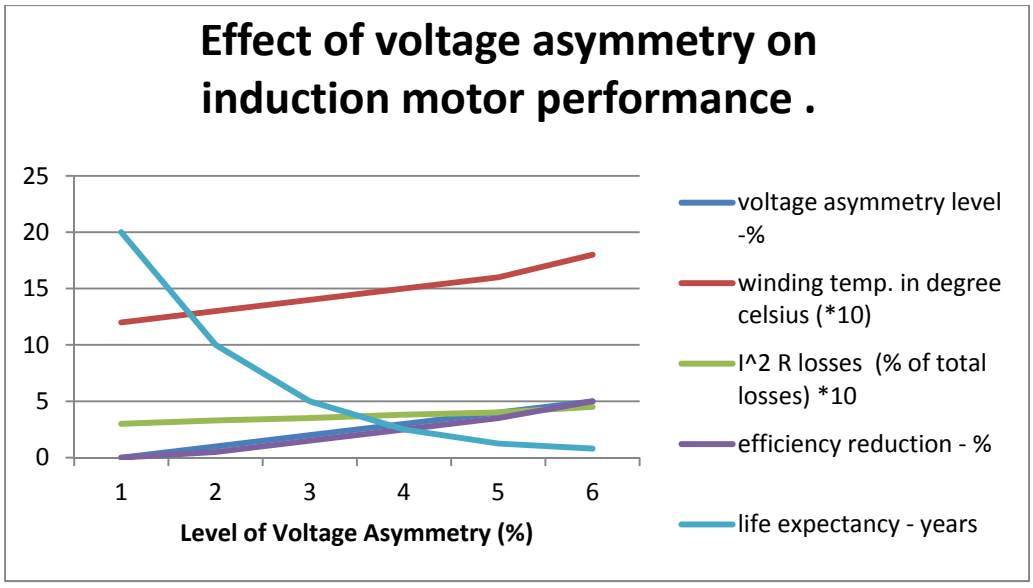

Figure 2.2 Negative effect of voltage asymmetry on induction motor performance based on data taken from ref. [17]

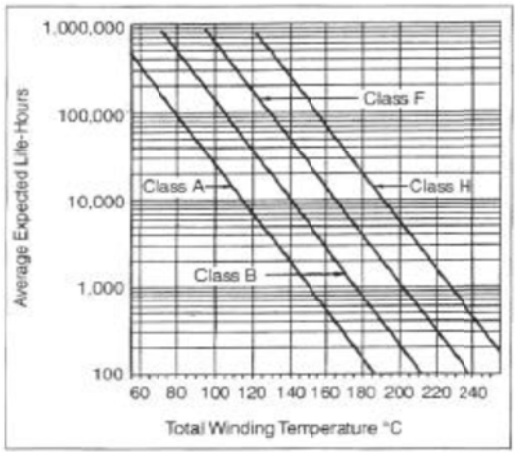

Figure 2.3 Average expected life-hrs. vs total winding temp for different classes of motors taken from ref. [11]

And the slip for negative sequence is:

$$s_n = \frac{-n_s - n_r}{-n_s} = 2 - s_p$$

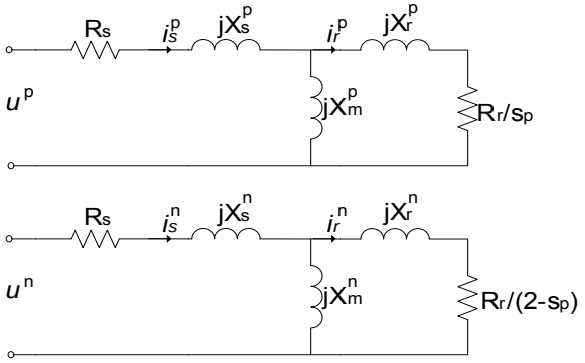

Figure 2.4**:** Positive and negative sequence equ**i**valent circuit diagram for a three-phase induction motor.

Since the frequencies are different:

$$\omega^p = s_p 2\pi$$

$$\omega^n = s_n 2\pi$$

Therefore their reactances are also different.

The negative sequence voltage creates a reverse rotating field with the slip s_n refs. [16], [11], [6] and [62]. This reduces the speed of the rotor ref. [61] and [62]. For example, a 3% voltage

asymmetry would double the slip and reduce the speed of a 4-pole pump motor with a synchronous speed of 1800 rpm that operates at 1764 rpm under normal operating balance voltage, to 1728 rpm [17].

2.1.1.4. Torque

In a response to supply voltage asymmetry i.e the presence of the positive and negative sequence components, the induction motor draws a current which contains positive and negative sequence components. These components depend on the slip. At voltage asymmetry the negative sequence current produces a magnetic field that rotates in the opposite direction to the field created by the positive sequence current as show in figure 2.5. In effect, the rotating field is elliptical rather than circular. This results in a net torque reduction. As a result the motor will operate at a higher slip which intern increases the rotor losses and heat dissipation ref. [14], [6] and [61]. According to ref. [6], a 6.35% (NEMA equation) voltage asymmetry can cause a torque reduction of 23%. Furthermore, the torque pulsation (at double system frequency) on the three-phase induction motor can create mechanical stress ref. [17] on the mechanical component such as the gearbox which will cause noise and vibration that will eventually lead ref. [6] to failure of the motor. A typical torque – speed characteristics is shown in figure 2.6 below. The upper curve is due to the positive sequence torque while the lower curve is due to the negative sequence torque. Therefore, the net torque is less than that produce by a balanced system. Reduction in the peak torque will mitigate the ability of the motor to ride through voltage dips and sags which can affect the stability of the system [16] [62]. The stator and rotor will heat excessively with the flow of this negative sequence current.

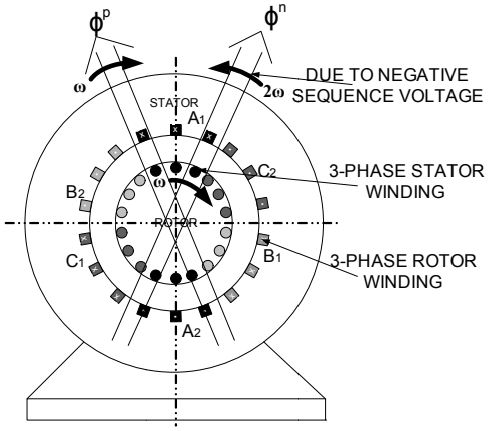

Figure 2.5 Induction motor showing reverse rotation due to voltage asymmetry

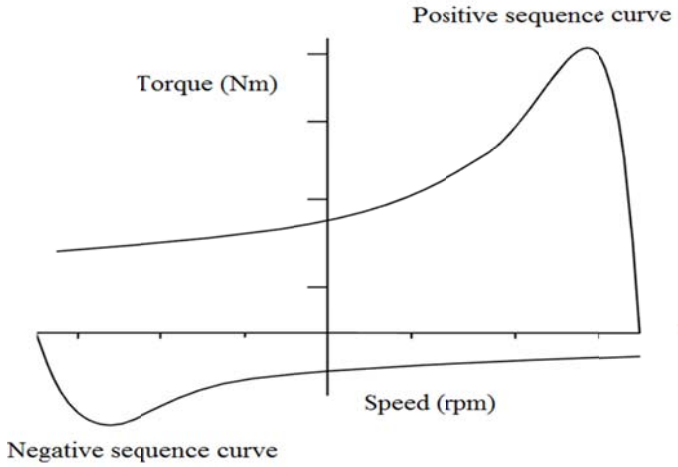

Figure 2.6 Torque-speed characteristic under voltage asymmetry

Starting torque**:** The motor will take a longer time to ramp up to speed or stall if it is supplied with voltage asymmetry ref. [62] and [63]. A detailed analysis performed on a three-phase squirrel-cage 25hp, 240V induction motor is compiled in ref. [63]. The torque-speed characteristic was analyzed under a 6% voltage asymmetry. The motor operate at a slip of 3.54% at rated torque. According to this analysis, the starting torque variation can exceed 60% of the full-load torque of the motor when supplied with asymmetrical voltage. It further states that if the load of the motor demands a starting torque at a very low speed, such as with compressors, conveyor belt system in the bauxite industry and cranes, then this reduction in starting torque could lead to stalling at the starting of the motor.

2.1.1.5 Efficiency

Voltage asymmetry reduces efficiency refs. [17], [60], [62], [63] and [64]. With the slip as stated above, the efficiency will reduce by about 2% [17]. However, according to ref. [60] [62] and [63] the effects of voltage asymmetry on a three-phase induction motor must not only be assessed based on the negative sequence alone but also on the positive sequence. For instance with the same voltage asymmetry factor, a higher positive sequence voltage leads to a higher motor efficiency and a lower power factor.

2.1.1.6 Costs Associated with Motor Failures and Performance Deterioration

Replacement or repair for premature motor failure, unscheduled downtime, loss of production and wasted energy are the financial impact of voltage asymmetry. According to ref. [53] it is estimated that in the United States of America between 1-2 billion dollars per year is attributed to motor loss of life expectancy due to the presence of harmonic and voltage asymmetry. For instance, according to ref. [17] the cost of downtime ($/hour) for a pulp and paper industry is approximately $15,000.00, for a Petro-chemical industry is approximately $150,000.00 and for a Computer manufacturing industry is approximately $4 million per incident. Furthermore ref. [17] stipulates that the cost to the United States industries could be approximately $28 billion a year due to voltage asymmetry. About 98% of the industry uses motor for their critical operation and an unscheduled down time – loss of production (due to current and voltage asymmetry) could cost more than expected ref. [43] and [44]. According to ref. [60] the electricity charge per year due to different voltage asymmetry such as under-voltage and over-voltage cases with 4% voltage asymmetric factor, for 1-5HP induction motor is shown in the bar graph below.

Where:

- 1-phase-uv is single-phase under-voltage asymmetry.

- 2-phase-uv is two-phase under-voltage asymmetry.
- 3-phase-uv is three-phase under-voltage asymmetry.
- 1-phase-ov is single-phase over-voltage asymmetry.
- 2-phase-ov is two-phase over -voltage asymmetry.
- 3-phase-ov is three-phase over -voltage asymmetry.
- 1-phase-α is unequal single-phase angle displacement.
- 2-phase-α is unequal two-phase angle displacement

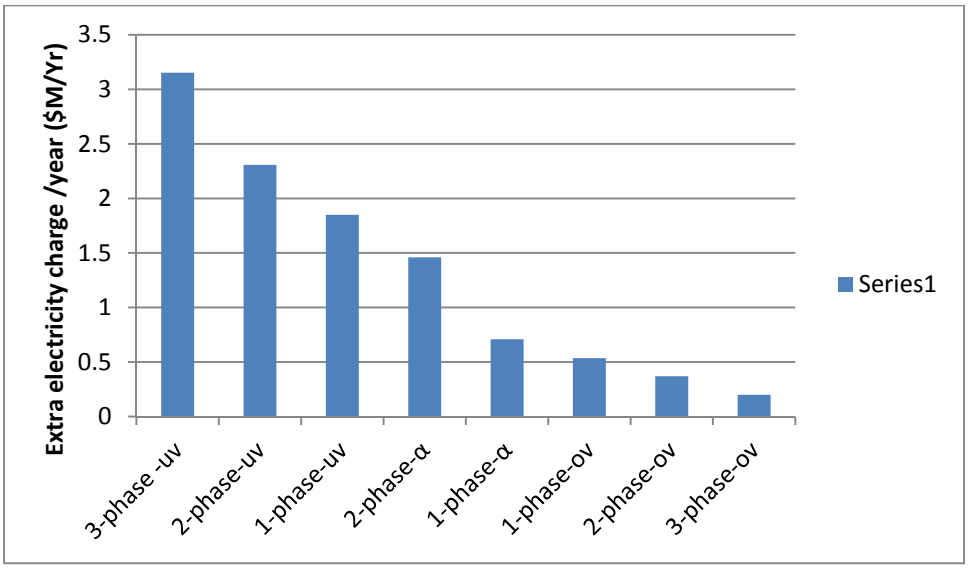

Figure 2.7 Effect of 4% voltage asymmetry on electricity cost – [60]

2.1.2 AC Adjustable Speed Drive (ASD) System

Although adjustable speed drives are used to improve motor operational efficiency, the presence of voltage asymmetry will negatively affect the ASD. Details can be found in refs. [18] and [40]. The structure of a typical ASD is shown in figure 2.7 below. The rectifier and the capacitor (sometimes also an inductor is used) should provide a dc voltage with the lowest ripples possible for the PWM inverter. The power and the motor speed of rotation are controlled by the PWM inverter output voltage magnitude and frequency.

The voltage asymmetry can affect the following areas of the ASD: the rectifier, DC link and the PWM inverter and eventually the motor is affected.

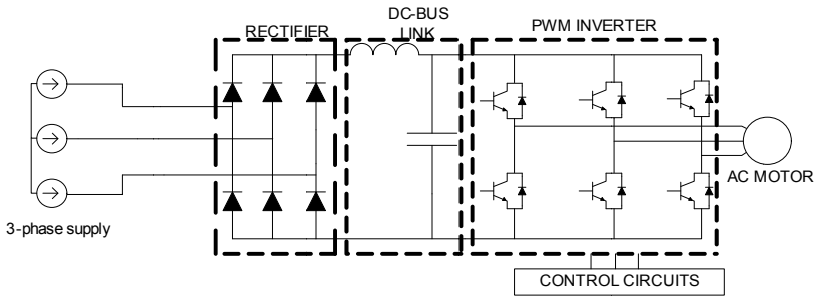

Figure 2.8 Circuit of a typical adjustable speed drive system

According to ref. [40], the positive sequence voltage component specifies the magnitude of the output voltage, while the negative sequence component contributes to ripples in the output voltage. Furthermore the supply current harmonics are influenced by the voltage asymmetry.

For the 6-pulse rectifier the output voltage is built of six pulses of 60 deg. duration. According to ref. [18], when supplied with symmetrical voltage, the rectifier has a current of the waveform as shown in figure 2.8. This current contains harmonics of the order 5^{th},7^{th}, 11^{th} , in general n = 6k ±1, referred to as characteristic harmonics.

Figure 2.9 Rectifier current waveform under symmetrical voltage supply [18].

However, the voltage asymmetry changes the waveform. The waveform change depends on the degree of voltage asymmetry. Figure 2.9 shows the input current waveform for the ASD system analyzed in ref. [18] with 0.3% and 3.75% voltage asymmetry.

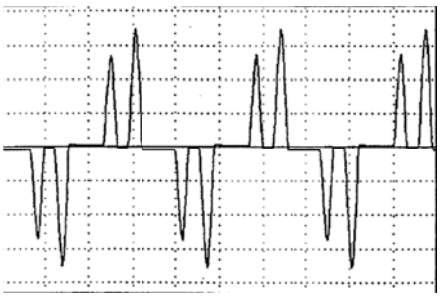

a. 0.3%

b. 3.75%

Figure 2.10 Input current waveform under a. 0.3% and b. 3.75% voltage asymmetry [18].

At asymmetry at the level of 3.75%, the current waveform changes, according to ref. [18], to a single pulse waveform, as shown in Fig. 2.9(b).

There are three main negative impacts of voltage asymmetry on ASD performance, discussed in refs. [54], [11] and [67]. First, voltage asymmetry results in the supply current asymmetry. It is stated in ref. [67] that a voltage asymmetry increase from 0.6% to 2.4% causes the current asymmetry increase from 13% to 52%. The increase in the voltage asymmetry causes the double pulse waveform of the input current to change into a single-pulse waveform as shown in figure 29. The increase in current asymmetry can cause an increase in the temperature of the rectifier diodes in some phases and this can also affect protective devices. For instance, it causes the tripping of the ASD drive system due to excessive ac input current on some phases and under or over voltage on the dc link.

Second, asymmetrical current harmonics of the 3rd and 9th order will increase with an increase of voltage asymmetry ref. [18], [40], [69], and [70]. The voltage ripples on the dc-bus voltage will also increase ref. [55]. This increases the electrical demand of the capacity of the dc-bus capacitor and or inductor. There is also an increase in the core losses on the dc-bus inductor. This increases the potential of magnetic saturation in the core. Ref. [54] further state that a typical voltage asymmetry can contribute to approximately 30% increase in core loss in a powder-core inductor when compared with a system supplied with symmetrical voltage.

Third, it increases the ripple torque in the ASD induction machine. Reference [55] further states that this cause unwanted low frequency harmonic current to flow in the machine. As a result the pulsating torque can cause acoustic noise and mechanical vibration. Also the increase in the bus ripple current increases the temperature of the electrolytic bus capacitors and thereby reduces the life of the capacitor. According to ref. [54], a 2.5% voltage asymmetry can reduce the life of the capacitor to approximately 50% when compared to the symmetrical case. Furthermore the conduction time of the transistors will be longer and the pulse will be longer in the PWM. This condition can lead to more power loss in the devices.

2.1.3 Transmission and Distribution Lines

The primary function of the transmission/distribution lines is to efficiently transmit energy to various destinations to be used by customers. The negative sequence voltage component contributes, along with other reasons, to the asymmetry of the line currents, meaning a negative sequence component occurs in the current. This current practically does not convey energy, because it is orthogonal to the positive sequence voltage. But it contributes to energy loss at the line resistance and this increases temperature of conductors. Therefore, the negative sequence current reduces the capacity of the transmission/distribution line.

2.1.4 Power System Restoration

If the transmission line quantities are not shifted by one-third of the period with respect to each other, or the RMS values of phase quantities are not mutually equal or both phase and RMS asymmetry occurring at the same time, then a power system restoration is not possible. This is because, when trying to synchronize a generator to an asymmetrical system, the phases will not match and therefore, will not be able to be synchronized. The extent of this condition depends on the characteristic of the line, such as the length of the line and the loading of the line at the time. In the case of a long, extra high voltage (EHV) transmission line, that is not transposed, the resulting voltage asymmetry is due to the flow of current (symmetrical in this case) through the different impedance of individual conductors. This voltage asymmetry also causes current asymmetry.

According to ref. [72], during system restoration, the voltage asymmetry;

- Impedes the synchronization of incoming generation. For example, a generator, in a mid-western utility, could not be synchronized to an energized 345KV incoming line because of the presence of 11% negative sequence voltage.
- Causes sequential tripping of generators that lead to section block out. For example, during a light-load period a utility in Australia experienced sequential tripping of their generators due to the excessive negative sequence voltage present on the 500 KV systems. This particular even caused a total blackout.
- Impedes remote starting of thermal units. According to ref. [72], a utility try to provide remote starting energy to a steam electric station via a 500 KV line but because of voltage asymmetry, the process had to be aborted, due to the damage it would cause to the equipment at that station such as rotating machinery.

According to the paper, one of the main reasons for the sequential tripping of the generators and the interference with the remote energization (cranking) operation is due to the imbalance in the line's capacitance. More details can be found in ref. [72].

2.2 Effects of Current Asymmetry

Current asymmetry reduces efficiency, productivity and profits at generation, transmission and distribution of electric energy. This is because the negative sequence component does not contribute to useful energy transmission, but to transmission of energy dissipated in power system equipment in the form of heat. As a consequence of this the ampacity of cables, transmission and distribution lines have to be selected based on the anticipated level of negative sequence current it will be subjected to during operations. Also the capacity of transformers and the efficiency of motors are reduced. In other words the negative sequence current increases losses in the cables, transmission and distribution lines, transformers and equipment on the power system ref. [14]. Furthermore, the negative sequence current cause voltage asymmetry. For instance, the current asymmetry caused by very large single-phase loads such as high speed traction systems and AC arc furnace contribute to different voltage drops on the symmetrical three-phases of the supply system and consequently, it produces voltage asymmetry. Some of the major impact of current asymmetry are compiled and discussed in more details below:

2.2.1 Generator

Synchronous generators essentially produce only positive sequence voltages, while the negative sequence voltage is negligible. Negative sequence current component can occur in the generator mainly due to imbalance loading conditions or faults.

The symmetrical voltage produced by a synchronous generator and its asymmetrical current can be expressed as three-phase vectors as shown below:

$$\boldsymbol{e} = \begin{bmatrix} e_R \\ e_S \\ e_T \end{bmatrix} = e^{\mathrm{p}} \qquad \boldsymbol{i} = \begin{bmatrix} i_R \\ i_S \\ i_T \end{bmatrix} = \boldsymbol{i}^{\mathrm{p}} + \boldsymbol{i}^{\mathrm{n}} \tag{2.1}$$

Thus, the active power delivered by the generator is:

$$P = \frac{1}{T}\int_0^T (e_R i_R + e_S i_S + e_T i_T)dt = \frac{1}{T}\int_0^T (\boldsymbol{e}^T(\mathrm{t})\boldsymbol{i}(\mathrm{t}))dt = (\boldsymbol{e}, \boldsymbol{i}) \tag{2.2}$$

$$= (\boldsymbol{e}^p, \boldsymbol{i}^p + \boldsymbol{i}^n) = (\boldsymbol{e}^p, \boldsymbol{i}^p) + (\boldsymbol{e}^p, \boldsymbol{i}^n)$$

$$(\boldsymbol{e}^p, \boldsymbol{i}^p) = P^p \tag{2.3}$$

$$(\boldsymbol{e}^p, \boldsymbol{i}^n) = 0 \tag{2.4}$$

The scalar product in equation 2.4 is zero because the positive and negative sequence components, as components of different sequences, are mutually orthogonal. Thus, the energy from the generator is delivered to the power system only by the positive sequence component of the generator voltage ($\boldsymbol{e}^{\mathrm{p}}$) and current ($\boldsymbol{i}^{\mathrm{p}}$). However, the negative sequence current $\boldsymbol{i}^{\mathrm{n}}$ contributes to the active power loss in the generator. This power loss in the generator stator resistance R_{s} due to the negative sequence current is $\Delta P_{\mathrm{s}} = R_{\mathrm{s}} ||\boldsymbol{i}^{\mathrm{n}}||^2$. There is also an additional loss in the generator due to the flow of eddy current which contributes to generator heating.

The negative sequence current component has three other main negative effects on the generator:

1. It creates a rotating magnetic field in the air gap that rotates at angular speed of $2\omega_1$ with respect to the rotor. This induces voltage $e(t) = 2\omega_1 N \Phi_{\mathrm{m}} \sin 2\omega_1 t$ in the rotor. The rotor current which occurs due to this voltage contributes to an increase in the active power loss on the rotor resistance. As a result, the temperature of the rotor, and consequently, also the generator, increases. This phenomenon, according to ref. [71], is enhanced by an increase in the rotor resistance due to the skin effect. This is much more visible for the negative sequence component because of the frequency of the voltage induced in the rotor.

2. The reverse field contributes to torque pulsation and mechanical vibration. The torque pulsates at twice the supply frequency and is proportional to the negative sequence current in the stator.

3. It causes terminal voltage asymmetry.

These effects of the current asymmetry on synchronous generators are discussed in many papers, in particular, in refs. [68], [71], [73] and [74]. According to these references, the degree of impact of the negative sequence current is dependent on the type of generator. For instance, the IEEE standard C37.102-1995 in ref. [71] shows the continuous negative sequence capabilities and short time current asymmetry limits for different generators. This data confirms that the cylindrical rotor generator is affected more by the negative sequence component than the salient pole generator. According to ref. [71], there are two types of rotor failure in the cylindrical rotor generator, which are caused by current asymmetry:

i. Overheating of the slot wedges. This causes hardening of material in the slot. Also there is a shear failure against the force of material in the slots, reported also in ref. [74].

ii. Failure of the retaining ring. The heat created by the negative sequence component can cause the shrink fitted retaining ring to become free of the rotor body. As a result the retaining ring is not realigned after it cools and this lead to vibration. Ref. [73] presents a method for analyzing the rotor current and loss distribution under the negative sequence conditions in the generator. In ref. [74], a detailed experiment was conducted to illustrate the effect on rotor surface heating.

Because of all these negative effects of the current asymmetry, generators are very sensitive to unbalanced loads connected in the vicinity of the generator. For instance, high power electric arc furnace (EAF) or a traction system operated in a close vicinity to a generator will cause current asymmetry to affect the generator. In refs. [45] and [46] it is concluded that, due to

the randomness of the EAF load (scrap metal size and type of metal) and the high current which is required for melting, the EAF generates a combination of harmonics and current asymmetry which cause reduced generator performance that could lead to failure of the generator, resulting in instability on the power system and also reduction in the life of the generator. In ref. [45] a situation is described, in which a 350MW steam turbine generator supplies two 60MVA electric arc furnaces (EAF) through a three-mile 230 KV transmission line. The EAF draws asymmetrical current, which causes voltage asymmetry. As a result, the following sequence of events occurred: the generator had a cracked shaft near the turbine-end coupling, then there was two failures of the rotating portion of the brushless exciter and then while operating close to full load the generator's exciter–end retaining ring of the rotor failed. This cost the company a significant amount of money and time to repair the generator. Therefore the nature of the load, the size of the load, the characteristic of the load (resistive, inductive, capacitive or a combination) help to determine the extent of the current asymmetry and hence the level of impact on the generator. Similar effects are studied in ref. [15].

3. The terminal voltage asymmetry is due to the presence of the negative sequence current $\boldsymbol{i}^{n}$. This current causes a voltage drop across the negative sequence impedance $\boldsymbol{Z}_{G}^{n}$ of the generator. Therefore when combined with the voltage drop across the positive sequence impedance $\boldsymbol{Z}_{G}^{p}$ of the generator, which is due to the positive sequence current $\boldsymbol{i}^{p}$, the resulting terminal voltage of the generator is asymmetrical. This will lead to the propagation of voltage asymmetry in the power system. The negative effects of voltage asymmetry are already discussed and therefore will not be repeated here. Figure 2.10 illustrate the voltage drops discussed above.

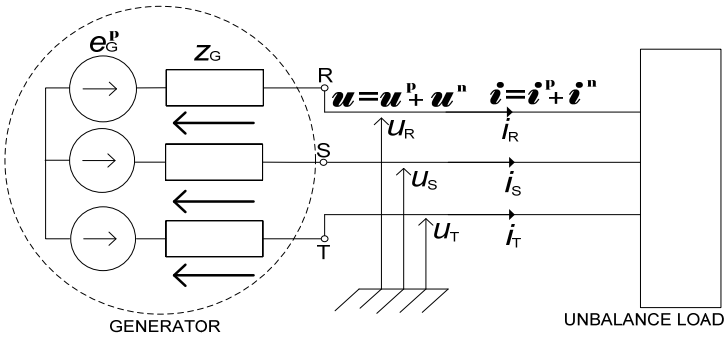

Figure 2.11 Typical generator feeding an unbalance load

Induction generators are affected in a similar way as the induction motors. A detailed experiment is conducted on a wind turbine generator in ref. [15].

2.2.2 Transformers

The transformer is affected based on the configuration, with regard to the connection of a neutral wire on the primary and or secondary shown by the data in appendix B. For example, if the connection is delta / wye-grounded, then the zero sequence current is converted into a circulating current in the delta side as shown in figure 2.11 and also in the ETAP model in figure 4.6. This circulating current cause energy loss and the windings heat as a result. The magnetic flux produced by this current is in phase with each other and as a result they do not cancel each other. This magnetic flux passes through the parts of the transformer causing eddy currents and energy losses. For instance, when case 1 and 2 in appendix B, is compared, the results show that when T2 in figure 4.6 is changed from delta/wye-grounded to wye-ground/wye-ground there are more losses in the system. This is because more transformers are subjected to the zero sequence components. This is shown in the branch loss summary report in appendix B. It shows an overall increase in losses from 82.5kw, 3301.0 kvar (case1) to 1661.6kw, 38359.6kvar (case 2). Another negative effect, however not validated by the ETAP model, is an increase in the acoustic noise of

the transformer. The positive and negative sequence components behave in the same way in the transformer, regardless of the configuration ref. [14] and [68].

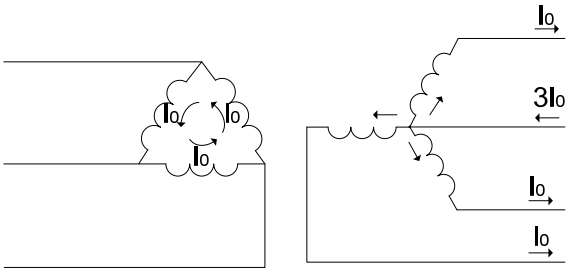

Figure 2.12 Circulating zero sequence current in delta winding

2.2.3 Micro-Grid

One of the objectives of the Micro-Grid is to provide local power using 'green energy' sources. Green sources included: wind, solar, hydro, fuel cells, biomass, diesels powered from synthetic fuels and methane from landfills which supply gas turbines or diesels. Because the load and the generating source (Range from 1KW to about 10KW) is electrically close, the impact of asymmetry can be very expensive and destructive. For example, these small units such as photovoltaic installations are connected to the grid at low voltage via single–phase power electronic inverter units. The impact on electronic converters/inverters has already been discussed and will not be repeated here. However base on that analysis the Micro-Grid will be susceptible to failure because of negative sequence current component. Also since a majority of loads could be single phase this will increase the possibility of negative sequence current flow to the three-phase loads on the system such as induction motors. Since there is no inertia in the Micro-Grid system, any instability or sudden change on the system could lead to the shutdown of the system.

2.2.6 Power Factor Reduction

According to CPC power theory ref. [49] and [75], asymmetry causes power factor reduction and as a result increases apparent power. A three-phase load is connected in delta

configuration as shown in figure 2.11, however any load topology could be used to illustrate how asymmetry mitigates the power factor of a system ref. [49].

$$\boldsymbol{i} = \begin{bmatrix} i_R \\ i_S \\ i_T \end{bmatrix} = \sqrt{2} Re \begin{bmatrix} I_R \\ I_S \\ I_T \end{bmatrix} e^{j\omega t} = \sqrt{2} Re(\boldsymbol{I} e^{j\omega t})$$

$$\boldsymbol{i} = \sqrt{2} Re\{[(G_e + jB_e)\boldsymbol{U} + A\boldsymbol{U}^{\#}]e^{j\omega t}\}$$

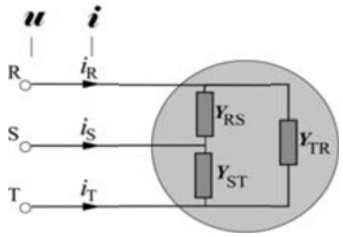

Figure 2.13 Equivalent circuit of a three-phase load

Where:

$$\boldsymbol{U} = \begin{bmatrix} U_R \\ U_S \\ U_T \end{bmatrix}, \qquad \boldsymbol{U}^{\#} = \begin{bmatrix} U_R \\ U_T \\ U_S \end{bmatrix}$$

Equivalent admittance:

$$G_e + jB_e = \boldsymbol{Y}_{RS} + \boldsymbol{Y}_{ST} + \boldsymbol{Y}_{TR} = \boldsymbol{Y}_e$$

Unbalance admittance:

$$Ae^{j\psi} = \boldsymbol{A} = -(\boldsymbol{Y}_{RS} + \alpha \boldsymbol{Y}_{ST} + \alpha^* \boldsymbol{Y}_{TR})$$

Active current:

$$\boldsymbol{i}_a = \sqrt{2} Re(G_e \boldsymbol{U} e^{j\omega t})$$

This current is associated with permanent energy flow from the supply to the load.

Reactive current:

$$\boldsymbol{i}_r = \sqrt{2} Re(jB_e \boldsymbol{U} e^{j\omega t})$$

This current is associated with phase-shift between the supply voltage and current.

Unbalance current:

$$\boldsymbol{i}_u = \sqrt{2} Re(\boldsymbol{A}\boldsymbol{U}^{\#} e^{j\omega t})$$

This current is associated with the supply asymmetry, caused by the load imbalance. The power equation is:

$$S^2 = P^2 + Q^2 + D_u^2$$

Apparent power:

$$S = || \boldsymbol{i} || \, || \boldsymbol{u} ||$$

Active power:

$$P = || \boldsymbol{i_a} || \, ||\boldsymbol{u} ||$$

Reactive power:

$$Q = \pm || \boldsymbol{i_r} || \, || \boldsymbol{u} ||$$

and unbalanced power:

$$D_u = || \boldsymbol{i_u} || \, || \boldsymbol{u} ||$$

Now the power factor is:

$$\lambda = \frac{P}{S} = \frac{P}{\sqrt{P^2 + Q^2 + D_u^2}} = \frac{|| \boldsymbol{i_a} ||}{\sqrt{|| \boldsymbol{i_a} ||^2 + || \boldsymbol{i_r} ||^2 + || \boldsymbol{i_u} ||^2}}$$

This shows that as the asymmetric current increase the power factor decreases.

CHAPTER 3

SOURCE AND LEVEL OF CURRENT AND VOLTAGE ASYMMETRY

3.1 Meaning of Asymmetry and Unbalance

There are three possible manifestations of asymmetry of three-phase quantities – currents and voltages. The first is ***phase asymmetry*** – phase quantities are not shifted by one-third of the period with respect to each other. Second: ***RMS asymmetry*** – RMS values of phase quantities are not mutually equal and the third: - both phase and RMS asymmetry occur at the same time.

The imbalance/unbalance term is used in association with the load. Therefore, the loads that have mutually different impedances of individual phases are referred to as ***imbalanced loads.***

3.2 Supply Quality

The symmetry of voltage, constant frequency, sinusoidal voltage, very low internal impedance – infinitely strong source, lack of transients, no harmonics and RMS variations are some of the quantities that represent an ideal supply quality. If any of these quantities deviate from the ideal case then the supply quality is regarded as a source with degraded supply quality. Therefore the characteristic of these quantities stipulate whether you have a good supply quality or not.

In this thesis the use of supply and loading quality deterioration will be in reference to asymmetry in the power system.

3.3 Loading Quality

If the load is balanced, resistive, linear, time-invariant, is not a source of high frequency noise and is not a source of transients then this constitutes an ideal loading quality. If any of these characteristics is not satisfied then the load is regarded as a load with a degraded loading

quality. For instance if the load is not balanced then it will cause negative sequence current to flow and as a result this will reduce the efficacy of energy use.

3.4 Definition and Quantification of the Voltage and Current Asymmetry.

Since asymmetry is inherent in the power system, standards were developed for evaluation of acceptable level of current and voltage asymmetry for generation, transmission and distribution equipment and also for customer's load. Therefore, it is imperative that the level of current and voltage asymmetry be calculated in an efficient and effective manner.

The level of asymmetry that is used in this thesis is specified as the ratio of the rms value of the negative sequence component to the rms value of the positive sequence component. This is not in-line with a variety of different approaches and standards. Some of these different approaches are due to the measurement technology that exists at the time and some are application oriented as discussed below.

Differences in definitions of asymmetry reflect differences in measurement technology and changes in its capabilities. Originally, only analog meters were available for asymmetry measurements, now sampling technology and digital signal processing can be used for that purpose. For example, in the twenties when this phenomenon was first investigated ref. [56], there was not much harmonics in the power system. Also the technology at that time did not support Fast Fourier Transform (FFT) that can be used to find complex quantities of current and voltages. Therefore, the measuring instrumentation was not capable of taking samples to generate complex quantities of currents and voltages.

Some definitions can be application oriented. For example, asymmetric definition from the point of view of synchronous generator operation can be different from that for three-phase rectifiers or ASD. For instance the continuous unbalance (asymmetric) capabilities (equation 3b) and the short time asymmetric current of the generator are calculated based on the negative

sequence current component. While for motors, it is important to have both phase angle and RMS magnitudes in its calculation of the VAF. Therefore equation (3a) would be the best to use in this case, because equation (1) and (2) both exclude phase angle asymmetry from there calculation of the voltage asymmetric factor (VAF), sometimes called "voltage unbalanced factor." and as a result will not be as accurate. The VAF is used rather than the IAF because motors are affected by the level of voltage asymmetry as stated in chapter 2.

Several papers, such as references [18], [41], [16] and [10] compared some definitions based on whether they use the phase angle or not in their calculation of the VAF. For example NEMA, IEEE, IEC and CIGRE all provide different ways to calculate the VAF. The concern regarding their respective definition of the level of asymmetric current and voltage is whether the calculation without the use of the phase angle will produce an accurate result of the asymmetric current and voltage level. NEMA uses line to line voltage while IEEE uses phase voltage in its calculation and as a result both exclude phase angle asymmetry from there calculation ref. [18], [41], [16] and [10]. However, IEC uses both phase angle and RMS magnitudes in its calculation. The respective differences are illustrated by the equations shown below.

NEMA:

Line voltage unbalance rate – LVUR

V_{maxdev} = Maximum voltage deviation from the average line voltage magnitude

$$= [|V_{ab} - V_{Lav}|, |V_{bc} - V_{Lav}|, |V_{ca} - V_{Lav}|]$$

$$V_{Lav} = [(V_{ab} + V_{bc} + V_{ca})/3]$$

$$\text{LVUR (\%)} = \frac{V_{maxdev}}{V_{Lav}} * 100 \qquad (1)$$

IEEE:

Phase voltage unbalance rate – PVUR

$V_{pmaxdev}$ = Maximum voltage deviation from the average phase voltage magnitude

$$= \left[|V_a - V_{pav}|, |V_b - V_{pav}|, |V_c - V_{pav}|\right]$$

$$V_{pav} = \frac{[(V_a + V_b + V_c)]}{3}$$

$$\text{PVUR (\%)} = \frac{V_{pmaxdev}}{V_{pav}} * 100 \ldots\ldots\ldots\ldots\ldots\ldots (2)$$

IEC:

Voltage unbalance factor – VUF

V^p= positive sequence voltage

V^n= negative sequence voltage

$$V^p = \frac{V_{ab} + \alpha V_{bc} + \alpha^2 V_{ca}}{3}$$

$$V^n = \frac{V_{ab} + \alpha^2 V_{bc} + \alpha V_{ca}}{3}$$

Where: $\alpha = 1 * e^{j\frac{2\pi}{3}}$

$$\text{VAF (\%)} = \frac{V^n}{V^p} * 100 \ldots\ldots\ldots\ldots (3)$$

In the case of equation 3, the system is assumed to be sinusoidal and in such a case do not contain any harmonics. However in all practical system there is always a level of harmonics present and as a result will increase the current and voltage RMS values. This is why equation 3a and 3b was derived to incorporate the impact of harmonics in the system.

$$\text{VAF (\%)} = \frac{V_1^n}{V_1^p} * 100 \ldots\ldots\ldots\ldots (3a)$$

Current asymmetric factor:

$$\text{IAF (\%)} = \frac{I_1^n}{I_1^p} * 100 \ldots\ldots\ldots\ldots (3b)$$

CIGRE:

Voltage unbalance factor – VUF

$$\text{VAF (\%)} = \sqrt{\frac{1-\sqrt{3-6*\beta}}{1+\sqrt{3-6*\beta}}} \text{.....(4)}$$

$$\beta = \frac{|V_{ab}^4| + |V_{bc}^4| + |V_{ca}^4|}{(|V_{ab}^2| + |V_{bc}^2| + |V_{ca}^2|)^2}$$

According to ref. [41] and [11], IEC is the most accurate, because it uses the ratio of negative sequence to positive sequence voltage. According to ref. [41] different voltage asymmetric conditions such as under-voltage asymmetry, over-voltage asymmetry etc. was undertaken to illustrate this finding. The under-voltage case produces a higher value of the voltage asymmetry factor (VAF) when compared to the over-voltage case due to the increase in the negative sequence voltage, while the positive sequence voltage decreases ref. [41] and [42]. Also because the change of the phase angle does not affect the magnitude of the phases but affect the sequence components it is evident that IEC would give a more accurate result. Therefore, equation 3 and 4 produces the same results and are the best formulas to use when calculating the voltage asymmetry factor. If the line-to-neutral voltages are used in the formulas, the zero sequence components can give erroneous results. Zero sequence current does not flow in a three wire system. Therefore, the calculation of a zero sequence voltage asymmetry factor is irrelevant however, for a four wire system it would be relevant. This would be the ratio of the zero sequence voltage to the positive sequence voltage but this will not be discussed in details here.

3.5 Standards for Voltage Asymmetry

There was a study conducted by the Edison electrical Institute, about twenty years ago, to investigate the trade-off between the cost of reducing system voltage asymmetry and the cost of designing motors to tolerate imbalance. The result of this study revealed that utility cost for asymmetry reduction below 2.5% increases exponentially whereas the manufacturer cost of a motor capable of operating at asymmetry higher than 3.25% also increases exponentially.

Therefore, by combining the two, the overall cost was minimized at an asymmetry of 3%. This is the basis on which the ANSI standard C84.1 was written. More details can be found in ref. [18].

ANSI C84.1-1995 recommends that the electrical supply systems should be design to accommodate a maximum voltage asymmetry limit of 3% when measured at the power utility meter under no load conditions ref. [18]. However, for motors the NEMA MG1-1993 standard (corresponds with the VAF formula) recommends that if the voltage asymmetry is greater than 1% then the motor should be derated according to the required factor which appears in figure 3.1 ref. [32], [33] and [18]. According to ref. [18], the above study, provides the rationalization for the apparent contradiction between NEMA MG1-1993 standard and ANSI C84.1-1995 standard. The IEC – International Electrotechnical Commission recommends that the maximum voltage asymmetric limit be 2% [18]. According to the information provided in ref. [14], the international standards EN-50160 and IEC 1000-3-x series state that for low voltage and medium voltage systems, the voltage asymmetric factor should be less than 2% and less than 1% for high voltage systems. These limits are based on a ten minute interval, with maximum instantaneous value of 4% VAF.

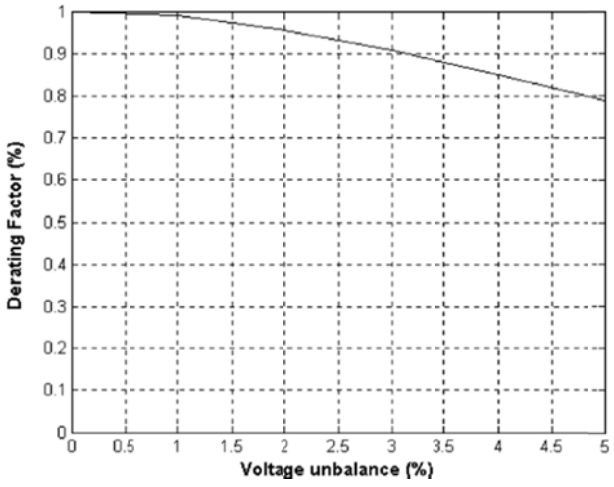

Figure 3.1 NEMA motor derating curve

3.6 Standards for Current Asymmetry

The standards set for the voltage asymmetry automatically set the standards for current asymmetry in some cases. For example, knowing that 1% voltage asymmetry corresponds to approximately 6% current asymmetry in induction motor, the standard can be set for the voltage asymmetry. However in some cases, such as with the generator, this is different. For example, according to refs. [46] and [71], the continuous negative sequence capabilities for the cylindrical rotor generator (indirectly cooled) is 10% and 5% (without connected amortisseur windings) for the salient-pole. More details on the different continuous negative sequence capabilities (permissible $||i^n||$ in percent) and the short time asymmetry current limits (permissible $(i^n)^2t$ can be found in ref. [71].

3.7 Sources of Voltage Asymmetry

3.7.1 Structural Asymmetry

The voltage asymmetry of the structural nature is caused by a physical asymmetry of generating and transmission equipment, such as:

- Generators
- Transformers
- Transmission lines
- Distribution lines

It means that some level of the voltage asymmetry is built in the system. This is a permanent source of asymmetry that can become worst if the system is loaded with unbalanced load. This can be seen by the data in case 4 in appendix B.

3.7.1.1 Generators

The generator can contribute to voltage asymmetry if the stator impedances for particular phases are not mutually equal. This can be attributed to some level of mechanical asymmetry of the

stator and its windings. For example, the eccentricity of the rotor causes variation of the air gap which will result in asymmetry of the phase inductances. Also asymmetry between leakage inductances can occur from asymmetry of winding heads and due to possible differences in the distribution of the coil conductors of different slots. However these are generally designed to be symmetrical.

3.7.1.2 Transformers.

Transformers can contribute to the voltage asymmetry in two ways. The first is through the transformer geometry. That is, the impedance can be asymmetrical. The second is through the configuration. However in this section the focus will be on the asymmetry caused by the structural features of the transformer. Figure shows the typical structure of a three limb transformer with magnetic flux.

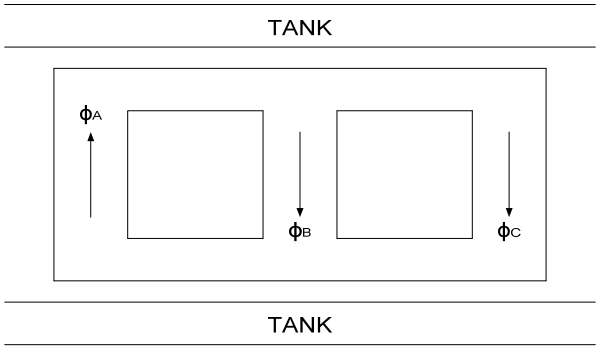

Figure 3.2 Typical three-phase three limb transformer structure

The induced voltage is:

$$e = N\frac{d\Phi}{dt} = \frac{d\lambda}{dt}$$

Due to the structural asymmetry:

$$e_A = N\frac{d\Phi_A}{dt} \neq e_B = N\frac{d\Phi_B}{dt} \neq e_C = N\frac{d\Phi_C}{dt}$$

Asymmetry will always exist in distribution transformers with cores of standard geometry ref. [1]. The transformer core, tank and frame geometric orientation contributes to

asymmetric conditions. This asymmetry is mainly due to the difference that exists between the mutual impedances of the transformer phases. Mutual reactance is directly proportional to the magnetic couplings between ports and the occurrence of stray losses produced in the tank and frames are associated with the mutual resistances. Figure 3.2 illustrate this. Therefore, even though there is some asymmetry due to stray losses, the main asymmetry is due to the electromagnetic couplings between the phases. If the magnetic path length associated with the central phase of a three-phase three-limbed core type transformer is shorter than that of either of the outer phases, then the magnetizing current and core loss value will be asymmetric, to the degree stipulated by the path length ratio. If the central path length is one-half that of either outer, then its magnetizing current is likely to be about 30% less, and this is independent on the peak flux density level.

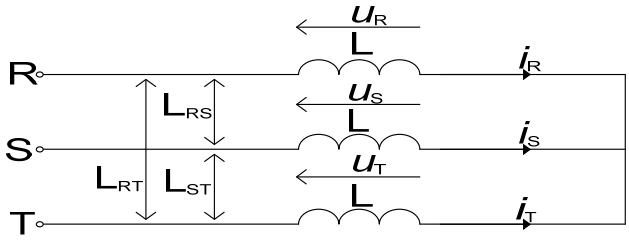

Figure 3.3 Simplified circuit of a transformer showing mutual inductance between phases.

The equation below shows the derivation of the relation between the current asymmetry and voltage asymmetry. This equation can be modified to illustrate a similar situation with transmission lines.

$$\begin{bmatrix} \boldsymbol{u}_R \\ \boldsymbol{u}_S \\ \boldsymbol{u}_T \end{bmatrix} = \begin{bmatrix} j\omega L & j\omega L_{RS} & j\omega L_{RT} \\ j\omega L_{SR} & j\omega L & j\omega L_{ST} \\ j\omega L_{TR} & j\omega L_{TS} & j\omega L \end{bmatrix} \begin{bmatrix} \boldsymbol{i}_R \\ \boldsymbol{i}_S \\ \boldsymbol{i}_T \end{bmatrix}$$

$$L_{RS} = L_{SR} = L_R$$

$$L_{RT} = L_{TR} = L_S$$

$$L_{ST} = L_{TR} = L_T$$

$$\begin{bmatrix} \boldsymbol{u}_R \\ \boldsymbol{u}_S \\ \boldsymbol{u}_T \end{bmatrix} = j\omega \begin{bmatrix} L & L_R & L_S \\ L_R & L & L_T \\ L_S & L_T & L \end{bmatrix} \begin{bmatrix} \boldsymbol{i}_R \\ \boldsymbol{i}_S \\ \boldsymbol{i}_T \end{bmatrix}$$

$$S = \begin{bmatrix} 1 & 1 & 1 \\ 1 & a^2 & a \\ 1 & a & a^2 \end{bmatrix}, \qquad S^{-1} = \frac{1}{3}\begin{bmatrix} 1 & a & a^2 \\ 1 & a^2 & a \\ 1 & 1 & 1 \end{bmatrix}, a = e^{j120}$$

$$S\begin{bmatrix} \boldsymbol{u}^p \\ \boldsymbol{u}^n \\ \boldsymbol{u}^o \end{bmatrix} = j\omega \begin{bmatrix} L & L_R & L_S \\ L_R & L & L_T \\ L_S & L_T & L \end{bmatrix} S \begin{bmatrix} \boldsymbol{i}^p \\ \boldsymbol{i}^n \\ \boldsymbol{i}^o \end{bmatrix}$$

For three-phase 3 wire systems $\boldsymbol{u}^o and\ \boldsymbol{i}^o = 0$

$$\begin{bmatrix} \boldsymbol{u}^p \\ \boldsymbol{u}^n \\ 0 \end{bmatrix} = j\omega \frac{1}{3}\begin{bmatrix} 1 & a & a^2 \\ 1 & a^2 & a \\ 0 & 0 & 0 \end{bmatrix} \begin{bmatrix} L & L_R & L_S \\ L_R & L & L_T \\ L_S & L_T & L \end{bmatrix} \begin{bmatrix} 0 & 0 & 0 \\ 1 & a^2 & a \\ 1 & a & a^2 \end{bmatrix} \begin{bmatrix} \boldsymbol{i}^p \\ \boldsymbol{i}^n \\ 0 \end{bmatrix}$$

$$\begin{bmatrix} \boldsymbol{u}^p \\ \boldsymbol{u}^n \end{bmatrix} = j\omega \frac{1}{3}\begin{bmatrix} L_R + aL + a^2L_T & L_S + aL_T + a^2L \\ a^2L_R + a^4L + a^3L_T & aL_S + a^3L_T + a^2L \end{bmatrix} \begin{bmatrix} \boldsymbol{i}^p \\ \boldsymbol{i}^n \end{bmatrix}$$

To evaluate the level of impedance asymmetry that could be attributed to a transformer or the generator, modeling of its magnetic field is needed. The following is a list of possible programs that can be used to evaluate the specific level of asymmetry due to structural imbalance:

- Maxwells 3D program
- 2D finite element method using the AC/DC module of COMSOL Multiphysics

Transformer Bank.

Three-phase transformer windings can be configured in delta or wye. It can be done on a common magnetic core or using separate single-phase transformers arranged in either configuration (transformer banks). On the distribution system there is a need to supply both single-phase and three-phase loads. To achieve this in the distribution system single phase transformers are arranged in transformer banks. Therefore by using a 4-wire system comprising of transformers with secondary windings connected in delta or open delta with a center tap

ground on one leg of the delta, these loads can be supplied. Also in the 4-wire grounded wye system, the secondary winding neutral point is grounded. The focus below will be on transformer banks connected in floating wye – delta and open wye – open delta configuration.

Delta – Delta and Floating Wye – Delta Banks: In this configuration the voltage asymmetry is caused by the dissimilarities between the single-phase transformers that make up the bank. The transformer to which the single-phase load is connected is referred to as the "lighting leg" (L) and the other transformer are referred to as "the power leg" (P). As a result the impedance is noted as Z_L and Z_p respectively. Figure 3.3 illustrates this.

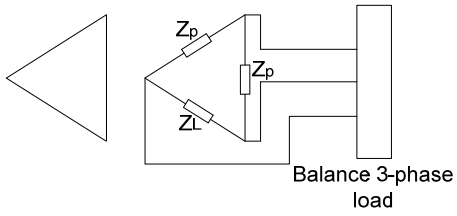

Figure 3.4 Delta-delta transformer bank configuration with balance 3-phase load

Even if both transformers have the same impedance (Z_L=Z_p), the maximum negative sequence voltage can be above 1%.

Open Wye-Open Delta or Open Delta-Open Delta: Voltage asymmetry is caused by the asymmetry of the transformer bank configured in open wye-open delta or open delta-open delta supplying a three-phase load. Figure 3.4 illustrates this kind of transformer bank configuration. The voltage asymmetry with the open delta bank can be significantly higher than that with a closed delta bank supplying the same load ref. [23]. However, according to ref. [23], due to the use of only two transformers (3% impedance) in the bank arrangement, the voltage asymmetry at nominal load is approximately 1.73%. This is achieved when the primary supply system is symmetrical. However, if an untransposed line produces a 1 to 2 % range of asymmetry in the primary system, then the load would experience an asymmetry in the range of 2.7 to 3.7%.

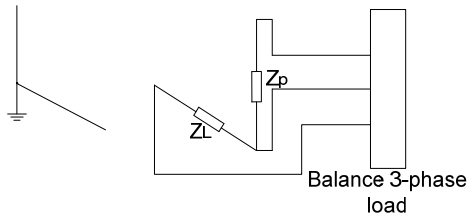

Figure 3.5 Open wye-open delta transformer bank

3.7.1.3 Transmission and Distribution Lines

The geometric positioning of transmission and distribution lines in space and to ground (earth) makes it impossible for the lines to be spaced equilaterally as shown in figure 3.6. Other similar structure and measurements can be found in ref. [76]. When the right-of-way consist of only one circuit it is easier to mitigate the voltage asymmetry. However, it is more difficult to do so when multi-circuit power lines exist in the right-of-way, especially when there are many load taps on the same circuit.

One Circuit – The distance each line is placed from each other and ground will never achieve equilibrium and this will influence the impedance of the lines. In other words the flux linkages and inductance of each phase are never the same and this will produce voltage asymmetry in the system. Also the capacitances of each phase to neutral is unequal and since it is a shunt between conductors then charging current flows in the transmission line. With this flow of charging current and the unbalance inductance there will be voltage drop along the line which will lead to voltage asymmetry in the system. One of the only effective methods to reduce the source of voltage asymmetry in the overhead lines in transmission and distribution system is phase transposition. In other words the geometric orientation of the phases should be placed in such a way that the average current induced (especially at maximum loading of the line/s) is reduce to an acceptable level ref. [2]. Figure 3.5 is an example of phase transposition.

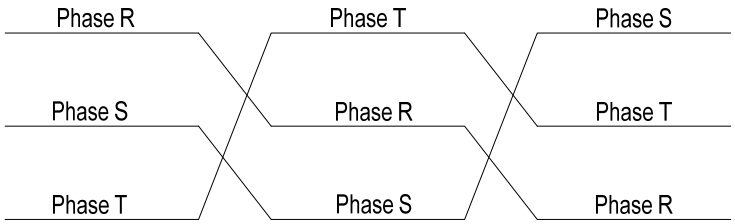

Figure 3.6 Cycle of a transposed line

Multi-Circuit – When the right-of-way has more than one circuit with load-taps, the voltage due to induction between the circuits will be asymmetrical. The situation gets worst when the magnitude of the induction in one or more circuits is higher than the others due to more loading of that circuit. A typical multi-circuit description and layout is shown in ref. [3].

In this situation we have to look at both phase transposition within each circuit as well as the transposition of the circuits in the right-of-way in order to mitigate voltage asymmetry. Another factor to consider will be the type of circuits that share the right-of-way. For instance if one circuit is a 345kv system and the other is a 138kv system, then the geographic spacing will be different than if the circuits were the same ref. [3]. A detailed description and analysis of multi-circuit is found in ref. [26-29].

Some other causes of voltage asymmetry are:

- Incorrect use or faulty capacitor banks - malfunction of power factor correction devices
- Voltage regulation of single phase system. For example, one section of the single phase may require the regulator to increase the voltage while another may require that the regulator reduce the voltage.

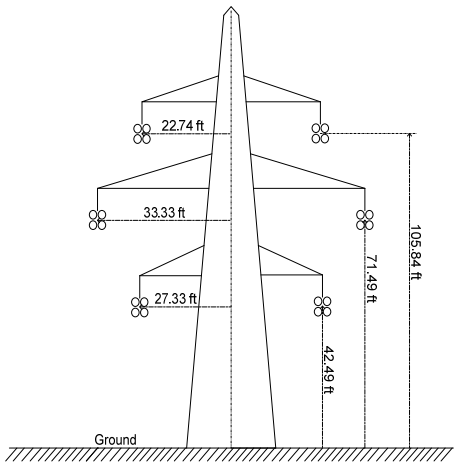

Figure 3.7 400kv transmission structure showing geometric spacing of conductors and ground

3.8 Sources of Current Asymmetry

The primary source of current asymmetry is load imbalance due to the single-phase arrangement of loads and/or large single-phase load on the distribution system or faults on the load side. Load imbalance, though, usually time-varying, can be regarded as permanent asymmetry. Faults are rather transient.

The supply system sees the entire user as a time-varying load, for example, the arc furnace load demand changes due to the kind and amount of scrap that it has to melt. In this case the supply system may see an unbalance load that is either: nonlinear, linear, resistive, capacitive, inductive and/or a combination. Therefore, the characteristic of the load will characterize the nature of the current asymmetry drawn due to the imbalance loading.

3.8.1 Permanent Imbalance

Permanent imbalance occurs under normal operating conditions of the system. The single or double phase loading of the three-phase 3-wire and three-phase 4-wire system and also unbalance three phase loads are the contributors to permanent imbalance. Single-phase loads such as traction systems and welders are examples of permanent imbalance on the power system.

Another load that contributes significantly to negative sequence current is the arc furnace. The nature of this load is nonlinear, random and also introduce harmonic into the system. These loads causes permanent imbalance in the system and they will be further discussed in details below.

3.8.1.1 Residential and Commercial Single-Phase Loading

The problem of unbalance loading in three-wire and four-wire systems is difficult to predict because the utility has no controls on the end user random use of the energy produced. For instance low voltage, single-phase loads such as PC's, commercial lighting, washing machines, domestic air condition units etc., is difficult to balance between phases of the three phase system. Furthermore, even if the system is designed balanced by distributing the load equally between phase per floor or houses, there will still be imbalance due to the fact that the energy demand in each phase by individual users will be different from each other ref. [39] and [14].

3.8.1.2 Traction Systems

Traction systems are electrically large single phase loads that can create current asymmetry. The loading characteristics or profile (when the train is in motion) of the AC traction system is nonlinear and time varying and produces imbalance loading. In other words as the position of the vehicle changes so does its geometry in relation to the power system to which it is connected ref. [34]. The large imbalanced traction loads (20MW for instance) may cause system current asymmetry and therefore overheat rotating machines, increase system losses, interfere with neighboring communication systems, and cause protection relays and measuring instruments to malfunction ref. [12]. As shown in ref. [13] the various transformer configurations are able to reduce the negative sequence current but not eliminate it.

3.8.1.3 Arc Furnaces

The central process of mini-mills, which produce steel from scrap, is the electric arc furnace (EAF). The nature of the scrap being melted creates the random and nonlinear load which causes current asymmetry in the power system. The evidence of this was shown in ref. [19] where the utility compared the asymmetric current period with a metal company's melting records and the findings were a match. The arc can change from zero to full load several times per hour as arcs are made and broken in the furnace. The current asymmetry that is produced can cause damage to generators that are electrically close to these metal plants. The arc providing the heat energy to melt the scrap is governed by the raising or lowering of the electrodes which depends on the voltage. The voltage is directly proportional to the arc length inside the furnace. This is also proportional to the current produced to provide the melting ref. [36]. Furthermore, some arc furnace electrodes have a triangular geographical orientation and the uneven distance between the electrodes and different position along the furnace wall result in an asymmetrical thermal load which in turn draws unequal current from the phases. Also the electromagnetic forces from the arc are deflected outwards from the center which is characterized as an imbalanced thermal load on the furnace walls – resistance and reactance in each phase is not the same ref. [37], [38]. This variation causes current asymmetry to flow in the system. This kind of characteristics of the arc furnace also causes harmonics which can also influence current and voltage asymmetry.

3.8.2 Transient Imbalance

Transient imbalances are unbalanced loading due mainly to faults on the power system. Single phase switching is also considered as transient imbalance. This condition last for approximately 60 cycles or more ref. [57]. During this time period the system experiences

current asymmetry. This negative sequence current can be very destructive to the surrounding equipment especially the generators.

3.8.2.1 Faults

The analysis of asymmetry due to faults is beyond the scope of the thesis. However, some basic information will be discussed. The following are possible cases of faults that produces critical asymmetric conditions on the power system:

- Single line to ground faults – these are the most likely fault on the power system.
- Line to line faults.
- Misoperation of one or more poles of a breaker.
- Blown fuse/s or loss of a phase.
- A blown fuse on a 3 phase bank of power factor improvement capacitors.
- Open phase on the primary of a 3 phase transformer on the distribution system.
- Faults in the power transformer.
- Large unbalanced industrial loads (such as multi-megawatts induction motors used in cement and mining industry) under single phase or two phase fault conditions.

Approximately 80% of the failure on the power system is single phase faults and only about 3% are three-phase faults. At the point of the phase to ground fault (or abnormal loading of one phase) the current increases while the voltage decrease. Therefore, while the current in one phase of the three phase system is abnormal the other two phases is significantly lower, producing a current asymmetry in the system. According to ref. [32] the grounded or ungrounded system exhibits different magnitude of current asymmetry due to phase to ground, phase to phase and phase to phase to ground faults. This is due to the different impedance values involved. For example the line-to-line fault generates the highest negative sequence current. The vector diagrams in ref. [32] clearly illustrate the variation of phase and magnitude of the current

asymmetry. This stipulates that the impedance of the system grounding connection, the location of the fault and the type of fault influence the nature of the current asymmetry that will result from the fault. The detail of all the fault conditions that can occur on the power system will not be covered in the thesis. However, the point being illustrated here is that a fault on the power system produces current asymmetry.

3.9 Interaction between Unbalanced Load and Supply Asymmetry

In some situations both the voltage and the current asymmetry have to be taken into account. This increases the complexity of the problem and modeling is usually required. This is done in figure 4.10 with the respective data in case 4 in appendix B. This is why it is important to clearly define loading quality and supply quality in sections 3.2 and 3.3. The interaction of both occurring as a source of asymmetry, occurs due to the structural asymmetry of the source and single-phase load unbalance. This could be a combination of any of the sources discussed above.

3.10 Voltage Response to Current Asymmetry

In some situation the supply is symmetric but the load is imbalance and as a result you have both current and voltage asymmetry resulting from the current asymmetry. For example, if there is a load connected to one-phase of a three-phase system in such a way that it causes an rms current to flow which is greater than the other phases, then this will cause a voltage drop to occur which will lower the voltage in that phase. This causes both current and voltage asymmetry to flow in the system. This is shown in figure 4.9 and the corresponding data in case 3 in appendix B. The voltage asymmetry depends on the impedance of the system and the magnitude of the current asymmetry which depend on the characteristic and nature of the load causing the imbalance. In this case the characteristic of the unbalance load is shown in figure 4.8. Figure 4.9 shows the respective asymmetric voltage drop on the cables and buses. Even though voltage

asymmetry will impact the power system negatively, current asymmetry contributes more to power losses on the power system.

3.11 Current Response to Voltage Asymmetry

The voltage asymmetry can originate in generation and transmission system as discussed above. However, even though the load is balanced, asymmetric current will flow due to the asymmetry in the supply. This voltage asymmetry can also amplify the current asymmetry. This is clearly visible in induction motors where 1% of voltage asymmetry causes a 6 to 10 % current asymmetry. This is because the negative sequence impedance is much lower than that of the positive sequence impedance. This is illustrated in figure 2.4 in chapter 2.

CHAPTER 4

PROPAGATION OF CURRENT AND VOLTAGE ASYMMETRY

Chapter 3 categorizes and classifies the possible source of current and voltage asymmetry which occurs in the process of generation, transmission, distribution and utilization of energy in the power system. This chapter will look at how asymmetric current and voltage propagate throughout the power system. In particular, does the transformer, equipment, transmission and distribution line attenuate, amplify and/or influence the current and voltage asymmetry in the power system? To answer this question we have to analyze the type of system (three-phase, 3-wire or three-phase, 4-wire), the source of the asymmetry and the characteristics of the devices in the power system.

Transformers, transmission and distribution lines does not attenuate or amplify current and voltage asymmetry. However, the way in which asymmetry propagates from upstream (HV) to downstream (LV) in the power system will depend on the type of system. That is, whether the system is a three-phase 4-wire system or a three-phase 3-wire system. The type of the system is dictated by the transformer configuration. The main difference of the two systems is that zero sequence current component flows in the 4-wire system, but does not flow in the 3-wire system.

The positive and negative sequence components affect the transformer in the same way. The impedances of both of these sequence components are the same in the case of the transmission lines and the transformers. However, the zero sequence impedance of the transmission lines depends on whether it is a cable or overhead line and also on the return path of the current. Furthermore the zero sequence impedance for the transformer depends on the rating and connection of the transformer ref. [10]. A simplified one line diagram of a power system is shown in figure 4.1. Figures 4.2 through 4.4, provides a basic illustration of the different sequence component in terms of an equivalent circuit.

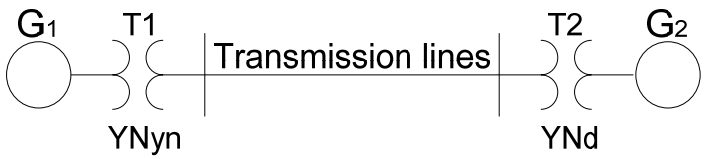

Figure 4.1 Simplified power system one line diagram.

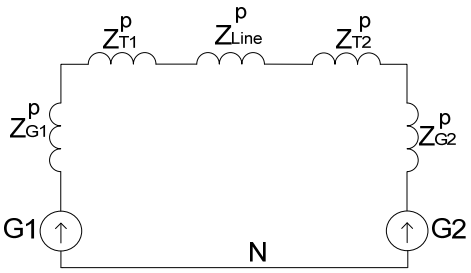

Figure 4.2 Equivalent circuit for the positive sequence

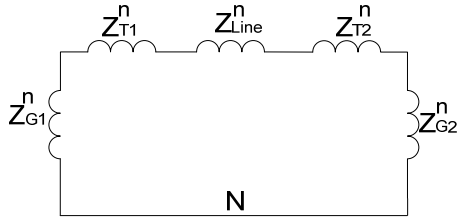

Figure 4.3 Equivalent circuit for the negative sequence

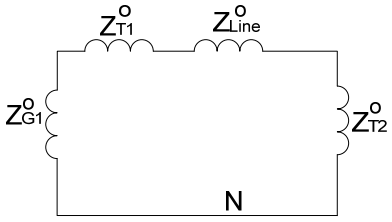

Figure 4.4 Equivalent circuit for the zero sequence

The negative effects of voltage asymmetry discussed in details in Chapter 2 accentuate the importance of understanding how the voltage asymmetry propagates in the power system. In assessing how asymmetry propagates in the system, the type of system has to be identified as stated about. Then the source of the asymmetry needs to be identified followed by the location of the asymmetry such as, HV MV or LV. The ETAP model in figure 4.5 will be used to illustrate the propagation of asymmetry in the power system. The ETAP unbalance load flow analysis uses

both three-phase 4-wire and three-phase 3-wire system. The details of the ETAP system model can be found in appendix A. Also a full description and detail of the calculation method used and the system parameters can be found in chapter 20 of the ETAP help 7.5.

4.1 Influence of Transformer Configuration on Asymmetry Propagation

Two cases will be analyzed base on the transformer configuration of the system. T2 will be the only transformer changed. The degree of source asymmetry is exaggerated for the purpose of this study.

Case1: The A phase of the supply is 80% of Va magnitude while B and C phase is 100% magnitude – without harmonics in the source. Transformer configuration T2- D/yn shown in figure 4.6. Figure 4.6 shows the unbalance load flow of the system.

Case 2: The A phase of the supply is 80% of Va magnitude while B and C phase is 100% magnitude – without harmonics in the source. Transformer configuration - (T2) YN/yn as shown in figure 4.7.

When the critical report data in appendix B was analyzed it is observed that the transformer configuration impedes or allow the flow of zero sequence components in the power system. For instance, for case 1 only bus 1, 2 and 3 had a critical zero sequence component alarm (VUF = 7.1%) as shown in the critical report in appendix B. However, for case 2, the zero sequence components propagate throughout the system wherever there is a YN/Yn configuration. Furthermore there are more losses associated with case 2 because of the flow of the zero sequence components in the system. This circulating current in the delta winding is converted to heat. This is shown in the branch losses summary report in appendix B.

The equipment and lines in red, in figure 4.7, is an indication that the rated current is exceeded as shown in the branch loading summary report in appendix B

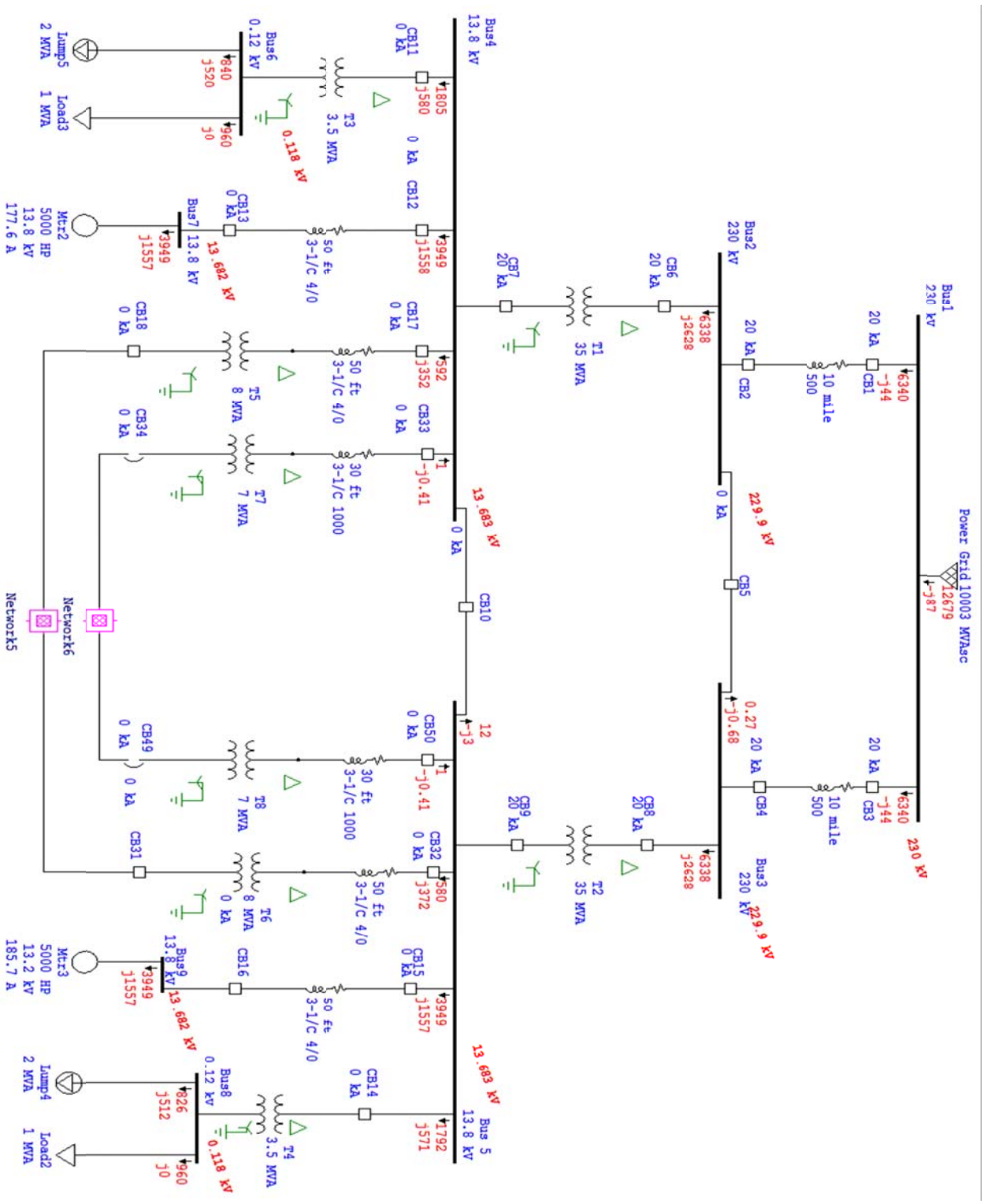

Figure 4.5 Balanced ETAP system with load flow information

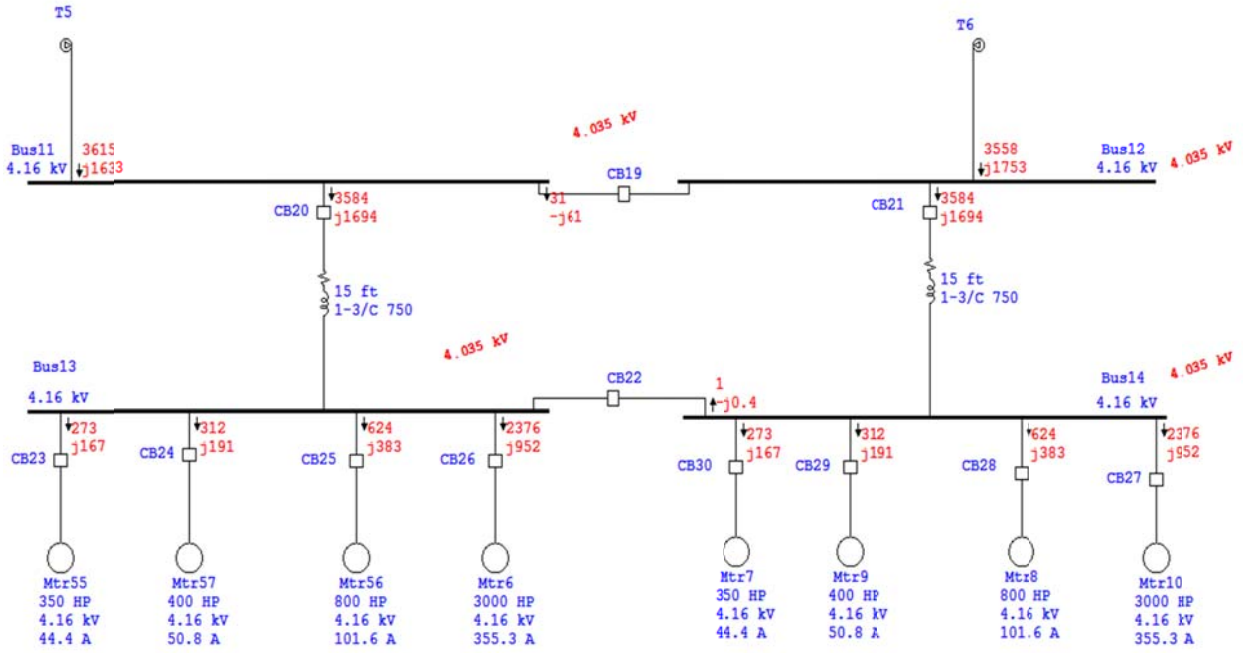

Figure 4.5a Balanced ETAP system with load flow information - Network 5

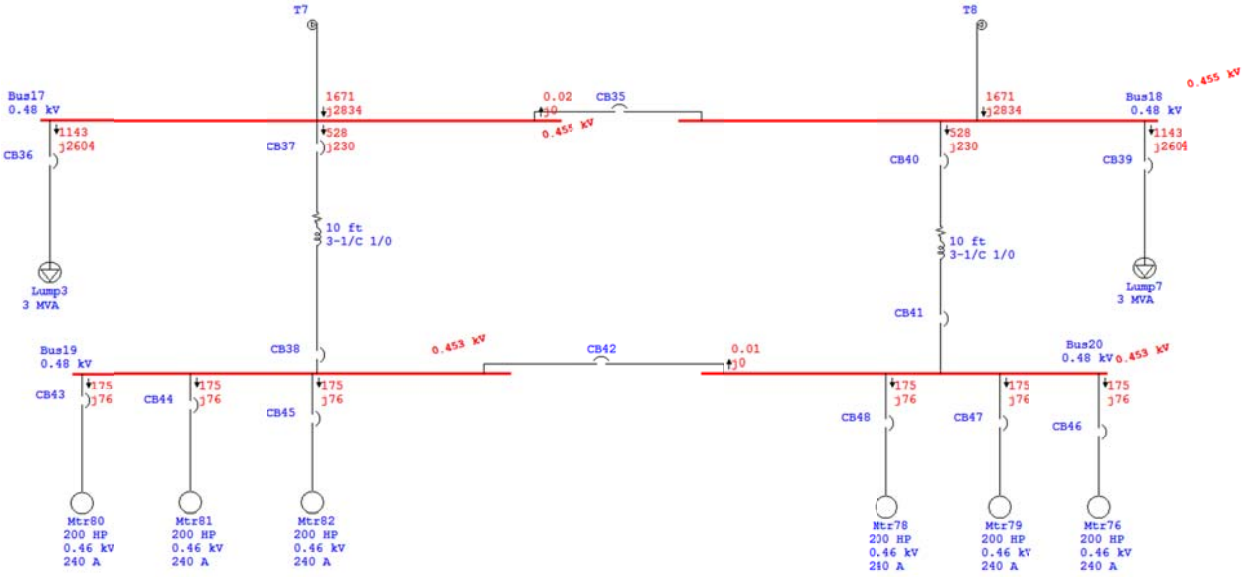

Figure 4.5b Balanced ETAP system with load flow information - Network 6

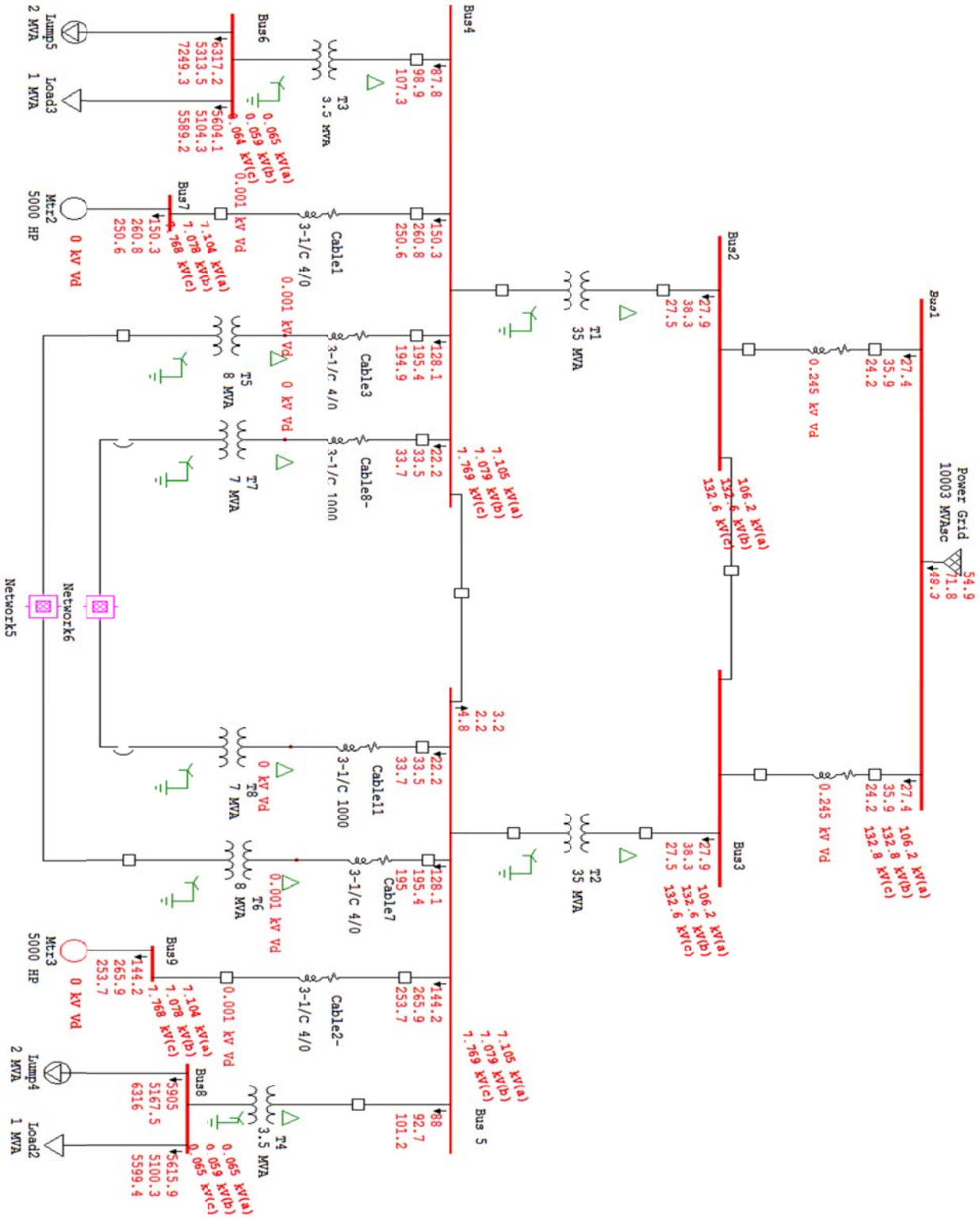

Figure 4.6 Source voltage asymmetry - Transformer configuration – all D/yn

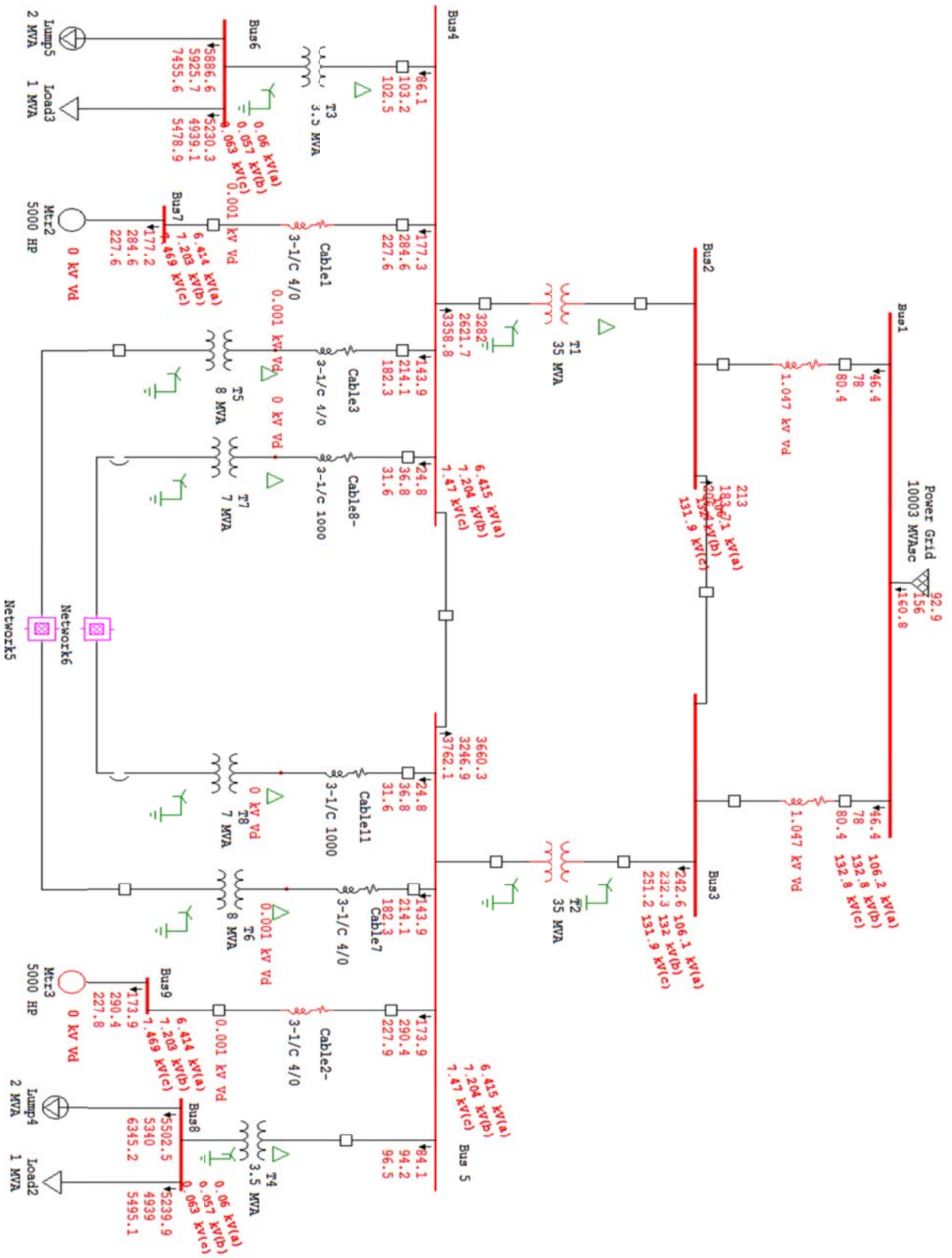

Figure 4.7 Source voltage asymmetry - Transformer configuration - (T2) YN/yn.

4.2 Influence of Different Sources of Asymmetry

The influence of different sources will be investigated using the following cases:

- In case 3, lump7 load, in network 6, has a single-phase unbalance parameter simulated as shown in figure 4.8.

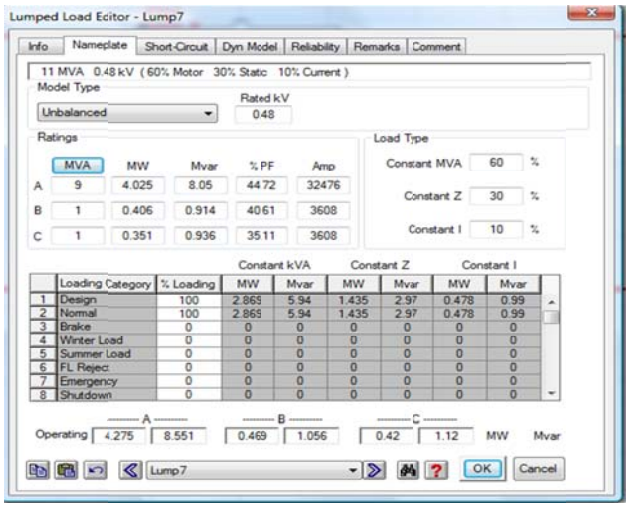

Figure 4.8 Parameters of lump7 load in network 6

- In case 4, there is a simulation of two sources of asymmetry. The sources are; the percent magnitude of phase A of the source is 90% and the condition of case 3.

Case 3: The only source of unbalance is due to the single-phase unbalance in lump7 load in network 6. Where phase A is heavily loaded in comparison to the other phases. Figure 4.9 shows the propagation of the sequence components from downstream LV to upstream HV. According to the Newton-Raphson current injection method use by ETAP, the negative sequence current propagates through the system resulting in a source current asymmetry of phase-A = 57A, phase-B = 83.6A and phase-C = 98.8A. The negative sequence component spread in the system in proportion to the respective system characteristic as shown in figure 4.9 and in more details by the data in the critical and unbalance load flow report in appendix B.

Case 4: According to the ETAP calculation the negative sequence component of the different sources are added vectorially at the point of common connection. This is evident by the

data in the critical report in appendix B which shows that when case 3 and 4 was compared, there is an increase in the respective sequence components. For example for case 3 the following values were obtained: max VUF2=7.5% and min VUF2 =2% and max IUF2=73% while min IUF2 = 5.6%. Now for case 4, max VUF2 increase to 7.8% and min VUF2 increase to 2.7% while max IUF2 increase to 74% and min IUF2 increase to 3.7%. The other increases are shown in the critical report in appendix B. Therefore, according to the current injection method used by the ETAP simulation there is a vectorial addition of the source's (grid) asymmetry and the asymmetry caused by the lump7 load in network 6. Figure 4.10 and the critical and unbalance load flow report in appendix B provides more individual and system details of the systematic propagation of the sequence component due to different source of asymmetry in the power system.

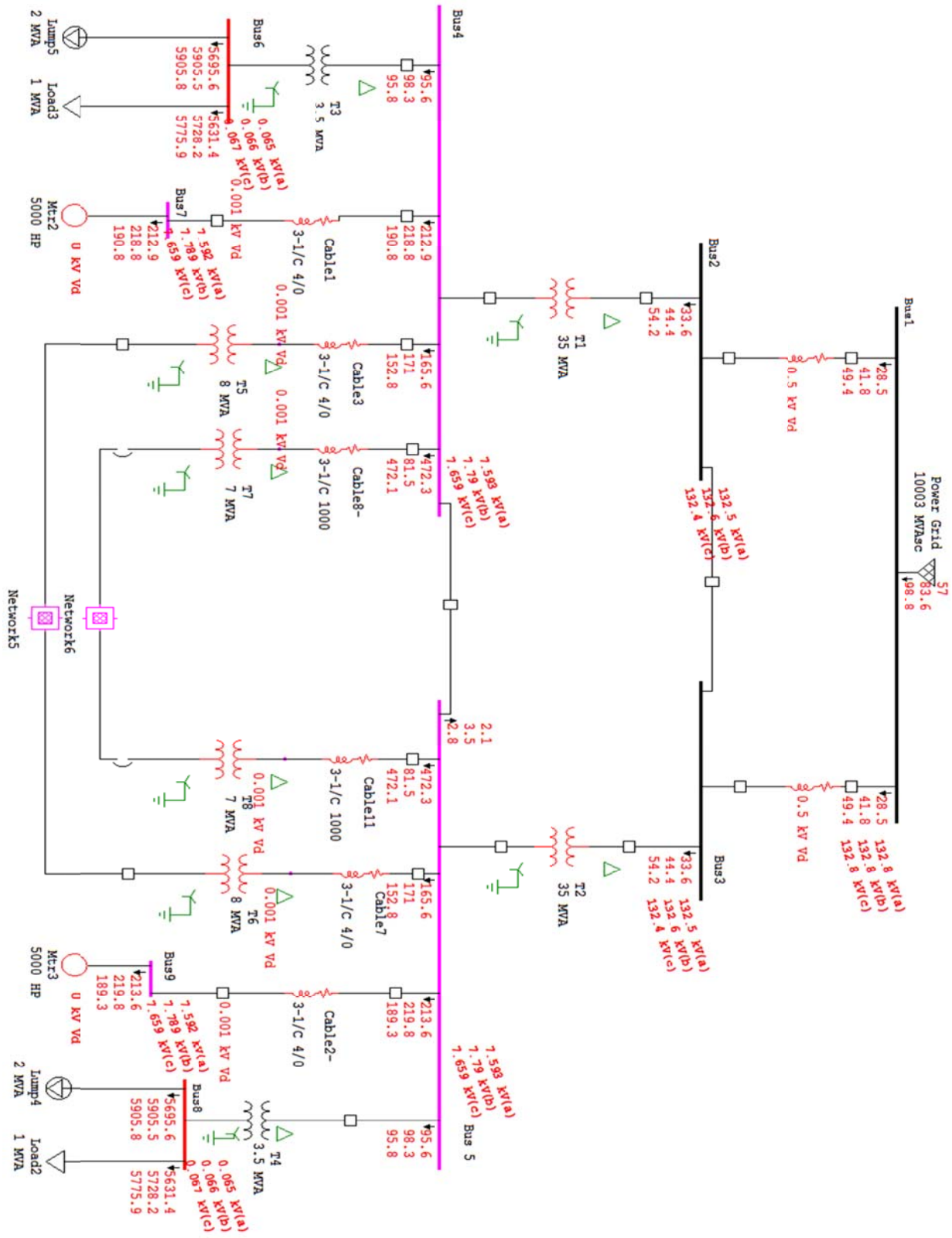

Figure 4.9 Propagation of sequence component from LV to HV

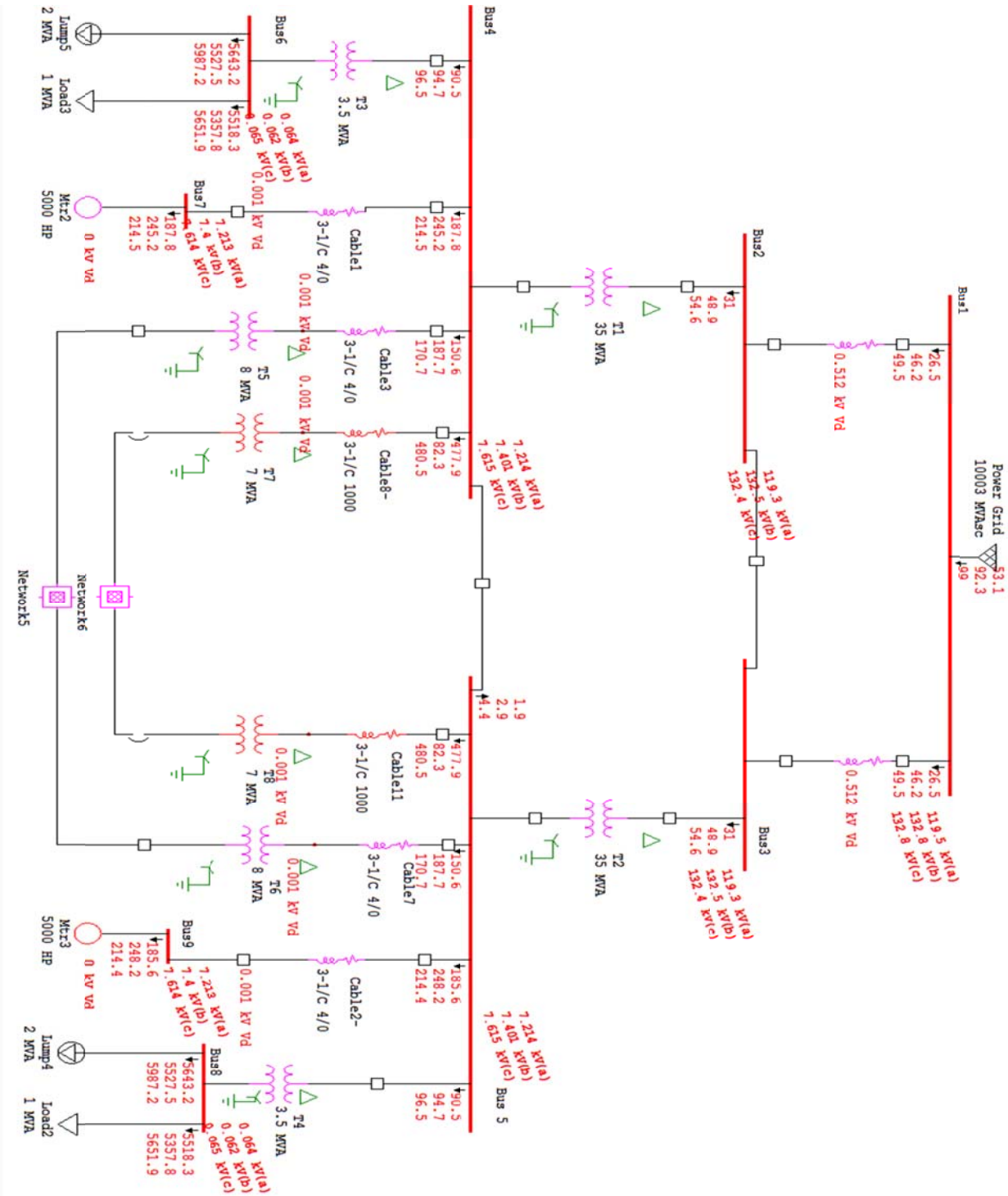

Figure 4.10 Source asymmetry and load unbalance simulation

CHAPTER 5

REDUCTION OF CURRENT AND VOLTAGE ASYMMETRY

There are a few approaches to the reduction of asymmetry in voltages and currents. These approaches are categorized in levels based on the source of the asymmetry and the most efficient and cost effective way of reduction.

Asymmetry can be confined or reduced by the following approaches:

1. Imposing regulation and standards with respect to:
   1.1 Equipment and transmission line construction.
   1.2 Adopting standards on acceptable levels of current and voltage asymmetry.
2. Structural modifications of single-phase loads – on both utility and customer sides.
3. Single-phase voltage regulators.
4. Balancing compensators.

5.1 Imposing Regulation and Standards

5.1.1 Equipment and Transmission Line Construction

Imposing regulation and standards with respect to equipment and transmission line design will provide a systematic and cost effective way of mitigating asymmetry in the power system. This initial stage of asymmetry reduction ensure that generators, transmission lines, transformers, switching equipment and three-phase motors are designed and manufactured to be symmetrical. For example, the impedance in each phase of the generator and motor is equal and symmetrical with respect to each other. Transmission and distribution lines are spaced and transposed to mitigate asymmetry. A detailed analysis and mitigation approach for reducing current asymmetry due to induction in heavily loaded multi-circuit power lines is presented in ref. [3].

5.1.2 Adopting Standards on Acceptable Levels of Current and Voltage Asymmetry

NEMA, IEEE and CIGRE/CIRED JWG C4.103 perform research and analysis to create standards for current and voltage asymmetry in the power system. When these standards are selected as the acceptable level of current and voltage asymmetry, fines can be impose on the respective entities to reduce asymmetry. For instance, fines can be imposed on utility and customers to keep asymmetry within the standard levels. Therefore, utilities are required to supply reliable power to customers and they are not allowed to have an asymmetric level beyond the level stipulated by the standards. Similarly, customers are not allowed to create asymmetry beyond the stipulated levels.

5.2 Structural Modifications of Single-Phase Loads

One of the main objectives of asymmetry mitigation is to use the most effective method of reduction in a cost effective way. Structural arrangement is one of those cost effective ways. For instance, the rearranging or redistributing of all single-phase loads equally among all the three phases can mitigate asymmetry. This refers to the distribution of the supply to individual homes or alternating connections in row of houses in residential subdivisions, per floor supply in commercial buildings or street lights. Also by arranging the connection phases between the distribution transformers and the primary feeder, the level of asymmetry can be reduced ref. [59]. For traction loads, the load scheduling of the trains in addition to the use of special transformers can improve the balance between the phases of the three-phase system. For instance, since the traction system is a large single phase load the scheduling in relation with other traction system is implemented in such a way that the loading on the three-phase system is balanced.

5.2.1 Traction System Transformer Connections Schemes.

1. V- connection
2. Single-phase connection

3. Scott transformers
4. Leblanc transformers
5. Steinmetz-transformer

Each scheme is discussed below and a simplified connection diagram showing the application for some of these schemes.

1. The schemes have different efficiency levels in asymmetry reduction. However, they can be selected based on the investment, operation and maintenance cost ref. [58]. For example, even though the V-connection is a source of asymmetry, according to ref. [58] the single-phase connection and the V-connection schemes are the most economical mitigation technique. This is because the V-connection has a high capacity utilization ratio and a simple structure. Also the V-connection scheme is more efficient when compared with the single-phase scheme. Reference [79] and [83] have compiled various comparison of transformers used in the electrified traction system.
2. Single–phase connection. In this arrangement the single transformer is feed with two phases. One of the output phases is connected to the catenary that supplies the train while the other is connected to the rails as the return current path as shown in figure 5.1. Therefore with this arrangement each of the different phases of the three-phase system can be balance by systematically distributing the phase connection base on the loading.

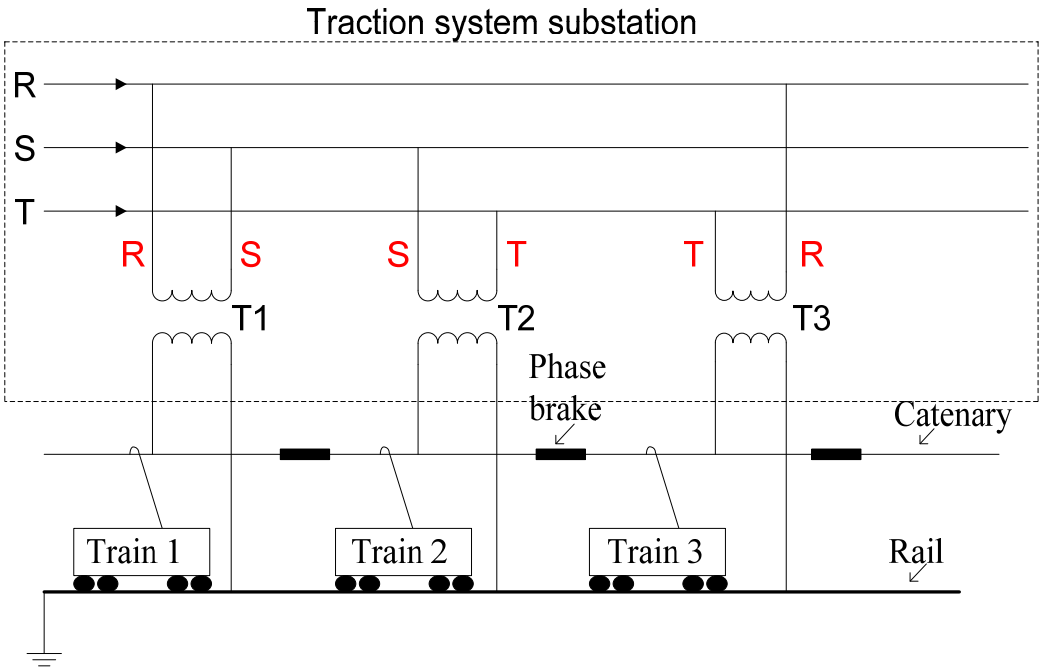

Figure 5.1 Single phase transformer connection of the traction load

3. The Scott transformer is two single phase transformers consisting of special winding ratios, which is connected to the three phase system as shown in figure 5.2. The connection is such that the output, which is a two-phase orthogonal voltage system, will provide connection of two single-phase systems. This configuration will mitigate the asymmetry in the system and with the addition of equal loading of the transformers can further reduce the asymmetry to approximately zero.

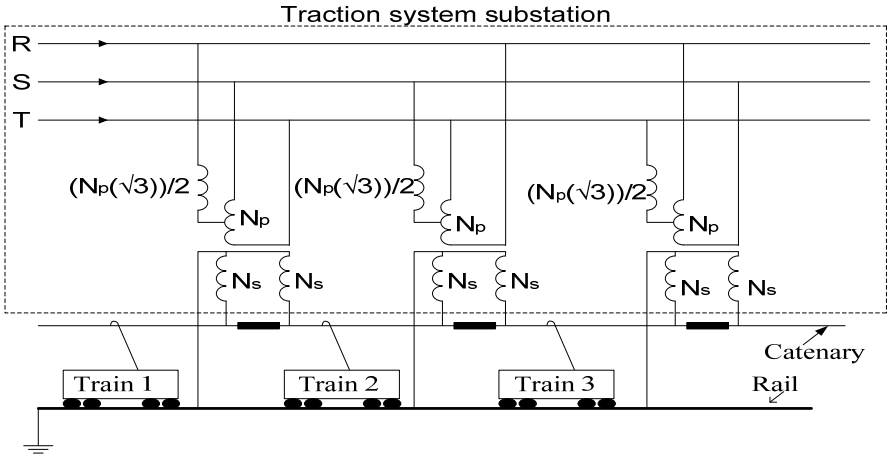

Figure 5.2 Scott transformer connection for traction load

4. Leblanc transformer

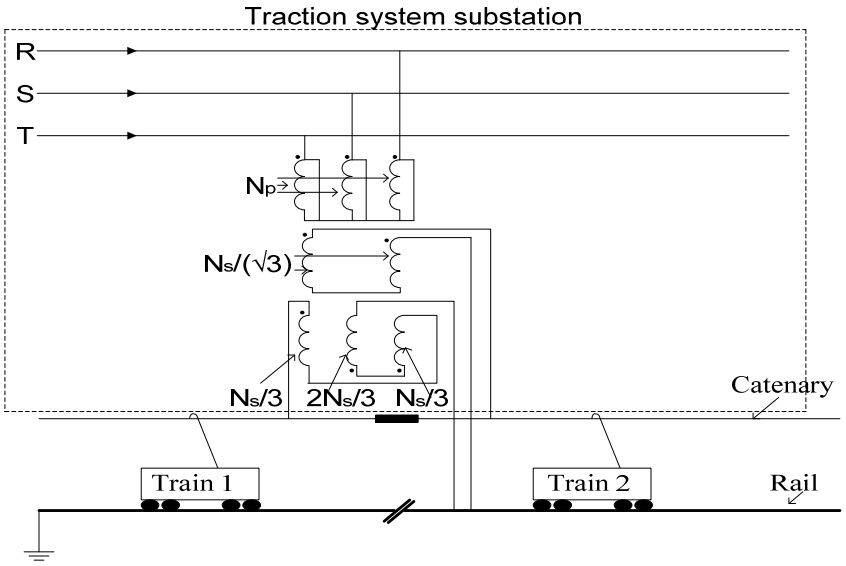

Figure 5.3 Leblanc transformer connection for traction load

5. According to ref. [14] the Steinmetz transformer is a three-phase transformer that is designed with a power balancing load feature. This consists of a capacitor and an inductor that is rated in such a way that the proportionality to the traction load will produce a balanced system.

For example:

When $Q_L + Q_C = \frac{mag.\ P}{\sqrt{3}}$, The three-phase supply sees a balanced load.

Where, Q_L is the reactive power of the inductor, Q_C is the reactive power of the capacitor and P is the active power of the load.

However, ref. [14] further states that the following condition must be realized if effective balancing is to be achieved: The three-phase rated power of the transformer must be equal to the active power of the single-phase load.

When structural modifications are not sufficient for reduction of asymmetry to a level impose by standards, some equipment which enables reducing of this asymmetry can be used. These include:

- Single-phase voltage regulators.
- Balancing compensators.

5.3 Single-Phase Voltage Regulators

Single-phase regulators are used to increase or decrease the voltage in each phase of a three-phase system, in such a way that symmetry is achieved. However, care must be exercised to ensure that they are controlled carefully not to increase asymmetry.

5.4 Balancing Compensators

This can be built as reactance devices or as switching compensators. There are some situations in which shunt switching compensators and reactance devices are the best mitigation techniques to use. For example, if the current asymmetry is caused by an arc furnace then a shunt switching compensator can be used. Shunt switching compensator not only mitigate current asymmetry but it also mitigate reactance current, harmonics and any other quantities that degrade supply and loading quality. Also if the current asymmetry is caused in an industrial environment where large single-phase fixed parameter loads cannot be reconfigured to obtain balance then a reactance balancing compensator can be used. However if the voltage asymmetry is caused by the source then a series compensator could be used to mitigate the voltage asymmetry. If it is from both then a hybrid (series and shunt compensator) can be used to mitigate the asymmetry.

The mitigation technique used must be selected meticulously. The first thing that needs to be done when considering the mitigation technique for use is to choose the correct power theory that correctly represents the phenomenon been mitigated. Therefore, the CPC power theory will be used to analyze the compensation technique used to reduce the current and voltage asymmetric effect on the power system [49]. The second thing is to ensure that the source/s of the asymmetry is clearly identified in the particular system. For example in some case by reducing current asymmetry you also reduce voltage asymmetry. While in other cases such as the

occurrence of both the supply voltage asymmetry caused by structural imbalance and the current asymmetry caused by load imbalance, this is not the case [56]. Third, it is imperative that the type of load (fixed or varying) causing the permanent asymmetry be identified. Finally the compensation method is chosen base on the three cases mentioned above.

5.4.1 Reactance Balancing Compensator

According to the CPC power theory, the current is one of the primary components of power which can be decomposed into three mutually orthogonal currents, i_a – active current, i_r – reactive current and i_u – unbalance current. As a result there exist three powers, active power (P) reactive power (Q) and unbalance power (D). Therefore $S^2 = P^2 + Q^2 + D^2$ and the objective of the compensator is to eliminate or mitigate D (i_u) and Q (i_r).

According to ref. [49]:

$$i_{rc} = \sqrt{2}Re[j\{B_e + (T_{ST} + T_{TR} + T_{RS})\}\boldsymbol{U}]e^{j\omega t} \quad \text{.....5.1.1a}$$

is reduced to zero when

$$B_e + (T_{ST} + T_{TR} + T_{RS}) = 0 \quad \text{.....5.1.1b}$$

also at the same time

$$i_{uc} = \sqrt{2}Re[[A - j(T_{ST} + \alpha T_{TR} + \alpha^* T_{RS})]\boldsymbol{U}^{\#}]e^{j\omega t} \quad \text{.....5.1.1c}$$

is reduced to zero when

$$A - j(T_{ST} + \alpha T_{TR} + \alpha^* T_{RS}) = 0 \quad \text{.....5.1.1d}$$

As a result the solution for calculating the admittances between the relevant phases is as follows:

$$T_{RS} = (\sqrt{3}ReA - ImA - B_e)/3 \quad \text{.....5.1.1e}$$

$$T_{ST} = (2ImA - B_e)/3 \quad \text{.....5.1.1f}$$

$$T_{TR} = (-\sqrt{3}ReA - ImA - B_e)/3 \quad \text{.....5.1.1g}$$

The following is a numerical example illustrating how current asymmetry can be compensated using reactance elements in a sinusoidal system:

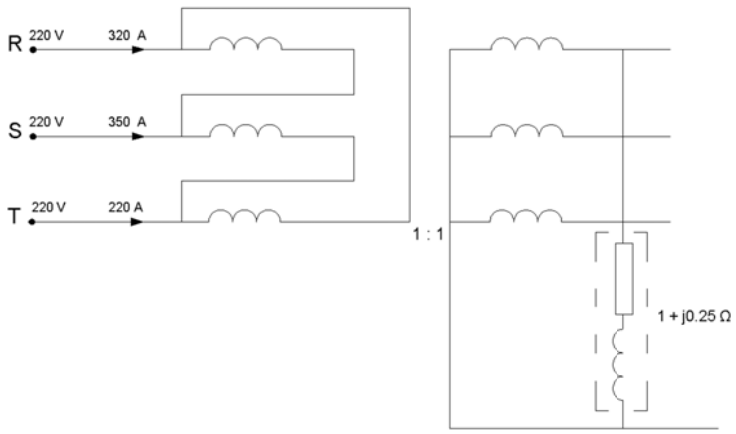

Figure 5.4 Symmetrical and sinusoidal supply feeding an imbalance load

$$\left||i|\right| = \sqrt{320^2 + 350^2 + 220^2} = 522.78A$$

$$||u|| = \sqrt{3} * 220 = 381V$$

$$Y_e = G_e + jB_e = Y_{RS} = \frac{1}{Z_R}$$

$$Y_{RS} = \frac{1}{1 + j0.25} = 0.94 - j0.24\ S = 0.97e^{-j14.32}S$$

$$A = -\alpha^* Y_{RS} = 0.97e^{j45.68}\ S$$

$$\left||i_a|\right| = G_e * ||u||$$

= 0.94 * 381

= 358.14 A

$$\left||i_u|\right| = A * ||u||$$

= 0.97 * 381

= 369.57 A

$$\left||i_r|\right| = B_e * ||u||$$

= 0.24 * 381

= 91.44 A

S = 381*522.78

= 199.18KVA

P = 358.14*381

= 136.45KW

Q = 381*91.44

= 34.84KVAR

$$D_u = 381 * 369.57$$

= 140.81KVA

$$T_{RS} = \frac{\left(\sqrt{3}Re(A) - Im(A) - B_e\right)}{3}$$

= 0.24 S

$$T_{ST} = \frac{(2 * Im(A) - B_e)}{3}$$

= 0.54 S

$$T_{TR} = \frac{\left(-\sqrt{3}Re(A) - Im(A) - B_e\right)}{3}$$

= - 0.54 S

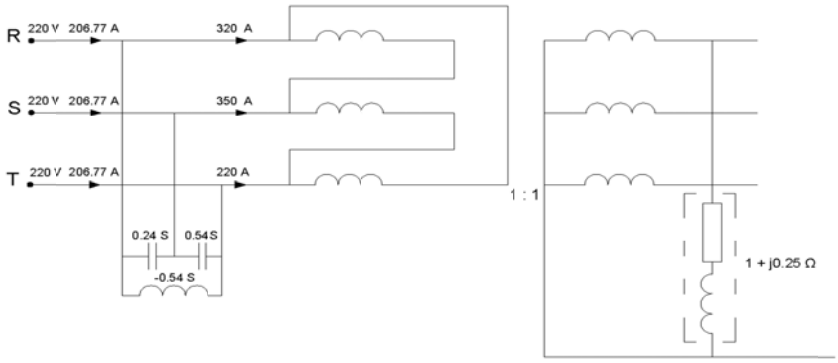

Figure 5.5 Compensation topology for imbalance load

$||i_a||$ = 358.14 A

$||i_u||$ = 0 A

$||i_r||$ = 0 A

$$||i|| = 358.14 \text{ A}$$

$$S = 136.45KW$$

However in the real power system there is harmonics present and therefore the following modification has to be adopted. The method of network synthesis has to be implemented as shown in the example below. The network topology which is created can have many different arrangement and values. A full detail description of the process of calculating this topology is provided in appendix C.

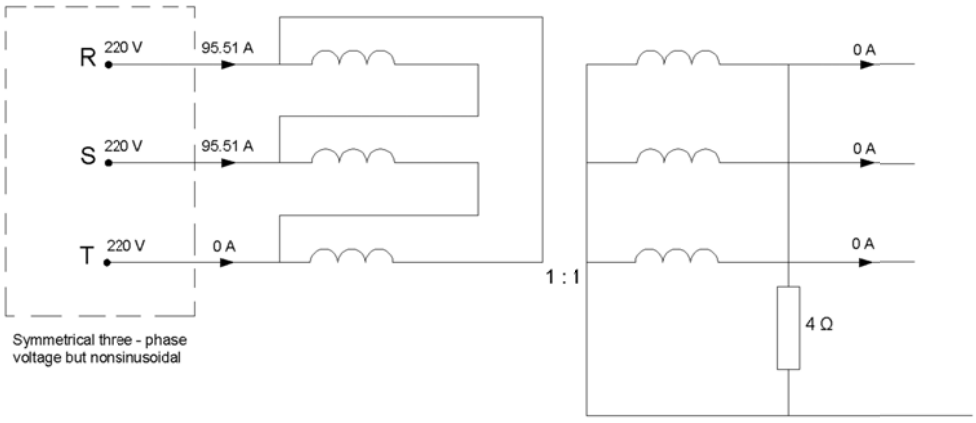

Figure 5.6 Symmetrical and non-sinusoidal supply feeding an imbalance load

$$u_1 = 220V$$

$$u_5 = 6\% * u_1 = 13.2V$$

$$||u|| = \sqrt{3 * 220^2 + 3 * 13.2^2} = 381.74V$$

$$Y_e = G_e + jB_e = Y_{RS} = \frac{1}{Z_R}$$

$$Y_{RS} = \frac{1}{4} = 0.25\ S$$

$$A = -\alpha^* Y_{RS} = 0.25e^{j60}\ S$$

$$\left||i_a|\right| = G_e * ||u||$$

$$= 0.25 * 381.74$$

= 95.43 A

$$\left||i_u|\right| = A * ||u||$$

= 0.25 * 381.74

= 95.43 A

$$||i||=\sqrt{95.43^2 + 95.43^2} = 134.96\ A$$

S = 381.74*134.96 = 51.52 KVA

P = 95.43*381.74 = 36.43 KW

$$\lambda = \frac{P}{S} = 0.71$$

$$T_{ST1} = \frac{(2 * (0.2165) - 0)}{3} = 0.1443\ S$$

$$T_{RS5} = -0.1443\ S$$

$$T_{TR1} = \frac{-\left(-1 * \sqrt{3}Re(A) - Im(A) - B_e\right)}{3} = -0.1443\ S$$

$$T_{TR5} = 0.1443\ S$$

$$Y(s) = A * \frac{(sz^2 + z^2)}{s}$$

$$= \mathrm{A}s + \frac{1}{s * \frac{1}{\mathrm{A} * z^2}}$$

$$= s\mathrm{C} + \frac{1}{s\mathrm{L}}$$

$$-j0.1443 = A * \frac{(j1)^2 + z^2}{j1}$$

$$j0.1443 = A * \frac{(j5)^2 + z^2}{j5}$$

$$z = \sqrt{\frac{-0.722 - 3.608}{-26}} = 0.408$$

$$A = -(0.1443 - 0.408^2) = 0.022$$

C = A = 0.022F

$$L = \frac{1}{A*z^2} = 273.059H$$

The individual compensation for each harmonic is not achievable and therefore the minimization of the unbalanced and reactive current is obtained using the following technique: Assuming that the frequency is normalize to $\omega_1 = 1\frac{rad}{s}$ and the resonant frequency of the LC branch is $\omega_r = 2.5\omega_1$. Then the parameters of the minimized compensator are:

$$C_{STopt} = \left[1 - \frac{{\omega_1}^2}{{\omega_r}^2}\right]\frac{T_{ST1}}{\omega_1} = 120.96mF$$

$$L_{ST} = \frac{1}{\omega_r^2 C_{STopt}} = 1.323H$$

$$L_{TRopt} = -\frac{1}{\omega_1 T_{ST1}} = 6.94H$$

5.4.2 Shunt Switching Compensator

Shunt switching compensators shape the current via the sequential switching of the transistors. Figure 5.7 below represents a shunt switching compensator. Let's say the supply is balanced but supplying an imbalance load such as a traction system or arc furnace, for example. The data acquisition system (DA) will take samples of the load voltage and current. This information is fed into a DSP (Digital Signal Processing) system which will perform FFT which will produce a current reference signal base on the CPC power theory. This signal is fed into the inverter switching control (ISC). The instruction of the ISC will cause the IGBT to switch in sequence which will shape the current in such a way that it will compensate the current asymmetry. The details are explained in appendix D. However, in general this system is a current control device because the current is control directly by switching and the voltage is indirectly affected in achieving compensation.

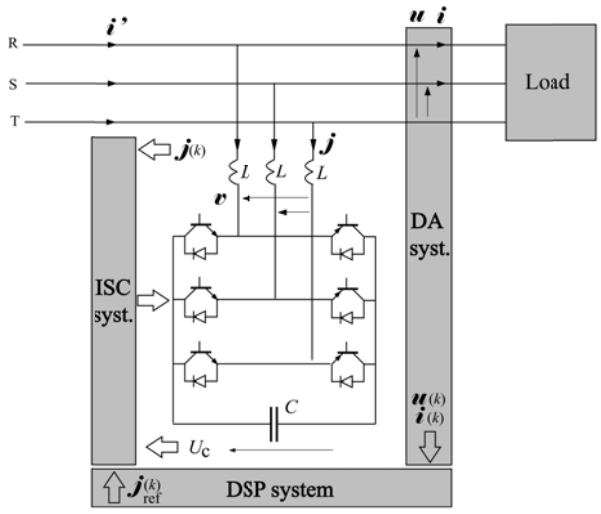

Figure 5.7 Structure of a three-phase system with shunt switching compensator.

The following formulas illustrate this principle mathematically:

$$\mathbf{U} = \begin{bmatrix} U_R \\ U_S \\ U_T \end{bmatrix}, \quad \boldsymbol{U}^{\#} = \begin{bmatrix} U_R \\ U_T \\ U_S \end{bmatrix}$$

$$\boldsymbol{A} = -(Y_{ST} + \alpha Y_{TR} + \alpha^{*} Y_{RS}) = \mathrm{A}e^{\mathrm{J}\Psi}\mathrm{S}$$

$$\boldsymbol{J_{1u}} = -\sqrt{2}Re(\boldsymbol{A U^{\#} e^{J\omega t}})\ \mathrm{A}$$

Using Clarke Transform:

Where $\boldsymbol{U_R} = \sqrt{2}U_R \cos(\omega_1 t + \alpha_R)\mathrm{V}$, $\boldsymbol{U_S} = \sqrt{2}U_R \cos(\omega_1 t + \alpha_R + \frac{2\pi}{3})\mathrm{V}$

$$\boldsymbol{J_{1u}^{C}(t)} = \begin{bmatrix} J_{1u\alpha}(t) \\ J_{1u\beta}(t) \end{bmatrix} = \boldsymbol{C}\begin{bmatrix} J_{1uR}(t) \\ J_{1uS}(t) \end{bmatrix} = -\sqrt{2}U_R \begin{bmatrix} \sqrt{\frac{3}{2}} & 0 \\ \frac{1}{\sqrt{2}} & \sqrt{2} \end{bmatrix} \begin{bmatrix} \cos(\omega_1 t + \alpha_R + \psi) \\ \cos(\omega_1 t + \alpha_R + \psi + \frac{2\pi}{3}) \end{bmatrix} \mathrm{A}$$

$$\boldsymbol{J_{1u}^{C}(t)} = -\sqrt{3}AU_R[\cos(\omega_1 t + \alpha_R + \psi) - j\sin(\omega_1 t + \alpha_R + \psi)] = -\sqrt{3}\boldsymbol{A U_R e^{-j\omega t}}\mathrm{A}$$

$$= -\boldsymbol{U^{C} A e^{-j\omega t}}\mathrm{A}$$

As a result of this the following voltage drop on the inductor occur:

$$\Delta U_{1u}^{C}(\mathrm{t}) = \mathrm{L}\frac{d}{dt}\boldsymbol{J_{1u}^{C}(t)} = -\mathbf{j}\omega_1 L \boldsymbol{J_{1u}^{C} e^{-j\omega t}}\ \mathbf{V}$$

Therefore, $V^C(t) = \boldsymbol{U^C e^{j\omega t}} \mp \Delta \boldsymbol{U^C e^{-j\omega t}}$ **V**, because of the rotation of vectors $\boldsymbol{U^C}$ and $\Delta \boldsymbol{U^C}$ in the opposite direction in certain instance of time.

Since the DSP system does not function on continuous voltage *U*(t) and reference current *J*(t), then the DA provide there discrete values at time instance $t_k = kT_s$, where T_s is the sampling period of the DA system.

U(k) = $U(kT_s)$

J(k) = $J(kT_s)$

CHAPTER 6

SUMMARY AND CONCLUSION

6.1 Summary

Generators: If the source of asymmetry is due to structural imbalance, then the terminal voltage of the generator will be asymmetric. This can be reduced by designing the generator as symmetric as financially possible. However if the source of asymmetry is due to imbalance loading, then a negative sequence current creates a rotating magnetic field in the air gap that rotates at angular speed of $2\omega_1$ with respect to the rotor frequency. This will cause the following:

- An induces voltage $e(t) = 2\omega_1 N\Phi_m \sin 2\omega_1 t$ in the rotor. This causes a rotor current which contribute to an increase in active power losses on the rotor resistance. This increases the temperature on the rotor and consequently the generator temperature increases.
- It contributes to a torque that pulsates at twice the supply frequency and causes mechanical vibration.
- It causes terminal voltage asymmetry.

This can be rectified by balancing the single phase loading and/or use shunt switching compensators.

Motors: The negative effects on motors are similar to that on generators. However the main source of asymmetry is voltage asymmetry. The following is a list of the negative effect of voltage asymmetry on the motor:

- According to NEMA a 1% voltage asymmetry causes a 6-10% increase in the current asymmetry. This is because the negative sequence impedance of an induction motor is smaller than the positive sequence impedance.

- The negative sequence voltage causes a negative sequence current that creates a reverse rotating magnetic field in the air gap. The current sequence components are a function of the voltage asymmetry, the motor parameters and the slip.
- It increases losses and by extension increase temperature which leads to reduced life-expectation.

The sequence of events is as follows:

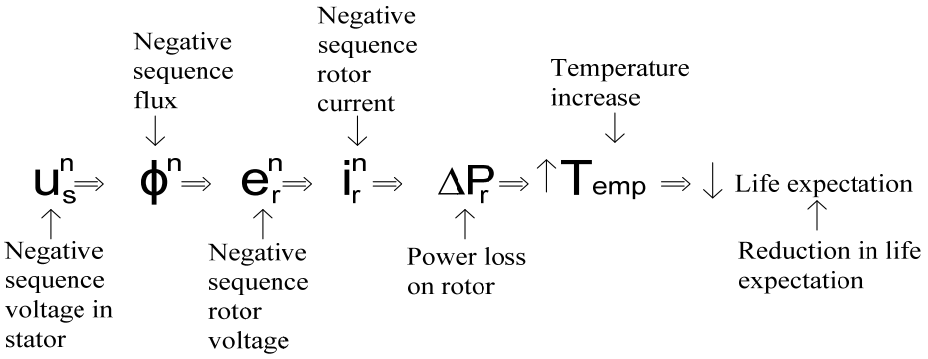

- It causes torque pulsation and reduction, increased vibration and mechanical stresses.
- It reduces motor efficiency and increases cost of production in the industry.

When the source of the asymmetry is clearly identified, if it cannot be reduce by imposing regulation and standards or ensuring that the system is structurally symmetric, then the impact can be reduced by derating the motor according to NEMA derating curve or use series switching compensation. A similar process can be adopted for the ASD system.

Adjustable Speed Drive: The supply voltage asymmetry impedes the performance of the ASD. The voltage asymmetry affects three main areas of the ASD: the rectifier, DC link and the PWM inverter.

- The supply voltage asymmetry causes asymmetrical current harmonics of the 3rd and 9th order. This increases the temperature of the rectifier diodes.
- There is an increase in voltage ripples on the DC-bus.

- It generates harmonics on the induction motor terminal.
- It causes ripple torque in the induction motor via the pulse width modulator inverter (PWM).

Transmission and Distribution Lines: The capacity of the lines is reduced if they are exposed to voltage and current asymmetry. However by transposing the phases the asymmetry can be reduced.

Transformers: Positive and negative sequence components affects the transformer in the same way. However, the zero sequence components affect the transformer in a different way. For instance, if the configuration is a delta/yn then the zero sequence current circulate in it and produce heat and losses.

6.2 Conclusion

The economic benefits of energy providers and users is strongly dependent on the supply reliability, security and efficiency of the power system and consequently, on the supply and loading quality. Current and voltage asymmetry is an inherent phenomenon in the power system that causes loading and supply quality degradation. However, it is not economically practical to totally eliminate asymmetry. However it can be mitigated to an economically justified level by making informed trade-offs. The data base provided in this thesis can be used for this purpose. This is why it is important to be aware of the negative impacts, the source of the negative impact and how it propagates in the system. Then, finally the most economical solution can be implemented.

There are several technical solutions available for reducing asymmetry. However, when using compensators, the correct power theory must be used in designing the mitigation techniques and therefore the CPC power theory should be used.

REFERENCES

[1] R. Escarela-Perez, S. V. Kulkarni, J. Alvarez-Ramirez and K. Kaushik, Analytical Description of the Load-Loss Asymmetry Phenomenon in Three-Phase Three-Limb Transformers, IEEE Transactions on Power Delivery, Vol. 24, No. 2, pp. 695-702, 2009.

[2] Z. Emin and D.S. Crisford "Negative Phase-Sequence Voltages on E&W Transmission System" IEEE Transaction on Power Delivery, Vol. 21, No. 3, pp. 1607-1612, July 2006.

[3] Jinxi Ma; Fortin, S.; Dawalibi, F.P, "Analysis and Mitigation of Current Unbalance Due to Induction in Heavily Loaded Multicircuit Power Lines", IEEE Transactions on Power Delivery, Vol. 19 , No. 3,pp. 1378 – 1383, 2004.

[4] J.M. Guerrero, L.G. de Vicuna, J. Matas, M. Castilla, J. Miret, "A wireless controller to enhance dynamic performance of parallel inverters in distributed generation systems", IEEE Trans. On Power Electronics, Vol. 19, No. 5, pp. 1205-1213, 2004.

[5] E. I. King and J. W. Batchelor "Effects of Unbalance Current on Turbine-Generator" IEEE Transaction on Power Apparatus and Systems, Vol. 84, No. 2, Feb. 1965.

[6] R. F. Woll "Effect of Unbalance Voltage on the Operation of Polyphase Induction Motors" IEEE Transactions on Inductry Applications, Vol. IA-II, No. 1, January/February 1975.

[7] Solanics, P.; Kozminski, K.; Bajpai, M.; Esztergalyos, J.; Fennell, E.; Gardell, J.; Mozina, C.; Patel, S.; Pierce, A.; Skendzic, V.; Waudby, P.; Williams, J."The Impact of Large Steel Mill Loads on Power Generating Units" IEEE Transactions on Power Delivery, Vol. 15, NO. 1, pp. 24-30, 2000.

[8] M.C. Chandorkar, D. M. Divan, R. Adapa, Control of parallel connected inverters in standalone AC supply systems, IEEE Trans. On Industry Applications, Vol. 29, No. 1, pp. 136-143, 1993.

[9] R.T. Jagaduri, G. Radman, Modeling and control of distributed generation systems including PEM fuel cell and gas turbine,

[10] M. Chindris, A. Cziker, Anca Miron, H.Bălan, A. Sudria "Propagation of Unbalance in Electric Power Systems" 9th International Conference –Electrical Power Quality and Utilisation, Barcelona, 9-11 October 2007.

[11] V.J. Gosbell, Sarath Perera, "Voltage Unbalance" Technical Note No. 6 October 2002

[12] B.R.Lakshmikantha, Dr Murugesh Mudaliar, Dr K.Balaraman, Dr R.Nagaraja "Mitigation of Voltage Unbalance in Traction System" Proceedings of the World Congress on Engineering and Computer Science 2008 WCECS 2008, October 22 – 24, 2008, San Francisco, USA.

[13] Farhad Shahnia, Rasoul Esmaeilzadeh "voltage unbalance problems and solutions for electrified railway systems" http://ezepdico.ir/papers/shahnia/railway-%20unbalance-%20eng-%20poland.pdf

[14] Dr Johan Driesen, Dr Thierry Van Craenenbroeck, "Voltage Disturbances Introduction to Unbalance" Power quality application guide Katholieke Universiteit Leuven May 2002.

[15] E. Muljadi, Senior Member, IEEE, T. Batan, Student Member, IEEE D. Yildirim, Student Member , IEEE C. P. Butterfield, Member, IEEE "Understanding the Unbalanced-Voltage Problem in Wind Turbine Generation" Presented at the 1999 IEEE Industry Applications Society Annual MeetingPhoenix, Arizona October 3-7, 1999

[16] K.V. Vamsi Krishna, "Effects of unbalance voltage on induction motor current and its operation performance" Lecon Systems

[17] Quality Energy "Eliminate Unbalanced Voltages-Take Action" www.quality-energy.com/PDF/Motor**UnbalancedVoltages**.pdf

[18] Annette von Jouanne, Senior Member, IEEE and Basudeb (Ben) Banerjee, Member, IEEE "Assessment of Voltage Unbalance" IEEE TRANSACTIONS ON POWER DELIVERY, VOL. 16, NO. 4, OCTOBER 2001

[19] Signature – A Power Quality Newsletter Spring 1996, Volume 6, Number 2

[20] Antonio Silva ABB Power T&D Company Inc. Raleigh NC Lars Hultqvist and Aleksander Wilk-Wilczynski ABB Power Systems AB Västerås Sweden "steel plant performance, power supply system design and power quality aspects"

[21] Dr. W. Z. Gandhare and D. D. Lulekar "Analyzing Electric Power Quality in Arc Furnaces" http://www.icrepq.com/icrepq07/272-gandhare.pdf

[22] Asheesh Kumar Singha, G. K. Singhb,R. Mitra "Impact of Source Voltage Unbalance on AC-DC Rectifier Performance" 2006 2nd International Conference on Power Electronics Systems and Applications

[23] ABB Distribution Transformer Guide, Revised March, 2002

[24] Ewald F. Fuchs, Fellow, IEEE, and Yiming You "Measeurement of λ-i Characteristics of Asymmetric Three—Phase Transformers and Their Applications" IEEE Transaction on Power Delivery, VOL 17, NO.4, October 2002.

[25] R. Escarela-Perez, Senior Member, IEEE, S. V. Kulkarni, Member, IEEE, J. Alavarez-Ramirez, and K. Kaushik, Student Member, IEEE, "Analytical Description of the Load-Loss Asymmetry Phenomenon in Three-Phase Three-Limb Transformers" IEEE Transactions on Power Delivery, Vol 24, No. 2, April 2009

[26] M. Harry Hesse, Senior Member, IEEE "Circulating Current in Paralleled Untransposed Multicircuit Lines: I-Numerical Evaluations" IEEE Transactions on Power Apparatus and Systems Vol. Pas-85, No. 7 July1966

[27] M. Harry Hesse, Senior Member, IEEE "Circulating Current in Paralleled Untransposed Multicircuit Lines: II-Methods for Estimating Current Unbalance" IEEE Transactions on Power Apparatus and Systems Vol. Pas-85, No. 7 July1966

[28] M. Harry Hesse, Senior Member, IEEE "Simplified approach for estimating current unbalances in e.h.v loop circuits" PROC. IEE, Vol.119, No. 11 November 1972

[29] Hesse, M.H.; Sabath, J,"EHV Double-Circuit Untransposed Transmission Line-Analysis and Tests" IEEE Transactions on Power Apparatus and Systems, Vol. PAS-90 , No. 3, pp. 984 – 992, 1971

[30] W.H Kersting, "Causes and Effects of Unbalanced Voltages Serving and Induction Motor" IEEE Transactions on Industry Applications, Vol. 37, No. 1, pp. 165 – 170, 2001

[31] Pradhakar Neti, Sudhasis Nandi, "Analysis and Modeling on a Synchronous Machine with Structural Asymmetries" CCECE '06. Canadian Conference on Electrical and Computer Engineering, 2006, pp. 1236 – 1239, 2006

[32] IEEE Standard Board "IEEE Recommended Practice for Electric Power Distribution for Industrial Plants(Red Book)" December 2, 1993

[33] "IEEE Recommended Practice for Electric Power Systems in Commercial Buildings" (Gray Book).

[34] R.J. Hill 'Electric railway traction" Part 3 Traction power supplies

[35] Antonio Silva, Lars Hultqvist, Aleksander Wilk-Wilczynski "STEEL PLANT PERFORMANCE, POWER SUPPLY SYSTEM DESIGN AND POWER QUALITY ASPECTS" 54th ELECTRIC FURNACE CONFERENCE – Dec. 96.

[36] CMP Techcommentary "Understanding Electric Arc Furnace Operations For Steel Production" Vol. 3, No. 2, 1987

[37] World Steel Association. http://www.steeluniversity.org/content/html/eng/default.asp?catid=25&pageid=2081271929

[38] Janusz Bialek, Andrzej Wasowski "Advantages of changing 3-phase arc furnaces asymmetry estimation criteria in international and European standards" Electrical Power Quality and Utilisation, Journal Vol. XI, No. 1, 2005

[39] Luis F. Ochoa, Rade M. Ciric, A. Padilha-Feltrin, Gareth P. Harrison "Evaluation of Distribution System Losses Due to Load Unbalance" 15th PSCC, session 10, paper 6, August 2005.

[40] Asheesh Kumar Singh, G.K. Singh, R. Mitra "Impact of Source Voltage Unbalance on AC-DC Rectifier Performance" 2nd International Conference on Power Electronics System and Applications – 2006.

[41] Asheesh K. Singh, G. K. Singh, R. Mitra "Some Observations on Definitions of Voltage Unbalance" NAPS '07. 39th North American Power Symposium, 2007, pp. 473 – 479, 2007

[42] Arfat Siddique, G.S Yadava and Bhim Singh "Effects of Voltage Unbalance on Induction Motors" IEEE International Symposium on Electrical Insulation, Indianapolis, IN USA 19-22 September 2004.

[43] Motor System Tip Sheet #7 September 2005

[44] Electric Power Research Institute, INC. "The Cost of Power Disturbances to Industrial and Digital Economy Companies" http://www.onpower.com/pdf/EPRICostOfPowerProblems.pdf

[45] Peter Solanics, Kevin Kozminski, Munnu Bajpai, Jules Esztergalyos, Everett Fennell, Jon Gardell, Chuck Mozina, Subhash Patel, Al Pierce, Veselin Skendzic, Phil Waudby and Jerome

[46] D.J. Graham, P.G. Brown and R.L. Winchester "Generator Protection With a New Static Negative Sequence Relay" IEEE Transactions on Power Apparatus and Systems, Vol.94, No. 4, pp. 1208 – 1213, 1975

[47] W. H. Kersting "Causes and Effects of Unbalance Voltages Serving and Induction Motor"

[48] Prabhakar Neti and subhasis Nandi "Analysis and Modeling of a Synchronous Machine with Structural Asymmetries" IEEE CCECE/CCGEI, Ottawa, May 2006

[49] Leszek S. Czarnecki "Currents' Physical Components (CPC) In Circuits with Nonsinusoidal Voltages and Currents – Part 2: Three-Phase Three- Wire Linear Circuits" Electric Power Quality and Utilization Journal, Vol. X, No.1.pp.1-14, 2006.

[50] Lawrence Berkeley, Joseph H. Eto, Hassan Nikkajoei, Robert H. Lasseter and Nancy J. Lewis "Microgrid fault Protection Based on Symmetrical and Differential Current Components" Consortium for Electrical Reliability Technology Solution (CERTS)

[51] D. R. Smith, H. R. Braunstein and J. D. Borst "Voltage Unbalance in 3-and 4-Wire Delta Secondary Systems", IEEE Transaction on Power Delivery, Vol. 3, No. 2, April 1988

[52] Charles J. Mozina "Impact-of-Green-Power-Generation-on-Distribution-Systems"

[53] Jose Policarpo G. de Abreu and Alexander Eigeles Emanuel, "Induction Motor Thermal Aging Caused by Voltage Distortion and Imbalance: Loss of Useful Life and Its Estimated Cost" IEEE Transactions on Industry Applications, VOL. 38, No. 1, January/February 2002.

[54] Kevin Lee, Thomas M. Jahns, Thomas A. Lipo, Giri Venkataramanan and William E. Berkopec "Impact of Input Voltage Sag and Unbalance on DC-Link Inductor and Capacitor

Stress in Adjustable-Speed Drives" IEEE Transactions on Industry Applications, Vol. 44, No. 6, November/December 2008.

[55] Kevin Lee, Thomas M. Jahns, Donald W. Novotny, Thomas A. Lipo, William E. Berkopec, and Vladimir Blasko, "Impact of Inductor Placement on the Performance of Adjustable-Speed Drives Under Input Voltage Unbalance and Sag Conditions" IEEE Transactions on Industry Applications, Vol.42, No. 5, pp.1230-1240, 2006

[56] Dr. L.S. Czarnecki, "Supply and loading quality improvement in sinusoidal power systems with unbalanced loads supplied with asymmetrical voltage" Archiv fur Elektrotechnik 77 (1994) 169-177.

[57] Richard Gutman, Sharma Kolluri and Anant Kumar "Application of Single Phase Switching on Entergy System: Three Phase Unbalance Studies", Power Engineering Society Summer Meeting, 2001. IEEE, Vol.2, pp. 778 – 783, 2001

[58] Giulio Burchi, Cristian Lazaroiu, Nicolae Golovanov and Mariacristina Roscia "Estimation on Voltage Unbalance in Power Systems Supplying High Speed Railway" Electrical Power Quality and Utility, Journal Vol. XI, No. 2, 2005.

[59] Tsai-Hsiang Chen and Jeng-Tyan Cherng "Optimal Phase Arrangement of Distribution Transformers Connected to a Primary Feeder for System Unbalance Improvement and Loss Reduction Using a Genetic Algorithm" 1999 IEEE

[60] Ching-Yin Lee, Bin-Kwie Chen, Wei-Jen Lee and Yen-Feng Hsu "Effects of Various Unbalanced Voltages on the Operation Performance of an Induction Motor under the Same Voltage Unbalance factor Condition" IEEE Industrial and Commercial Power Systems Technical Conference, pp. 51-59, May 1997.

[61] A A Ansari and D M Deshpande "Investigation of Performance of 3-Phase Asynchronous Machine Under Voltage Unbalance" Journal of Theoretical and Applied Information Technology 2005-2009 JATIT.

[62] Pragasen Pillay, Peter Hofmann and Marubini Manyage "Derating of Induction Motors Operating with a Combination of Unbalanced Voltages and Over or Undervoltages" IEEE Transaction on Energy Conversion, Vol.17, No.4, 2002, pp.485-491.

[63] J. Faiz, H. Ebrahimpour and P. Pillay, "Influence of Unbalanced Voltage on the Steady-State Performance of a Three-Phase Squirrel-Cage Induction Motor" IEEE Transaction on Energy Conversion, Vol.19, No.4, 2004, pp.657-662.

[64] J. E. Williams, "Operating of three-phase induction motors on unbalanced voltages," AIEE Trans., pt. IIIA, vol. 73, pp. 125–132, 1954.

[65] Gafford, W. C. Duesterhoef, and C. C. Mosher, "Heating of induction motors on unbalanced voltages," AIEE Trans., Pt. III-A, Power App. Syst., vol. PAS-78, pp. 282–297, June 1959.

[66] Cumings et al., "Protection of induction motors against unbalanced

voltage operation," IEEE Trans. Ind. Applicat., vol. IA-21, pp. 778–792, May/June 1985.

[67] Kevin Lee, Giri Venkataramanan and Thomas M. Jahns "Source Current harmonics Analysis of Adjustable Speed Drives Under Input Voltage Unbalance and Sag Conditions" 2004 11th Internationa; Conference on Harmonics and Quality of Power.

[68] R. Gutman and L.B. Wagenaar, "EHV Transformer Bank Unbalance: Practical Issues and Solutions" IEEE Transactions on Power Delivery, Vol.11, No. 4, October 1996.

[69] D. Rendusara, A. Von Jouanne, P. Enjeti and D.A. Paice "Design Consideration for Six Pulse and Twelve Pulse Diode Rectifier Systems Operating Under Voltage Unbalance and Pre-existing Voltage Distortion With Some Corrective Measures" Industry Applications Conference, 1995. Thirtieth IAS Annual Meeting, IAS '95, Conference Record of the 1995 IEEE, Vol. 3, pp. 2549-2556, 1995

[70] P. Enjeti and P. D. Ziogas, "Analysis of a Static Power Converter Under Unbalance – A Novel Approach", IEEE Transactions On Industrial Electronics, Vol. 37, No. 1, Feb. 1990, pp. 91-93.

[71] Donald Reimert "Protective Relaying for Power Generation Systems" Published in 2006 by CRC Press – Taylor and Francis Group.

[72] M.M. Adibi, D.P. Milanicz and T.L. Volkmann "Asymmetry Issues in Power System Restoration" IEEE Transactions on Power System, Vol. 14, No. 3, August 1999.

[73] A.C. Williamson and E.B. Urquhart "Analysis of the losses in a turbine-generator rotor caused by unbalanced loading" Proc. IEE, Vol. 123, No. 12, December 1976.

[74] A.C. Williamson "Measurement of rotor temperatures of a 500 MW turbine generator with unbalanced loading" Proc. IEE, Vol. 123, No. 8, August 1976.

[75] Leszek S. Czarnechi "Currents' Physical Components (CPT) concept: a fundamental of Power Theory. Przeglad Elektrotechniczny, R84, No. 6/2008, pp. 28-37

[76] Westinghouse Electric Corporation, "Electrical Transmission and Distribution Reference Book"

[77] Tristan A. Kneschke "Control of Utility System Unbalance Caused by Single-Phase Electric Traction" IEEE Transactions on Industry Applications, Vol. 1A-21, No. 6, November/December 1985.

[78] Hung-Yuan Kuo and Tsai-Hsiang Chin "Rigorous Evaluation of the Voltage Unbalance Due to High-Speed Railway Demand" IEEE Transactions on Vehicular Technology, Vol. 47, No.4, November 1998.

[79] Hu Yu, Yuan Yue, Chen Zhe, Chen Zhifei and Tao Ye, "Research on the Selection of Railway Traction Transformer" IPEC, 2010 Conference Proceedings, pp. 677-681

[80] William S. Einwechter and Blair A. Ross “Electrified Railroad Supply from Utility Transmission Systems” IEEE Transactions on Industry and General Applications,Vol. IGA-3, No. 4, July/August 1967.

[81] Tsai-Hsiang Chin, “Criteria to Estimate the Voltage Unbalances due to High-Speed Railway Demands” IEEE Transactions on Power Systems, Vol. 9, No. 3, August 1994.

[82] John J. Marczewski “Utility Interconnection Issues” IEEE Power Engineering Society Summer meeting Vol. 1, pp. 439-444, 1999

[83] T. H. Chen and H. Y. Kuo, “Network Modeling of Traction Substation Transformers for Studying unbalance effects” IEE Preceedings, Generation, Transmission and Distribution Vol. 142, No. 2, pp. 103-108, March 1995.

[84] Nelson Martins, Vander DaCosta, Sandoval Carneiro, Jose Pereira and Paulo Garcia, “Three -Phase Power Flow Calculations Using the Current Injection Method” IEEE Transactions on Power Systems, Vol. 15 No. 2, May 2000.

APPENDIX A – ETAP SYSTEM DATA

Project:	ETAP	Page:	1
Location:	7.5.0E	Date:	04-17-2011
Contract:		SN:	LOUSINSTSA
Engineer:		Revision:	Base
Filename: THESIS	Study Case: ULF2	Config.:	Normal

Electrical Transient Analyzer Program

Unbalanced Load Flow Analysis

Loading Category (2):	Normal
Generation Category (2):	Normal
Load Diversity Factor:	Bus Maximum

	Swing	V-Control	Load	Total
Number of Buses:	1	0	20	21

	XFMR2	XFMR3	Reactor	Line	Cable	Impedance	Tie PD	Total
Number of Branches:	8	0	0	2	10	0	6	26

Method of Solution:	Current Injection Method
Maximum No. of Iteration:	99
Precision of Solution:	0.000100
System Frequency:	60 Hz
Unit System:	English
Project Filename:	THESIS
Output Filename:	C:\Users\user\Desktop\Thesis Research papers\ETAP analysis\Thesis.UL1

Adjustments

Tolerance	Apply Adjustments	Individual /Global	Percent
Transformer Impedance:	Yes	Individual	
Reactor Impedance:	Yes	Individual	
Overload Heater Resistance:	No		
Transmission Line Length:	Yes	Individual	
Cable Length:	No		

Temperature Correction	Apply Adjustments	Individual /Global	Degree C
Transmission Line Resistance:	Yes	Individual	
Cable Resistance:	Yes	Individual	

Bus Input Data

Bus						Initial Voltage		Generation		Load		Mvar Limits	
ID	Conn.	Type	kV	Sub-sys	Fh	% Mag.	Ang.	MW	Mvar	MW	Mvar	Max.	Min.
Bus1	3 phase	Swing	230.000	1	A	80.0	0.0	5.829	-0.137	0	0		
					B	100.0	-120.0	9.224	2.418	0	0		
					C	100.0	120.0	5.822	2.691	0	0		
Bus2	3 phase	Load	230.000	1	A	79.9	-0.1	0	0	0	0		
					B	99.9	-120.1	0	0	0	0		
					C	99.9	119.9	0	0	0	0		
Bus3	3 phase	Load	230.000	1	A	79.9	-0.1	0	0	0	0		
					B	99.9	-120.1	0	0	0	0		
					C	99.9	119.9	0	0	0	0		
Bus4	3 phase	Load	13.800	1	A	89.2	-35.3	0	0	0	0		
					B	88.9	-148.9	0	0	0	0		
					C	97.5	88.0	0	0	0	0		
Bus 5	3 phase	Load	13.800	1	A	89.2	-35.3	0	0	0	0		
					B	88.9	-148.9	0	0	0	0		
					C	97.5	88.0	0	0	0	0		
Bus6	3 phase	Load	0.120	1	A	93.2	-67.1	0	0	0.748	0.265		
					B	84.9	175.6	0	0	0.729	0.151		
					C	92.9	58.6	0	0	0.835	0.243		
Bus7	3 phase	Load	13.800	1	A	89.2	-35.3	0	0	1.034	0.269		
					B	88.8	-148.9	0	0	1.807	0.377		
					C	97.5	88.0	0	0	1.602	1.106		
Bus8	3 phase	Load	0.120	1	A	93.4	-67.1	0	0	0.761	0.240		
					B	84.8	175.7	0	0	0.753	0.189		
					C	93.1	58.8	0	0	0.799	0.230		
Bus9	3 phase	Load	13.800	1	A	89.2	-35.3	0	0	0.995	0.244		
					B	88.8	-148.9	0	0	1.848	0.357		
					C	97.5	88.0	0	0	1.599	1.151		
Bus10	3 phase	Load	13.800	1	A	89.2	-35.3	0	0	0	0		
					B	88.8	-148.9	0	0	0	0		
					C	97.5	88.0	0	0	0	0		
Bus11	3 phase	Load	4.160	1	A	93.0	-66.4	0	0	0	0		
					B	85.3	175.9	0	0	0	0		
					C	92.5	58.8	0	0	0	0		
Bus12	3 phase	Load	4.160	1	A	93.0	-66.4	0	0	0	0		
					B	85.3	175.9	0	0	0	0		
					C	92.5	58.8	0	0	0	0		
Bus13	3 phase	Load	4.160	1	A	93.0	-66.4	0	0	0.934	0.649		
					B	85.3	175.9	0	0	1.032	0.172		
					C	92.5	58.8	0	0	1.406	0.696		
Bus14	3 phase	Load	4.160	1	A	93.0	-66.4	0	0	0.934	0.649		
					B	85.3	175.9	0	0	1.032	0.172		
					C	92.5	58.8	0	0	1.406	0.696		
Bus15	3 phase	Load	13.800	1	A	89.2	-35.3	0	0	0	0		
					B	88.8	-148.9	0	0	0	0		
					C	97.5	88.0	0	0	0	0		

Bus						Initial Voltage		Generation		Load		Mvar Limits	
ID	Conn.	Type	kV	Sub-sys	Fh	% Mag.	Ang.	MW	Mvar	MW	Mvar	Max.	Min.
Bus16	3 phase	Load	13.800	1	A	89.2	-35.3	0	0	0	0		
					B	88.9	-148.9	0	0	0	0		
					C	97.5	88.0	0	0	0	0		
Bus17	3 phase	Load	0.480	1	A	94.5	-65.3	0	0	0	0		
					B	85.9	177.4	0	0	0	0		
					C	94.2	60.6	0	0	0	0		
Bus18	3 phase	Load	0.480	1	A	94.5	-65.3	0	0	0	0		
					B	85.9	177.4	0	0	0	0		
					C	94.2	60.6	0	0	0	0		
Bus19	3 phase	Load	0.480	1	A	94.2	-65.3	0	0	0.167	0.111		
					B	85.5	177.3	0	0	0.178	0.028		
					C	93.7	60.6	0	0	0.247	0.118		
Bus20	3 phase	Load	0.480	1	A	94.2	-65.3	0	0	0.167	0.111		
					B	85.5	177.3	0	0	0.178	0.028		
					C	93.7	60.6	0	0	0.247	0.118		
Bus21	3 phase	Load	13.800	1	A	89.2	-35.3	0	0	0	0		
					B	88.9	-148.9	0	0	0	0		
					C	97.5	88.0	0	0	0	0		
Total Number of Buses: 21								20.876	4.972	21.438	8.168		

Cable Input Data

Cable								Ohms/1000 ft per Conductor		
				Length						
ID	Conn.	Library	Size	Adj. (ft)	% Tol.	#/Phase	T (°C)	R	X	Y
Cable1	3 phase	15NCUS1	4/0	50.0	0.0	1	75	0.064000	0.046600	
Cable2-	3 phase	15NCUS1	4/0	50.0	0.0	1	75	0.064000	0.046600	
Cable3	3 phase	15NCUS1	4/0	50.0	0.0	1	75	0.064000	0.046600	
Cable5	3 phase	5.0MCUS3	750	15.0	0.0	1	75	0.022300	0.036400	
Cable6-	3 phase	5.0MCUS3	750	15.0	0.0	1	75	0.022300	0.036400	
Cable7	3 phase	15NCUS1	4/0	50.0	0.0	1	75	0.064000	0.046600	
Cable8-	3 phase	0.6NCJN1	1000	30.0	0.0	1	75	0.015000	0.037000	
Cable9	3 phase	0.6MCUS1	1/0	10.0	0.0	1	75	0.109450	0.060000	
Cable10	3 phase	0.6MCUS1	1/0	10.0	0.0	1	75	0.109450	0.060000	
Cable11	3 phase	0.6NCJN1	1000	30.0	0.0	1	75	0.015000	0.037000	

Cable resistances are listed at the specified temperatures.

Impedance/Line Input Data

			Length		Operating
ID	Type	Connection	Adj. (ft)	% Tol.	Temp °C
Line 1	Line	3 phase	52788.7	0.0	75
Line 2	Line	3 phase	52788.7	0.0	75

Line resistances are listed at the specified temperatures.

Series Impedance/Shunt Admittance Matrices (Phase Domain)

Line ID	Line ID	Length miles		R (ohms)			X (ohms)			Y (micro-siemens)		
				A	B	C	A	B	C	A	B	C
Line 1	Line 1	9.998	A	3.16129	0.91109	0.91109	13.87503	5.48107	5.48107	44.183	-6.489	-6.489
			B	0.91109	3.16129	0.91109	5.48107	13.87503	5.48107	-6.489	44.183	-6.489
			C	0.91109	0.91109	3.16129	5.48107	5.48107	13.87503	-6.489	-6.489	44.183
Line 2	Line 2	9.998	A	3.16129	0.91109	0.91109	13.87503	5.48107	5.48107	44.183	-6.489	-6.489
			B	0.91109	3.16129	0.91109	5.48107	13.87503	5.48107	-6.489	44.183	-6.489
			C	0.91109	0.91109	3.16129	5.48107	5.48107	13.87503	-6.489	-6.489	44.183

2-Winding Transformer Input Data

Transformer	Rating								Z Variation		% Tap Setting		Adjusted		Phase Shift	
ID	MVA	Prim. kV	Sec. kV	% Z1	% Z0	X1/R1	X0/R0	% Tol.	+ 5%	- 5%	Prim.	Sec.	% Z 1	% Z 0	Type	Angle
T1	35.000	230.000	13.800	10.00	10.00	27.30	27.30	0	0	0	0	0	10.0000	10.0000	Std Pos. Seq.	-30.000
T2	35.000	230.000	13.800	10.00	10.00	27.30	27.30	0	0	0	0	0	10.0000	10.0000	Std Pos. Seq.	-30.000
T3	3.500	13.800	0.120	5.75	5.75	11.41	11.41	0	0	0	0	0	5.7500	5.7500	Std Pos. Seq.	-30.000
T4	3.500	13.800	0.120	5.75	5.75	11.41	11.41	0	0	0	0	0	5.7500	5.7500	Std Pos. Seq.	-30.000
T5	8.000	13.800	4.160	6.50	6.50	14.23	14.23	0	0	0	0	0	6.5000	6.5000	Std Pos. Seq.	-30.000
T6	8.000	13.800	4.160	6.50	6.50	27.30	27.30	0	0	0	0	0	6.5000	6.5000	Std Pos. Seq.	-30.000
T7	7.000	13.800	0.480	6.75	6.75	13.55	13.55	0	0	0	0	0	6.7500	6.7500	Std Pos. Seq.	-30.000
T8	7.000	13.800	0.480	6.75	6.75	13.55	13.55	0	0	0	0	0	6.7500	6.7500	Std Pos. Seq.	-30.000

Branch Connections

CKT/Branch			Connected Bus ID		% Impedance, Pos. Seq., 100 MVAb			
ID	Conn.	Type	From Bus	To Bus	R	X	Z	Y
Cable1	3 phase	Cable	Bus4	Bus7	0.17	0.12	0.21	
Cable2-	3 phase	Cable	Bus 5	Bus9	0.17	0.12	0.21	
Cable3	3 phase	Cable	Bus4	Bus10	0.17	0.12	0.21	
Cable5	3 phase	Cable	Bus11	Bus13	0.19	0.32	0.37	
Cable6-	3 phase	Cable	Bus12	Bus14	0.19	0.32	0.37	
Cable7	3 phase	Cable	Bus 5	Bus15	0.17	0.12	0.21	
Cable8-	3 phase	Cable	Bus4	Bus16	0.02	0.06	0.06	
Cable9	3 phase	Cable	Bus17	Bus19	47.50	26.04	54.17	
Cable10	3 phase	Cable	Bus18	Bus20	47.50	26.04	54.17	
Cable11	3 phase	Cable	Bus 5	Bus21	0.02	0.06	0.06	
T1	3 phase	2W XFMR	Bus2	Bus4	1.05	28.55	28.57	
T2	3 phase	2W XFMR	Bus3	Bus 5	1.05	28.55	28.57	
T3	3 phase	2W XFMR	Bus4	Bus6	14.34	163.66	164.29	
T4	3 phase	2W XFMR	Bus 5	Bus8	14.34	163.66	164.29	
T5	3 phase	2W XFMR	Bus10	Bus11	5.70	81.05	81.25	
T6	3 phase	2W XFMR	Bus15	Bus12	2.97	81.20	81.25	
T7	3 phase	2W XFMR	Bus16	Bus17	7.10	96.17	96.43	
T8	3 phase	2W XFMR	Bus21	Bus18	7.10	96.17	96.43	
CB5	3 phase	Tie Circuit	Bus3	Bus2	0.00	0.00	0.00	
CB10	3 phase	Tie Circuit	Bus 5	Bus4	0.00	0.00	0.00	
CB19	3 phase	Tie Circuit	Bus12	Bus11	0.00	0.00	0.00	
CB22	3 phase	Tie Circuit	Bus14	Bus13	0.00	0.00	0.00	
CB35	3 phase	Tie Circuit	Bus17	Bus18	0.00	0.00	0.00	
CB42	3 phase	Tie Circuit	Bus19	Bus20	0.00	0.00	0.00	

Equipment Cable Input Data

Equipment Cable	Equipment			Ohms or Siemens/1000 ft per Conductor									O/L Heater	
						Length							Resistance	
ID	ID	Conn.	Type	Library	Size	Adj. (ft)	% Tol.	#/ph	T (°C)	R	X	Y	Adj (ohm)	% Tol.
Cable17	Mtr2	3 phase	Ind. Motor	15MCUS1	4/0	0.0	0.0	1	75	1.#IND0	1.#IND01.#IND00			0.00
Cable23	Mtr3	3 phase	Ind. Motor	15MCUS1	3/0	0.0	0.0	1	75	1.#IND0	1.#IND01.#IND00			0.00
Cable12	Mtr4	3 phase	Ind. Motor	5.0MCUS3	6	0.0	0.0	1	75	1.#IND0	1.#IND01.#IND00			0.00
Cable15	Mtr6	3 phase	Ind. Motor	5.0MCUS1	500	0.0	0.0	1	75	1.#IND0	1.#IND01.#IND00			0.00
Cable19	Mtr8	3 phase	Ind. Motor	5.0MCUS3	6	0.0	0.0	1	75	1.#IND0	1.#IND01.#IND00			0.00
Cable21	Mtr10	3 phase	Ind. Motor	5.0MCUS1	500	0.0	0.0	1	75	1.#IND0	1.#IND01.#IND00			0.00

APPENDIX B – ETAP RESULTS

CASE 1

Alert-Basic Summary Report

	% Alert Settings	
	Critical	Marginal
Loading		
Bus	100.0	95.0
Cable	100.0	95.0
Reactor	100.0	95.0
Line	100.0	95.0
Transformer	100.0	95.0
Panel	100.0	95.0
Protective Device	100.0	95.0
Generator	100.0	95.0
Bus Voltage		
OverVoltage	105.0	102.0
UnderVoltage	95.0	98.0
Generator Excitation		
OverExcited (Q Max.)	100.0	95.0
UnderExcited (Q Min.)	100.0	

Alert-Advanced Summary Report

	% Alert Settings	
	Critical	Marginal
Bus Voltage		
Line Voltage Unbalanced Rate (LVUR)	100.0	100.0
Voltage Unbalanced Factor (VUF) Neg. Seq.	5.4	2.0
Voltage Unbalanced Factor (VUF) Zero Seq.	7.1	2.0
Branch Current		
Line Current Unbalanced Rate (LIUR)	100.0	100.0
Current Unbalanced Factor (IUF) Neg. Seq.	33.0	7.6
Current Unbalanced Factor (IUF) Zero Seq.	3.0	2.0

Critical Report

Device ID	Type	Condition	Rating/Limit	Unit	Operating A	Operating B	Operating C	%Op. A	%Op. B	%Op. C
Bus1	Bus	Under Voltage	230.000	kV	106.232	132.791	132.791	80.0	100.0	100.0
Bus1	Bus	VUF 2 (Neg. Seq.)	214.667	kV	15.333	0.000	0.000	7.1	0.0	0.0
Bus1	Bus	VUF 0 (Zero Seq.)	123.938	kV	8.853	0.000	0.000	7.1	0.0	0.0
Bus2	Bus	Under Voltage	230.000	kV	106.151	132.611	132.632	79.9	99.9	99.9
Bus2	Bus	VUF 2 (Neg. Seq.)	214.424	kV	15.227	0.000	0.000	7.1	0.0	0.0
Bus2	Bus	VUF 0 (Zero Seq.)	123.798	kV	8.856	0.000	0.000	7.2	0.0	0.0
Bus3	Bus	Under Voltage	230.000	kV	106.151	132.611	132.632	79.9	99.9	99.9
Bus3	Bus	VUF 2 (Neg. Seq.)	214.424	kV	15.227	0.000	0.000	7.1	0.0	0.0
Bus3	Bus	VUF 0 (Zero Seq.)	123.798	kV	8.856	0.000	0.000	7.2	0.0	0.0
Bus4	Bus	Under Voltage	13.800	kV	7.105	7.080	7.771	89.2	88.9	97.5
Bus4	Bus	VUF 2 (Neg. Seq.)	12.664	kV	0.797	0.000	0.000	6.3	0.0	0.0
Bus 5	Bus	Under Voltage	13.800	kV	7.105	7.080	7.771	89.2	88.9	97.5
Bus 5	Bus	VUF 2 (Neg. Seq.)	12.664	kV	0.797	0.000	0.000	6.3	0.0	0.0
Bus6	Bus	Under Voltage	0.120	kV	0.065	0.059	0.065	93.5	84.8	93.2
Bus6	Bus	VUF 2 (Neg. Seq.)	0.108	kV	0.007	0.000	0.000	6.2	0.0	0.0
Bus7	Bus	Under Voltage	13.800	kV	7.105	7.079	7.770	89.2	88.8	97.5
Bus7	Bus	VUF 2 (Neg. Seq.)	12.662	kV	0.797	0.000	0.000	6.3	0.0	0.0
Bus8	Bus	Under Voltage	0.120	kV	0.065	0.059	0.065	93.5	84.8	93.2
Bus8	Bus	VUF 2 (Neg. Seq.)	0.108	kV	0.007	0.000	0.000	6.2	0.0	0.0
Bus9	Bus	Under Voltage	13.800	kV	7.105	7.079	7.770	89.2	88.8	97.5
Bus9	Bus	VUF 2 (Neg. Seq.)	12.662	kV	0.797	0.000	0.000	6.3	0.0	0.0
Bus10	Bus	Under Voltage	13.800	kV	7.105	7.079	7.770	89.2	88.8	97.5
Bus10	Bus	VUF 2 (Neg. Seq.)	12.662	kV	0.797	0.000	0.000	6.3	0.0	0.0
Bus11	Bus	Under Voltage	4.160	kV	2.235	2.048	2.222	93.1	85.3	92.5
Bus11	Bus	VUF 1 (Neg. Seq.)	3.753	kV	0.206	0.000	0.000	5.5	0.0	0.0
Bus12	Bus	Under Voltage	4.160	kV	2.235	2.048	2.222	93.1	85.3	92.5
Bus12	Bus	VUF 1 (Neg. Seq.)	3.753	kV	0.206	0.000	0.000	5.5	0.0	0.0
Bus13	Bus	Under Voltage	4.160	kV	2.235	2.048	2.222	93.1	85.3	92.5
Bus13	Bus	VUF 1 (Neg. Seq.)	3.753	kV	0.206	0.000	0.000	5.5	0.0	0.0
Bus14	Bus	Under Voltage	4.160	kV	2.235	2.048	2.222	93.1	85.3	92.5
Bus14	Bus	VUF 1 (Neg. Seq.)	3.753	kV	0.206	0.000	0.000	5.5	0.0	0.0
Bus15	Bus	Under Voltage	13.800	kV	7.105	7.079	7.770	89.2	88.8	97.5
Bus15	Bus	VUF 1 (Neg. Seq.)	12.662	kV	0.797	0.000	0.000	6.3	0.0	0.0
Bus16	Bus	Under Voltage	13.800	kV	7.105	7.080	7.771	89.2	88.9	97.5
Bus16	Bus	VUF 1 (Neg. Seq.)	12.663	kV	0.797	0.000	0.000	6.3	0.0	0.0
Bus17	Bus	Under Voltage	0.480	kV	0.262	0.238	0.261	94.6	85.8	94.2
Bus17	Bus	VUF 1 (Neg. Seq.)	0.439	kV	0.027	0.000	0.000	6.1	0.0	0.0
Bus18	Bus	Under Voltage	0.480	kV	0.262	0.238	0.261	94.6	85.8	94.2
Bus18	Bus	VUF 1 (Neg. Seq.)	0.439	kV	0.027	0.000	0.000	6.1	0.0	0.0
Bus19	Bus	Under Voltage	0.480	kV	0.261	0.237	0.260	94.2	85.5	93.7
Bus19	Bus	VUF 1 (Neg. Seq.)	0.437	kV	0.027	0.000	0.000	6.1	0.0	0.0
Bus20	Bus	Under Voltage	0.480	kV	0.261	0.237	0.260	94.2	85.5	93.7

Critical Report

Device ID	Type	Condition	Rating/Limit	Unit	Operating A	Operating B	Operating C	%Op. A	%Op. B	%Op. C
Bus20	Bus	VUF : (Neg. Seq.)	0.437	kV	0.027	0.000	0.000	6.1	0.0	0.0
Bus21	Bus	UnderVoltage	13.800	kV	7.105	7.080	7.771	89.2	88.9	97.5
Bus21	Bus	VUF : (Neg. Seq.)	12.663	kV	0.797	0.000	0.000	6.3	0.0	0.0
Cable2-	Cable	IUF 2 (Neg. Seq.)	216.028	Amp	72.832	72.832	72.832	33.7	33.7	33.7
Cable5	Cable	Overload	700.604	Amp	508.710	510.663	706.505	72.6	72.9	100.8
Cable6-	Cable	Overload	700.604	Amp	508.710	510.663	706.505	72.6	72.9	100.8
Cable9	Cable	Overload	1000.000	Amp	766.974	760.895	1054.215	76.7	76.1	105.4
Cable10	Cable	Overload	1000.000	Amp	766.974	760.895	1054.215	76.7	76.1	105.4
Cable23	Cable	Overload	233.810	Amp	143.954	266.076	253.770	61.6	113.8	108.5
Cable23	Cable	IUF 2 (Neg. Seq.)	216.028	Amp	72.832	72.832	72.832	33.7	33.7	33.7
Cable8	Cable	Overload	546.692	Amp	388.920	403.355	554.575	71.1	73.8	101.4
Cable21	Cable	Overload	546.692	Amp	388.920	403.355	554.575	71.1	73.8	101.4

Marginal Report

Device ID	Type	Condition	Rating/Limit	Unit	Operating A	Operating B	Operating C	%Op. A	%Op. B	%Op. C
Line 1	Line	IUF : (Neg. Seq.)	28.539	Amp	7.426	7.426	7.426	26.0	26.0	26.0
Line 2	Line	IUF : (Neg. Seq.)	28.539	Amp	7.426	7.426	7.426	26.0	26.0	26.0
Cable1	Cable	IUF : (Neg. Seq.)	216.147	Amp	66.627	66.627	66.627	30.8	30.8	30.8
Cable3	Cable	IUF : (Neg. Seq.)	170.451	Amp	42.548	42.548	42.548	25.0	25.0	25.0
Cable5	Cable	IUF : (Neg. Seq.)	565.379	Amp	141.129	141.129	141.129	25.0	25.0	25.0
Cable6-	Cable	IUF : (Neg. Seq.)	565.379	Amp	141.129	141.129	141.129	25.0	25.0	25.0
Cable7	Cable	IUF : (Neg. Seq.)	170.463	Amp	42.551	42.551	42.551	25.0	25.0	25.0
Cable8-	Cable	IUF : (Neg. Seq.)	29.438	Amp	7.231	7.231	7.231	24.6	24.6	24.6
Cable9	Cable	IUF : (Neg. Seq.)	846.352	Amp	207.882	207.882	207.882	24.6	24.6	24.6
Cable10	Cable	IUF : (Neg. Seq.)	846.352	Amp	207.882	207.882	207.882	24.6	24.6	24.6
Cable11	Cable	IUF : (Neg. Seq.)	29.438	Amp	7.231	7.231	7.231	24.6	24.6	24.6
T1	2W XFMR	IUF : (Neg. Seq.)	30.494	Amp	7.426	7.426	7.426	24.4	24.4	24.4
T2	2W XFMR	IUF : (Neg. Seq.)	30.494	Amp	7.426	7.426	7.426	24.4	24.4	24.4
T5	2W XFMR	IUF : (Neg. Seq.)	170.451	Amp	42.548	42.548	42.548	25.0	25.0	25.0
T6	2W XFMR	IUF : (Neg. Seq.)	170.463	Amp	42.551	42.551	42.551	25.0	25.0	25.0
T7	2W XFMR	IUF : (Neg. Seq.)	29.438	Amp	7.231	7.231	7.231	24.6	24.6	24.6
T8	2W XFMR	IUF : (Neg. Seq.)	29.438	Amp	7.231	7.231	7.231	24.6	24.6	24.6
Cable17	Cable	IUF : (Neg. Seq.)	216.147	Amp	66.627	66.627	66.627	30.8	30.8	30.8
Cable12	Cable	IUF : (Neg. Seq.)	126.550	Amp	27.045	27.045	27.045	21.4	21.4	21.4
Cable8	Cable	IUF : (Neg. Seq.)	440.509	Amp	114.161	114.161	114.161	25.9	25.9	25.9
Cable19	Cable	IUF : (Neg. Seq.)	126.550	Amp	27.045	27.045	27.045	21.4	21.4	21.4
Cable21	Cable	IUF : (Neg. Seq.)	440.509	Amp	114.161	114.161	114.161	25.9	25.9	25.9

Branch Losses Summary Report

CKT / Branch		From-To Bus Flow		To-From Bus Flow		Losses		% Bus Voltage		Vd % Drop
ID	Phase	MW	Mvar	MW	Mvar	kW	kvar	From	To	in Vmag
Line 1	A	2.902	-0.064	-2.900	-0.520	1.7	-583.4	80.0	79.9	0.06
	B	4.572	1.186	-4.589	-2.055	-16.8	-869.5	100.0	99.9	0.14
	C	2.908	1.317	-2.887	-2.192	21.3	-875.6	100.0	99.9	0.12
Line 2	A	2.902	-0.064	-2.900	-0.520	1.7	-583.4	80.0	79.9	0.06
	B	4.572	1.186	-4.589	-2.055	-16.8	-869.5	100.0	99.9	0.14
	C	2.908	1.317	-2.887	-2.192	21.3	-875.6	100.0	99.9	0.12
Cable1	A	1.032	0.268	-1.032	-0.268	0.1	0.1	89.2	89.2	0.01
	B	1.809	0.376	-1.809	-0.376	0.2	0.2	88.9	88.8	0.01
	C	1.603	1.108	-1.602	-1.108	0.2	0.1	97.5	97.5	0.01
Cable2-	A	0.994	0.243	-0.994	-0.242	0.1	0.0	89.2	89.2	0.01
	B	1.850	0.356	-1.850	-0.356	0.2	0.2	88.9	88.8	0.01
	C	1.600	1.153	-1.600	-1.153	0.2	0.2	97.5	97.5	0.01
Cable3	A	0.848	0.326	-0.848	-0.326	0.1	0.0	89.2	89.2	0.01
	B	1.325	0.399	-1.325	-0.399	0.1	0.1	88.9	88.8	0.01
	C	1.234	0.879	-1.234	-0.879	0.1	0.1	97.5	97.5	0.01
Cable5	A	0.933	0.650	-0.933	-0.649	0.1	0.1	93.1	93.1	0.01
	B	1.032	0.171	-1.032	-0.171	0.1	0.1	85.3	85.3	0.01
	C	1.407	0.697	-1.407	-0.697	0.2	0.3	92.5	92.5	0.02
Cable6-	A	0.933	0.650	-0.933	-0.649	0.1	0.1	93.1	93.1	0.01
	B	1.032	0.171	-1.032	-0.171	0.1	0.1	85.3	85.3	0.01
	C	1.407	0.697	-1.407	-0.697	0.2	0.3	92.5	92.5	0.02
Cable7	A	0.837	0.354	-0.837	-0.354	0.1	0.0	89.2	89.2	0.01
	B	1.311	0.443	-1.311	-0.443	0.1	0.1	88.9	88.8	0.01
	C	1.204	0.920	-1.204	-0.920	0.1	0.1	97.5	97.5	0.01
Cable8-	A	0.148	0.054	-0.148	-0.054	0.0	0.0	89.2	89.2	0.00
	B	0.229	0.063	-0.229	-0.063	0.0	0.0	88.9	88.9	0.00
	C	0.218	0.146	-0.218	-0.146	0.0	0.0	97.5	97.5	0.00
Cable9	A	0.167	0.111	-0.167	-0.111	0.6	0.4	94.6	94.2	0.34
	B	0.179	0.029	-0.178	-0.028	0.6	0.3	85.8	85.5	0.32
	C	0.248	0.119	-0.247	-0.118	1.2	0.7	94.2	93.7	0.47
Cable10	A	0.167	0.111	-0.167	-0.111	0.6	0.4	94.6	94.2	0.34
	B	0.179	0.029	-0.178	-0.028	0.6	0.3	85.8	85.5	0.32
	C	0.248	0.119	-0.247	-0.118	1.2	0.7	94.2	93.7	0.47
Cable11	A	0.148	0.054	-0.148	-0.054	0.0	0.0	89.2	89.2	0.00
	B	0.229	0.063	-0.229	-0.063	0.0	0.0	88.9	88.9	0.00
	C	0.218	0.146	-0.218	-0.146	0.0	0.0	97.5	97.5	0.00
T1	A	2.900	0.520	-2.598	-0.846	302.0	-326.3	79.9	89.2	9.24
	B	4.589	2.055	-3.993	-1.042	596.1	1013.9	99.9	88.9	11.01
	C	2.887	2.192	-3.769	-2.433	-881.8	-241.2	99.9	97.5	2.34
T2	A	2.900	0.520	-2.598	-0.846	302.0	-326.3	79.9	89.2	9.24
	B	4.589	2.055	-3.993	-1.042	596.1	1013.9	99.9	88.9	11.01
	C	2.887	2.192	-3.769	-2.433	-881.8	-241.2	99.9	97.5	2.34

CKT / Branch		From-To Bus Flow		To-From Bus Flow		Losses		% Bus Voltage		Vd % Drop
ID	Phase	MW	Mvar	MW	Mvar	kW	kvar	From	To	in Vmag
T3	A	0.594	0.197	-0.675	-0.211	-81.1	-14.1	89.2	93.5	4.27
	B	0.617	0.191	-0.562	-0.150	55.0	41.3	88.9	84.8	4.08
	C	0.731	0.257	-0.698	-0.203	33.3	53.9	97.5	93.2	4.37
T4	A	0.594	0.197	-0.675	-0.211	-81.1	-14.1	89.2	93.5	4.27
	B	0.617	0.191	-0.562	-0.150	55.0	41.3	88.9	84.8	4.08
	C	0.731	0.257	-0.698	-0.203	33.3	53.9	97.5	93.2	4.37
T5	A	0.848	0.326	-0.944	-0.634	-95.8	-308.1	89.2	93.1	3.89
	B	1.325	0.399	-1.035	-0.154	290.0	245.4	88.8	85.3	3.56
	C	1.234	0.879	-1.418	-0.673	-184.2	205.6	97.5	92.5	5.01
T6	A	0.837	0.354	-0.922	-0.665	-85.5	-311.2	89.2	93.1	3.89
	B	1.311	0.443	-1.029	-0.188	281.7	255.0	88.8	85.3	3.56
	C	1.204	0.920	-1.395	-0.721	-190.9	199.3	97.5	92.5	5.01
T7	A	0.148	0.054	-0.167	-0.111	-19.3	-56.8	89.2	94.6	5.38
	B	0.229	0.063	-0.179	-0.029	50.2	34.8	88.9	85.8	3.01
	C	0.218	0.146	-0.248	-0.119	-30.5	27.0	97.5	94.2	3.33
T8	A	0.148	0.054	-0.167	-0.111	-19.3	-56.8	89.2	94.6	5.38
	B	0.229	0.063	-0.179	-0.029	50.2	34.8	88.9	85.8	3.01
	C	0.218	0.146	-0.248	-0.119	-30.5	27.0	97.5	94.2	3.33
						82.5	-3301.0			

CASE 2

Alert-Basic Summary Report

	% Alert Settings	
	Critical	Marginal
Loading		
Bus	100.0	95.0
Cable	100.0	95.0
Reactor	100.0	95.0
Line	100.0	95.0
Transformer	100.0	95.0
Panel	100.0	95.0
Protective Device	100.0	95.0
Generator	100.0	95.0
Bus Voltage		
OverVoltage	105.0	102.0
UnderVoltage	95.0	98.0
Generator Excitation		
OverExcited (Q Max.)	100.0	95.0
UnderExcited (Q Min.)	100.0	

Alert-Advanced Summary Report

	% Alert Settings	
	Critical	Marginal
Bus Voltage		
Line Voltage Unbalanced Rate (LVUR)	100.0	100.0
Voltage Unbalanced Factor (VUF) Neg. Seq.	7.1	5.4
Voltage Unbalanced Factor (VUF) Zero Seq.	7.1	3.6
Branch Current		
Line Current Unbalanced Rate (LIUR)	100.0	100.0
Current Unbalanced Factor (IUF) Neg. Seq.	31.1	6.9
Current Unbalanced Factor (IUF) Zero Seq.	20.9	11.8

Critical Report

Device ID	Type	Condition	Rating/Limit	Unit	Operating A	Operating B	Operating C	%Op. A	%Op. B	%Op. C
Bus1	Bus	Under Voltage	230.000	kV	106.232	132.791	132.791	80.0	100.0	100.0
Bus1	Bus	VUF - (Neg. Seq.)	214.667	kV	15.333	0.000	0.000	7.1	0.0	0.0
Bus1	Bus	VUF 0 (Zero Seq.)	123.938	kV	8.853	0.000	0.000	7.1	0.0	0.0
Bus2	Bus	Under Voltage	230.000	kV	106.068	132.000	131.937	79.9	99.4	99.4
Bus2	Bus	VUF - (Neg. Seq.)	213.622	kV	15.177	0.000	0.000	7.1	0.0	0.0
Bus3	Bus	Under Voltage	230.000	kV	106.068	132.000	131.937	79.9	99.4	99.4
Bus3	Bus	VUF - (Neg. Seq.)	213.622	kV	15.177	0.000	0.000	7.1	0.0	0.0
Bus4	Bus	Under Voltage	13.800	kV	6.415	7.205	7.473	80.5	90.4	93.8
Bus 5	Bus	Under Voltage	13.800	kV	6.415	7.205	7.473	80.5	90.4	93.8
Bus6	Bus	Under Voltage	0.120	kV	0.060	0.057	0.063	87.2	82.1	91.5
Bus7	Bus	Under Voltage	13.800	kV	6.414	7.204	7.472	80.5	90.4	93.8
Bus8	Bus	Under Voltage	0.120	kV	0.060	0.057	0.063	87.2	82.1	91.5
Bus9	Bus	Under Voltage	13.800	kV	6.414	7.204	7.472	80.5	90.4	93.8
Bus10	Bus	Under Voltage	13.800	kV	6.415	7.204	7.472	80.5	90.4	93.8
Bus11	Bus	Under Voltage	4.160	kV	2.091	1.977	2.175	87.1	82.3	90.6
Bus12	Bus	Under Voltage	4.160	kV	2.091	1.977	2.175	87.1	82.3	90.6
Bus13	Bus	Under Voltage	4.160	kV	2.091	1.977	2.175	87.0	82.3	90.6
Bus14	Bus	Under Voltage	4.160	kV	2.091	1.977	2.175	87.0	82.3	90.6
Bus15	Bus	Under Voltage	13.800	kV	6.414	7.204	7.472	80.5	90.4	93.8
Bus16	Bus	Under Voltage	13.800	kV	6.415	7.205	7.473	80.5	90.4	93.8
Bus17	Bus	Under Voltage	0.480	kV	0.245	0.230	0.256	88.3	83.1	92.5
Bus18	Bus	Under Voltage	0.480	kV	0.245	0.230	0.256	88.3	83.1	92.5
Bus19	Bus	Under Voltage	0.480	kV	0.244	0.229	0.255	87.9	82.7	92.0
Bus20	Bus	Under Voltage	0.480	kV	0.244	0.229	0.255	87.9	82.7	92.0
Bus21	Bus	Under Voltage	13.800	kV	6.415	7.205	7.473	80.5	90.4	93.8
Cable1	Cable	Overload	282.300	Amp	177.046	284.761	227.618	62.7	100.9	80.6
Cable2-	Cable	Overload	282.300	Amp	173.649	290.570	227.837	61.5	102.9	80.7
Cable2-	Cable	IUF - (Neg. Seq.)	224.902	Amp	70.123	70.123	70.123	31.2	31.2	31.2
Cable5	Cable	Overload	700.604	Amp	476.500	605.068	710.276	68.0	86.4	101.4
Cable6-	Cable	Overload	700.604	Amp	476.500	605.068	710.276	68.0	86.4	101.4
Cable9	Cable	Overload	1000.800	Amp	717.703	900.353	1061.249	71.8	90.0	106.1
Cable10	Cable	Overload	1000.800	Amp	717.703	900.353	1061.249	71.8	90.0	106.1
T1	2W XFMR	Overload	36.800	MVA	21.065	18.935	25.114	175.5	157.8	209.3
T2	2W XFMR	Overload	36.800	MVA	25.927	27.851	31.265	216.1	232.1	260.5
Cable23	Cable	Overload	233.810	Amp	173.647	290.568	227.835	74.3	124.3	97.4
Cable23	Cable	IUF - (Neg. Seq.)	224.900	Amp	70.123	70.123	70.123	31.2	31.2	31.2
Cable8	Cable	Overload	546.692	Amp	364.355	478.641	554.375	66.6	87.6	101.4
Cable21	Cable	Overload	546.692	Amp	364.355	478.641	554.375	66.6	87.6	101.4

Marginal Report

Device ID	Type	Condition	Rating/Limit	Unit	Operating A	Operating B	Operating C	%Op.A	%Op. B	%Op. C
Bus2	Bus	VUF 0 (Zero Seq.)	123.335	kV	8.504	0.000	0.000	6.9	0.0	0.0
Bus3	Bus	VUF 0 (Zero Seq.)	123.335	kV	8.504	0.000	0.000	6.9	0.0	0.0
Bus4	Bus	VUF 2 (Neg. Seq.)	12.171	kV	0.767	0.000	0.000	6.3	0.0	0.0
Bus4	Bus	VUF 0 (Zero Seq.)	7.027	kV	0.255	0.000	0.000	3.6	0.0	0.0
Bus 5	Bus	VUF 2 (Neg. Seq.)	12.171	kV	0.767	0.000	0.000	6.3	0.0	0.0
Bus 5	Bus	VUF 0 (Zero Seq.)	7.027	kV	0.255	0.000	0.000	3.6	0.0	0.0
Bus6	Bus	VUF 2 (Neg. Seq.)	0.104	kV	0.006	0.000	0.000	6.2	0.0	0.0
Bus7	Bus	VUF 2 (Neg. Seq.)	12.169	kV	0.767	0.000	0.000	6.3	0.0	0.0
Bus7	Bus	VUF 0 (Zero Seq.)	7.026	kV	0.255	0.000	0.000	3.6	0.0	0.0
Bus8	Bus	VUF 2 (Neg. Seq.)	0.104	kV	0.006	0.000	0.000	6.2	0.0	0.0
Bus9	Bus	VUF 2 (Neg. Seq.)	12.169	kV	0.767	0.000	0.000	6.3	0.0	0.0
Bus9	Bus	VUF 0 (Zero Seq.)	7.026	kV	0.255	0.000	0.000	3.6	0.0	0.0
Bus10	Bus	VUF 2 (Neg. Seq.)	12.170	kV	0.767	0.000	0.000	6.3	0.0	0.0
Bus10	Bus	VUF 0 (Zero Seq.)	7.026	kV	0.255	0.000	0.000	3.6	0.0	0.0
Bus11	Bus	VUF 2 (Neg. Seq.)	3.602	kV	0.198	0.000	0.000	5.5	0.0	0.0
Bus12	Bus	VUF 2 (Neg. Seq.)	3.602	kV	0.198	0.000	0.000	5.5	0.0	0.0
Bus13	Bus	VUF 2 (Neg. Seq.)	3.601	kV	0.198	0.000	0.000	5.5	0.0	0.0
Bus14	Bus	VUF 2 (Neg. Seq.)	3.601	kV	0.198	0.000	0.000	5.5	0.0	0.0
Bus15	Bus	VUF 2 (Neg. Seq.)	12.170	kV	0.767	0.000	0.000	6.3	0.0	0.0
Bus15	Bus	VUF 0 (Zero Seq.)	7.026	kV	0.255	0.000	0.000	3.6	0.0	0.0
Bus16	Bus	VUF 2 (Neg. Seq.)	12.171	kV	0.767	0.000	0.000	6.3	0.0	0.0
Bus16	Bus	VUF 0 (Zero Seq.)	7.027	kV	0.255	0.000	0.000	3.6	0.0	0.0
Bus17	Bus	VUF 2 (Neg. Seq.)	0.422	kV	0.026	0.000	0.000	6.1	0.0	0.0
Bus18	Bus	VUF 2 (Neg. Seq.)	0.422	kV	0.026	0.000	0.000	6.1	0.0	0.0
Bus19	Bus	VUF 2 (Neg. Seq.)	0.420	kV	0.026	0.000	0.000	6.1	0.0	0.0
Bus20	Bus	VUF 2 (Neg. Seq.)	0.420	kV	0.026	0.000	0.000	6.1	0.0	0.0
Bus21	Bus	VUF 2 (Neg. Seq.)	12.171	kV	0.767	0.000	0.000	6.3	0.0	0.0
Bus21	Bus	VUF 0 (Zero Seq.)	7.027	kV	0.255	0.000	0.000	3.6	0.0	0.0
Line 1	Line	IUF 2 (Neg. Seq.)	67.597	Amp	10.788	10.788	10.788	16.0	16.0	16.0
Line 1	Line	IUF 0 (Zero Seq.)	67.597	Amp	14.066	14.066	14.066	20.8	20.8	20.8
Line 2	Line	IUF 2 (Neg. Seq.)	67.597	Amp	10.788	10.788	10.788	16.0	16.0	16.0
Line 2	Line	IUF 0 (Zero Seq.)	67.597	Amp	14.066	14.066	14.066	20.8	20.8	20.8
Cable1	Cable	IUF 2 (Neg. Seq.)	225.018	Amp	64.148	64.148	64.148	28.5	28.5	28.5
Cable3	Cable	IUF 2 (Neg. Seq.)	177.700	Amp	40.965	40.965	40.965	23.1	23.1	23.1
Cable5	Cable	IUF 2 (Neg. Seq.)	589.424	Amp	135.879	135.879	135.879	23.1	23.1	23.1
Cable6-	Cable	IUF 2 (Neg. Seq.)	589.424	Amp	135.879	135.879	135.879	23.1	23.1	23.1
Cable7	Cable	IUF 2 (Neg. Seq.)	177.712	Amp	40.968	40.968	40.968	23.1	23.1	23.1
Cable8-	Cable	IUF 2 (Neg. Seq.)	30.655	Amp	6.962	6.962	6.962	22.7	22.7	22.7
Cable9	Cable	IUF 2 (Neg. Seq.)	881.628	Amp	200.148	200.148	200.148	22.7	22.7	22.7
Cable10	Cable	IUF 2 (Neg. Seq.)	881.628	Amp	200.148	200.148	200.148	22.7	22.7	22.7
Cable11	Cable	IUF 2 (Neg. Seq.)	30.655	Amp	6.962	6.962	6.962	22.7	22.7	22.7
T1	2W XFMR	IUF 2 (Neg. Seq.)	3059.740	Amp	281.156	281.156	281.156	9.2	9.2	9.2

Marginal Report

Device ID	Type	Condition	Rating/Limit	Unit	Operating A	Operating B	Operating C	%Op. A	%Op. B	%Op. C
T1	2W XFMR	IUF 0 (Zero Seq.)	3059.740	Amp	468.878	468.878	468.878	15.3	15.3	15.3
T3	2W XFMR	IUF 2 (Neg. Seq.)	90.110	Amp	6.777	6.777	6.777	7.5	7.5	7.5
T4	2W XFMR	IUF 2 (Neg. Seq.)	90.110	Amp	6.777	6.777	6.777	7.5	7.5	7.5
T5	2W XFMR	IUF 2 (Neg. Seq.)	177.700	Amp	40.965	40.965	40.965	23.1	23.1	23.1
T6	2W XFMR	IUF 2 (Neg. Seq.)	177.712	Amp	40.968	40.968	40.968	23.1	23.1	23.1
T7	2W XFMR	IUF 2 (Neg. Seq.)	30.665	Amp	6.962	6.962	6.962	22.7	22.7	22.7
T8	2W XFMR	IUF 2 (Neg. Seq.)	30.665	Amp	6.962	6.962	6.962	22.7	22.7	22.7
Cable17	Cable	IUF 2 (Neg. Seq.)	225.006	Amp	64.148	64.148	64.148	28.5	28.5	28.5
Cable12	Cable	IUF 2 (Neg. Seq.)	131.944	Amp	26.039	26.039	26.039	19.7	19.7	19.7
Cable8	Cable	IUF 2 (Neg. Seq.)	459.326	Amp	109.914	109.914	109.914	23.9	23.9	23.9
Cable19	Cable	IUF 2 (Neg. Seq.)	131.944	Amp	26.039	26.039	26.039	19.7	19.7	19.7
Cable21	Cable	IUF 2 (Neg. Seq.)	459.326	Amp	109.914	109.914	109.914	23.9	23.9	23.9

Branch Losses Summary Report

CKT / Branch		From-To Bus Flow		To-From Bus Flow		Losses		% Bus Voltage		Vd % Drop
ID	Phase	MW	Mvar	MW	Mvar	kW	kvar	From	To	in Vmag
Line 1	A	3.008	3.896	-3.010	-4.473	-2.4	-577.4	80.0	79.9	0.12
	B	3.618	9.661	-3.604	-10.482	14.1	-821.0	100.0	99.4	0.60
	C	4.414	9.679	-4.389	-10.481	25.4	-801.9	100.0	99.4	0.64
Line 2	A	3.008	3.896	-3.010	-4.473	-2.4	-577.4	80.0	79.9	0.12
	B	3.618	9.661	-3.604	-10.482	14.1	-821.0	100.0	99.4	0.60
	C	4.414	9.679	-4.389	-10.481	25.4	-801.9	100.0	99.4	0.64
Cable1	A	1.130	0.110	-1.130	-0.110	0.1	0.1	80.5	80.5	0.01
	B	1.957	0.615	-1.957	-0.615	0.3	0.2	90.4	90.4	0.01
	C	1.356	1.028	-1.355	-1.028	0.2	0.1	93.8	93.8	0.01
Cable2-	A	1.112	0.074	-1.111	-0.074	0.1	0.1	80.5	80.5	0.01
	B	2.001	0.616	-2.001	-0.616	0.3	0.2	90.4	90.4	0.01
	C	1.331	1.062	-1.331	-1.062	0.2	0.1	93.8	93.8	0.01
Cable3	A	0.896	0.217	-0.896	-0.217	0.1	0.0	80.5	80.5	0.01
	B	1.438	0.561	-1.438	-0.560	0.1	0.1	90.4	90.4	0.01
	C	1.075	0.837	-1.075	-0.837	0.1	0.1	93.8	93.8	0.01
Cable5	A	0.874	0.477	-0.874	-0.477	0.1	0.1	87.1	87.0	0.01
	B	1.170	0.250	-1.170	-0.250	0.1	0.2	82.3	82.3	0.01
	C	1.328	0.790	-1.327	-0.790	0.2	0.3	90.6	90.6	0.02
Cable6-	A	0.874	0.477	-0.874	-0.477	0.1	0.1	87.1	87.0	0.01

	B	1.170	0.250	-1.170	-0.250	0.1	0.2	82.3	82.3	0.01
	C	1.328	0.790	-1.327	-0.790	0.2	0.3	90.6	90.6	0.02
Cable7	A	0.888	0.247	-0.888	-0.247	0.1	0.0	80.5	80.5	0.01
	B	1.418	0.608	-1.418	-0.608	0.1	0.1	90.4	90.4	0.01
	C	1.046	0.873	-1.046	-0.873	0.1	0.1	93.8	93.8	0.01
Cable8-	A	0.155	0.035	-0.155	-0.035	0.0	0.0	80.5	80.5	0.00
	B	0.250	0.090	-0.250	-0.090	0.0	0.0	90.4	90.4	0.00
	C	0.190	0.140	-0.190	-0.140	0.0	0.0	93.8	93.8	0.00
Cable9	A	0.156	0.081	-0.155	-0.081	0.6	0.3	88.3	87.9	0.32
	B	0.203	0.042	-0.202	-0.042	0.9	0.5	83.1	82.7	0.39
	C	0.236	0.135	-0.235	-0.135	1.2	0.7	92.5	92.0	0.48
Cable10	A	0.156	0.081	-0.155	-0.081	0.6	0.3	88.3	87.9	0.32
	B	0.203	0.042	-0.202	-0.042	0.9	0.5	83.1	82.7	0.39
	C	0.236	0.135	-0.235	-0.135	1.2	0.7	92.5	92.0	0.48
Cable11	A	0.155	0.035	-0.155	-0.035	0.0	0.0	80.5	80.5	0.00
	B	0.250	0.090	-0.250	-0.090	0.0	0.0	90.4	90.4	0.00
	C	0.190	0.140	-0.190	-0.140	0.0	0.0	93.8	93.8	0.00
T1	A	-19.536	6.034	19.868	-7.001	332.0	-967.1	79.9	80.5	0.64
	B	-29.513	7.970	18.838	1.914	-1674.2	9883.6	99.4	90.4	8.97
	C	-21.834	11.085	24.753	-4.243	1919.5	6842.8	99.4	93.8	5.56
T2	A	25.556	2.912	-25.230	5.970	325.3	8881.9	79.9	80.5	0.64
	B	27.720	12.994	-27.422	-4.870	297.6	8124.7	99.4	90.4	8.97
	C	31.611	9.877	-31.263	-0.360	348.6	9517.2	99.4	93.8	5.56

CKT / Branch		From-To Bus Flow		To-From Bus Flow		Losses		% Bus Voltage		Vd % Drop
ID	Phase	MW	Mvar	MW	Mvar	kW	kvar	From	To	in Vmag
T3	A	0.513	0.157	-0.589	-0.181	-76.4	-23.9	80.5	87.2	6.67
	B	0.635	0.188	-0.540	-0.144	95.7	44.3	90.4	82.1	8.31
	C	0.661	0.262	-0.674	-0.206	-12.6	55.9	93.8	91.5	2.32
T4	A	0.513	0.157	-0.589	-0.181	-76.4	-23.9	80.5	87.2	6.67
	B	0.635	0.188	-0.540	-0.144	95.7	44.3	90.4	82.1	8.31
	C	0.661	0.262	-0.674	-0.206	-12.6	55.9	93.8	91.5	2.32
T5	A	0.896	0.217	-0.882	-0.463	13.5	-245.4	80.5	87.1	6.54
	B	1.438	0.560	-1.174	-0.230	263.5	330.3	90.4	82.3	8.10
	C	1.075	0.837	-1.341	-0.768	-266.2	69.1	93.8	90.6	3.22
T6	A	0.888	0.247	-0.867	-0.492	21.7	-244.8	80.5	87.1	6.54
	B	1.418	0.608	-1.166	-0.269	252.3	339.0	90.4	82.3	8.09
	C	1.046	0.873	-1.314	-0.813	-268.3	60.1	93.8	90.6	3.22
T7	A	0.155	0.035	-0.156	-0.081	-0.3	-46.5	80.5	88.3	7.74
	B	0.250	0.090	-0.203	-0.042	46.4	47.6	90.4	83.1	7.30
	C	0.190	0.140	-0.236	-0.135	-45.7	4.3	93.8	92.5	1.31
T8	A	0.155	0.035	-0.156	-0.081	-0.3	-46.5	80.5	88.3	7.74
	B	0.250	0.090	-0.203	-0.042	46.4	47.6	90.4	83.1	7.30
	C	0.190	0.140	-0.236	-0.135	-45.7	4.3	93.8	92.5	1.31
						1661.6	38359.6			

CASE 3

Alert-Basic Summary Report

	% Alert Settings	
	Critical	Marginal
Loading		
Bus	100.0	95.0
Cable	100.0	95.0
Reactor	100.0	95.0
Line	100.0	95.0
Transformer	100.0	95.0
Panel	100.0	95.0
Protective Device	100.0	95.0
Generator	100.0	95.0
Bus Voltage		
OverVoltage	105.0	102.0
UnderVoltage	95.0	98.0
Generator Excitation		
OverExcited (Q Max.)	100.0	95.0
UnderExcited (Q Min.)	100.0	

Alert-Advanced Summary Report

	% Alert Settings	
	Critical	Marginal
Bus Voltage		
Line Voltage Unbalanced Rate (LVUR)	100.0	100.0
Voltage Unbalanced Factor (VUF) Neg. Seq.	7.5	2.0
Voltage Unbalanced Factor (VUF) Zero Seq.	6.0	2.0
Branch Current		
Line Current Unbalanced Rate (LIUR)	100.0	100.0
Current Unbalanced Factor (IUF) Neg. Seq.	73.0	5.6
Current Unbalanced Factor (IUF) Zero Seq.	76.0	2.0

Critical Report

Device ID	Type	Condition	Rating/Limit	Unit	Operating A	Operating B	Operating C	%Op. A	%Op. B	%Op. C
Bus6	Bus	UnderVoltage	0.120	kV	0.065	0.066	0.067	93.6	95.2	96.0
Bus8	Bus	UnderVoltage	0.120	kV	0.065	0.066	0.067	93.6	95.2	96.0
Bus11	Bus	UnderVoltage	4.160	kV	2.251	2.284	2.303	93.7	95.1	95.9
Bus12	Bus	UnderVoltage	4.160	kV	2.251	2.284	2.303	93.7	95.1	95.9
Bus13	Bus	UnderVoltage	4.160	kV	2.251	2.284	2.302	93.7	95.1	95.9
Bus14	Bus	UnderVoltage	4.160	kV	2.251	2.284	2.302	93.7	95.1	95.9
Bus17	Bus	UnderVoltage	0.480	kV	0.217	0.263	0.265	78.2	94.9	95.7
Bus17	Bus	VUF 2 (Neg. Seq.)	0.430	kV	0.033	0.000	0.000	7.6	0.0	0.0
Bus17	Bus	VUF 0 (Zero Seq.)	0.248	kV	0.015	0.000	0.000	6.0	0.0	0.0
Bus18	Bus	UnderVoltage	0.480	kV	0.217	0.263	0.265	78.2	94.9	95.7
Bus18	Bus	VUF 2 (Neg. Seq.)	0.430	kV	0.033	0.000	0.000	7.6	0.0	0.0
Bus18	Bus	VUF 0 (Zero Seq.)	0.248	kV	0.015	0.000	0.000	6.0	0.0	0.0
Bus19	Bus	UnderVoltage	0.480	kV	0.217	0.263	0.265	78.2	94.9	95.7
Bus19	Bus	VUF 2 (Neg. Seq.)	0.430	kV	0.033	0.000	0.000	7.6	0.0	0.0
Bus19	Bus	VUF 0 (Zero Seq.)	0.248	kV	0.015	0.000	0.000	6.0	0.0	0.0
Bus20	Bus	UnderVoltage	0.480	kV	0.217	0.263	0.265	78.2	94.9	95.7
Bus20	Bus	VUF 2 (Neg. Seq.)	0.430	kV	0.033	0.000	0.000	7.6	0.0	0.0
Bus20	Bus	VUF 0 (Zero Seq.)	0.248	kV	0.015	0.000	0.000	6.0	0.0	0.0
Cable8-	Cable	IUF 2 (Neg. Seq.)	312.378	Amp	230.893	230.893	230.893	73.9	73.9	73.9
Cable11	Cable	IUF 2 (Neg. Seq.)	312.378	Amp	230.893	230.893	230.893	73.9	73.9	73.9
T7	2W XFMR	Overload	7.500	MVA	4.846	0.603	0.607	193.9	24.1	24.3
T7	2W XFMR	LIUR (Pos. Seq.)	8982.193	Amp	13384.600	6689.082	6695.520	149.0	74.5	74.5
T7	2W XFMR	IUF 2 (Neg. Seq.)	8980.880	Amp	6638.176	6638.176	6638.176	73.9	73.9	73.9
T8	2W XFMR	Overload	7.500	MVA	4.846	0.603	0.607	193.9	24.1	24.3
T8	2W XFMR	LIUR (Pos. Seq.)	8982.193	Amp	13384.600	6689.082	6695.520	149.0	74.5	74.5
T8	2W XFMR	IUF 2 (Neg. Seq.)	8980.880	Amp	6638.176	6638.176	6638.176	73.9	73.9	73.9

Marginal Report

Device ID	Type	Condition	Rating/Limit	Unit	Operating A	Operating B	Operating C	%Op. A	%Op. B	%Op. C
Bus4	Bus	UnderVoltage	13.800	kV	7.593	7.790	7.659	95.3	97.8	96.1
Bus 5	Bus	UnderVoltage	13.800	kV	7.593	7.790	7.659	95.3	97.8	96.1
Bus7	Bus	UnderVoltage	13.800	kV	7.592	7.789	7.659	95.3	97.8	96.1
Bus9	Bus	UnderVoltage	13.800	kV	7.592	7.789	7.659	95.3	97.8	96.1
Bus10	Bus	UnderVoltage	13.800	kV	7.592	7.789	7.659	95.3	97.8	96.1
Bus15	Bus	UnderVoltage	13.800	kV	7.592	7.789	7.659	95.3	97.8	96.1
Bus16	Bus	UnderVoltage	13.800	kV	7.593	7.790	7.659	95.3	97.8	96.1
Bus21	Bus	UnderVoltage	13.800	kV	7.593	7.790	7.659	95.3	97.8	96.1
Line 1	Line	IUF 2 (Neg. Seq.)	38.995	Amp	12.097	12.097	12.097	31.0	31.0	31.0
Line 2	Line	IUF 2 (Neg. Seq.)	38.995	Amp	12.097	12.097	12.097	31.0	31.0	31.0
Cable1	Cable	IUF 2 (Neg. Seq.)	207.194	Amp	16.771	16.771	16.771	8.1	8.1	8.1

Marginal Report

Device ID	Type	Condition	Rating/Limit	Unit	Operating A	Operating B	Operating C	%Op. A	%Op. B	%Op. C
Cable2-	Cable	IUF 2 (Neg. Seq.)	207.172	Amp	18.333	18.333	18.333	8.8	8.8	8.8
Cable3	Cable	IUF 2 (Neg. Seq.)	162.971	Amp	10.710	10.710	10.710	6.5	6.6	6.6
Cable5	Cable	IUF 2 (Neg. Seq.)	540.568	Amp	35.524	35.524	35.524	6.5	6.6	6.6
Cable6-	Cable	IUF 2 (Neg. Seq.)	540.568	Amp	35.524	35.524	35.524	6.5	6.6	6.6
Cable7	Cable	IUF 2 (Neg. Seq.)	162.982	Amp	10.711	10.711	10.711	6.5	6.6	6.6
T1	2W XFMR	IUF 2 (Neg. Seq.)	43.217	Amp	12.094	12.094	12.094	28.0	28.0	28.0
T2	2W XFMR	IUF 2 (Neg. Seq.)	43.217	Amp	12.094	12.094	12.094	28.0	28.0	28.0
T5	2W XFMR	IUF 2 (Neg. Seq.)	540.626	Amp	35.528	35.528	35.528	6.5	6.6	6.6
T6	2W XFMR	IUF 2 (Neg. Seq.)	540.652	Amp	35.530	35.530	35.530	6.5	6.6	6.6
T7	2W XFMR	IUF 0 (Zero Seq.)	8980.880	Amp	6747.738	6747.738	6747.738	75.1	75.1	75.1
T8	2W XFMR	IUF 0 (Zero Seq.)	8980.880	Amp	6747.738	6747.738	6747.738	75.1	75.1	75.1
Cable17	Cable	IUF 2 (Neg. Seq.)	207.194	Amp	16.771	16.771	16.771	8.1	8.1	8.1
Cable23	Cable	IUF 2 (Neg. Seq.)	207.172	Amp	18.333	18.333	18.333	8.8	8.8	8.8
Cable12	Cable	IUF 2 (Neg. Seq.)	121.138	Amp	6.808	6.808	6.808	5.5	5.6	5.6
Cable8	Cable	IUF 2 (Neg. Seq.)	421.069	Amp	28.736	28.736	28.736	6.8	6.8	6.8
Cable19	Cable	IUF 2 (Neg. Seq.)	121.138	Amp	6.808	6.808	6.808	5.5	5.6	5.6
Cable21	Cable	IUF 2 (Neg. Seq.)	421.069	Amp	28.736	28.736	28.736	6.8	6.8	6.8

UNBALANCED LOAD FLOW REPORT

Bus			Voltage		Generation		Load		Load Flow						XFMR
ID	kV	Phase	kV	Ang	MW	Mvar	MW	Mvar	ID	Phase	MW	Mvar	Amp	% PF	% Tap
* Bus1	230.000	A	132.791	0.0	5.299	5.402	0	0	Bus2	A	2.650	2.701	28.5	70.0	
		B	132.791	-120.0	10.535	3.518	0	0		B	5.268	1.759	41.8	94.9	
		C	132.791	120.0	9.549	8.995	0	0		C	4.774	4.497	49.4	72.8	
									Bus3	A	2.650	2.701	28.5	70.0	
		B	0.000	0.0	0	0	0	0		B	5.268	1.759	41.8	94.9	
		C	0.000	0.0	0	0	0	0		C	4.774	4.497	49.4	72.8	
Bus2	230.000	A	132.547	0.0	0	0	0	0	Bus1	A	-2.648	-3.585	33.6	59.4	
		B	132.562	-120.1	0	0	0	0		B	-5.263	-2.636	44.4	89.4	
		C	132.397	119.9	0	0	0	0		C	-4.768	-5.366	54.2	66.4	
									Bus4	A	2.648	3.585	33.6	59.4	
		B	0.000	0.0	0	0	0	0		B	5.263	2.636	44.4	89.4	
		C	0.000	0.0	0	0	0	0		C	4.768	5.366	54.2	66.4	
									Bus3	A	0.000	0.000	0.0	0.0	
										B	0.000	0.000	0.0	0.0	
										C	0.000	0.000	0.0	0.0	
Bus3	230.000	A	132.547	0.0	0	0	0	0	Bus1	A	-2.648	-3.585	33.6	59.4	
		B	132.562	-120.1	0	0	0	0		B	-5.263	-2.636	44.4	89.4	
		C	132.397	119.9	0	0	0	0		C	-4.768	-5.366	54.2	66.4	
									Bus 5	A	2.648	3.585	33.6	59.4	
		B	0.000	0.0	0	0	0	0		B	5.263	2.636	44.4	89.4	
		C	0.000	0.0	0	0	0	0		C	4.768	5.366	54.2	66.4	
									Bus2	A	0.000	0.000	0.0	0.0	
										B	0.000	0.000	0.0	0.0	
										C	0.000	0.000	0.0	0.0	
Bus4	13.800	A	7.593	-31.6	0	0	0	0	Bus7	A	1.540	0.492	212.9	95.3	
		B	7.790	-151.9	0	0	0	0		B	1.545	0.720	218.8	90.6	
		C	7.659	81.0	0	0	0	0		C	1.358	0.540	190.8	92.9	
									Bus10	A	1.157	0.468	165.6	92.8	
		B	0.000	0.0	0	0	0	0		B	1.181	0.617	171.0	88.6	
		C	0.000	0.0	0	0	0	0		C	1.058	0.499	152.8	90.4	
									Bus16	A	-0.216	3.580	472.3	6.0	
										B	0.235	0.590	81.5	37.0	
										C	2.690	2.417	472.1	74.4	
									Bus2	A	-3.178	-4.778	755.7	55.4	
										B	-3.679	-2.194	549.8	85.9	
										C	-5.789	-3.702	897.1	84.3	
									Bus6	A	0.691	0.223	95.6	95.2	
										B	0.727	0.242	98.3	94.9	
										C	0.697	0.230	95.8	95.0	

Bus			Voltage		Generation		Load		Load Flow						XFMR
ID	kV	Phase	kV	Ang.	MW	Mvar	MW	Mvar	ID	Phase	MW	Mvar	Amp	% PF	% Tap
									Bus 5	A	-0.004	0.015	2.1	24.3	
										B	-0.009	0.025	3.5	34.1	
										C	-0.014	0.016	2.8	67.4	
Bus 5	13.800	A	7.593	-31.6	0	0	0	0	Bus9	A	1.548	0.484	213.6	95.5	
		B	7.790	-151.9	0	0	0	0		B	1.548	0.732	219.8	90.4	
		C	7.659	88.0	0	0	0	0		C	1.347	0.536	189.3	92.9	
									Bus15	A	1.151	0.507	165.6	91.5	
		B	0.000	0.0	0	0	0	0		B	1.159	0.657	171.0	87.0	
		C	0.000	0.0	0	0	0	0		C	1.041	0.534	152.8	89.0	
									Bus21	A	-0.216	3.580	472.3	6.0	
										B	0.235	0.590	81.5	37.0	
										C	2.690	2.417	472.1	74.4	
									Bus3	A	-3.178	-4.778	755.7	55.4	
										B	-3.679	-2.194	549.8	85.9	
										C	-5.789	-3.702	897.1	84.3	
									Bus8	A	0.691	0.223	95.6	95.2	
										B	0.727	0.242	98.3	94.9	
										C	0.697	0.230	95.8	95.0	
									Bus4	A	0.004	-0.015	2.1	24.3	
										B	0.009	-0.025	3.5	34.1	
										C	0.014	-0.016	2.8	67.4	
Bus6	0.120	A	0.065	-64.6	0	0	0.680	0.193	Bus4	A	-0.680	-0.193	10901.6	96.2	
		B	0.066	176.6	0	0	0.710	0.203		B	-0.710	-0.203	11198.5	96.1	
		C	0.067	55.2	0	0	0.716	0.211		C	-0.716	-0.211	11217.9	95.9	
Bus7	13.800	A	7.592	-31.6	0	0	1.540	0.492	Bus4	A	-1.540	-0.492	212.9	95.3	
		B	7.789	-151.9	0	0	1.545	0.720		B	-1.545	-0.720	218.8	90.6	
		C	7.659	88.0	0	0	1.358	0.540		C	-1.358	-0.540	190.8	92.9	
Bus8	0.120	A	0.065	-64.6	0	0	0.680	0.193	Bus 5	A	-0.680	-0.193	10901.6	96.2	
		B	0.066	176.6	0	0	0.710	0.203		B	-0.710	-0.203	11198.5	96.1	
		C	0.067	55.2	0	0	0.716	0.211		C	-0.716	-0.211	11217.9	95.9	
Bus9	13.800	A	7.592	-31.6	0	0	1.548	0.483	Bus 5	A	-1.548	-0.483	213.6	95.5	
		B	7.789	-151.9	0	0	1.548	0.731		B	-1.548	-0.731	219.8	90.4	
		C	7.659	88.0	0	0	1.347	0.536		C	-1.347	-0.536	189.3	92.9	
Bus10	13.800	A	7.592	-31.6	0	0	0	0	Bus4	A	-1.167	-0.468	165.6	92.8	
		B	7.789	-151.9	0	0	0	0		B	-1.180	-0.617	171.0	88.6	
		C	7.659	88.0	0	0	0	0		C	-1.058	-0.499	152.8	90.4	
									Bus11	A	1.167	0.468	165.6	92.8	
		B	0.000	0.0	0	0	0	0		B	1.180	0.617	171.0	88.6	
		C	0.000	0.0	0	0	0	0		C	1.058	0.499	152.8	90.4	
Bus11	4.160	A	2.251	-64.1	0	0	0	0	Bus13	A	1.081	0.420	515.0	93.2	
		B	2.284	176.9	0	0	0	0		B	1.200	0.531	574.6	91.5	
		C	2.303	55.7	0	0	0	0		C	1.091	0.567	534.0	88.8	

Bus			Voltage		Generation		Load		Load Flow						XFMR
ID	kV	Phase	kV	Ang.	MW	Mvar	MW	Mvar	ID	Phase	MW	Mvar	Amp	% PF	% Tap
									Bus10	A	-1.088	-0.402	515.0	93.8	
		B	0.000	0.0	0	0	0	0		B	-1.209	-0.511	574.6	92.1	
		C	0.000	0.0	0	0	0	0		C	-1.101	-0.548	534.0	89.5	
									Bus12	A	0.007	-0.018	8.6	36.0	
										B	0.009	-0.020	9.6	40.3	
										C	0.009	-0.018	8.9	45.9	
Bus12	4.160	A	2.251	-64.1	0	0	0	0	Bus14	A	1.081	0.420	515.0	93.2	
		B	2.284	176.9	0	0	0	0		B	1.200	0.531	574.6	91.5	
		C	2.303	55.7	0	0	0	0		C	1.091	0.567	534.0	88.8	
									Bus15	A	-1.074	-0.438	515.1	92.6	
		B	0.000	0.0	0	0	0	0		B	-1.191	-0.551	574.7	90.8	
		C	0.000	0.0	0	0	0	0		C	-1.082	-0.585	534.1	88.0	
									Bus11	A	-0.007	0.018	8.6	36.0	
										B	-0.009	0.020	9.6	40.3	
										C	-0.009	0.018	8.9	45.9	
Bus13	4.160	A	2.251	-64.1	0	0	1.081	0.420	Bus11	A	-1.081	-0.420	515.0	93.2	
		B	2.284	176.9	0	0	1.200	0.531		B	-1.200	-0.531	574.6	91.5	
		C	2.302	55.7	0	0	1.091	0.566		C	-1.091	-0.566	534.0	88.8	

									Bus14	A	0.000	0.000	0.0	0.0
		B	0.000	0.0	0	0	0	0		B	0.000	0.000	0.0	0.0
		C	0.000	0.0	0	0	0	0		C	0.000	0.000	0.0	0.0
Bus14	4.160	A	2.251	-64.1	0	0	1.081	0.420	Bus12	A	-1.081	-0.420	515.0	93.2
		B	2.284	176.9	0	0	1.200	0.531		B	-1.200	-0.531	574.6	91.5
		C	2.302	55.7	0	0	1.091	0.566		C	-1.091	-0.566	534.0	88.8
									Bus13	A	0.000	0.000	0.0	0.0
		B	0.000	0.0	0	0	0	0		B	0.000	0.000	0.0	0.0
		C	0.000	0.0	0	0	0	0		C	0.000	0.000	0.0	0.0
Bus15	13.800	A	7.592	-31.6	0	0	0	0	Bus 5	A	-1.151	-0.507	165.6	91.5
		B	7.789	-151.9	0	0	0	0		B	-1.159	-0.656	171.0	87.0
		C	7.659	87.0	0	0	0	0		C	-1.041	-0.534	152.8	89.0
									Bus12	A	1.151	0.507	165.6	91.5
		B	0.000	0.0	0	0	0	0		B	1.159	0.656	171.0	87.0
		C	0.000	0.0	0	0	0	0		C	1.041	0.534	152.8	89.0
Bus16	13.800	A	7.593	-31.6	0	0	0	0	Bus4	A	0.216	-3.580	472.3	6.0
		B	7.790	-151.9	0	0	0	0		B	-0.235	-0.590	81.5	37.0
		C	7.659	87.0	0	0	0	0		C	-2.690	-2.416	472.1	74.4
									Bus17	A	-0.216	3.580	472.3	6.0
		B	0.000	0.0	0	0	0	0		B	0.235	0.590	81.5	37.0
		C	0.000	0.0	0	0	0	0		C	2.690	2.416	472.1	74.4
Bus17	0.480	A	0.217	-66.6	0	0	0	0	Bus19	A	0.000	0.000	0.0	0.0
		B	0.263	178.3	0	0	0	0		B	0.000	0.000	0.0	0.0
		C	0.265	57.0	0	0	0	0		C	0.000	0.000	0.0	0.0

Bus			Voltage		Generation		Load		Load Flow						XFMR
ID	kV	Phase	kV	Ang	MW	Mvar	MW	Mvar	ID	Phase	MW	Mvar	Amp	% PF	% Tap
									Bus16	A	-2.167	-4.335	22366.8	44.7	
		B	0.000	00	0	0	0	0		B	-0.245	-0.551	2293.1	40.6	
		C	0.000	00	0	0	0	0		C	-0.213	-0.568	2286.7	35.1	
									Bus18	A	2.167	4.335	22366.8	44.7	
										B	0.245	0.551	2293.1	40.6	
										C	0.213	0.568	2286.7	35.1	
Bus18	0.480	A	0.217	-666	0	0	4.335	8.670	Bus20	A	0.000	0.000	0.0	0.0	
		B	0.263	1783	0	0	0.490	1.103		B	0.000	0.000	0.0	0.0	
		C	0.265	570	0	0	0.426	1.136		C	0.000	0.000	0.0	0.0	
									Bus21	A	-2.167	-4.335	22366.8	44.7	
		B	0.000	00	0	0	0	0		B	-0.245	-0.551	2293.1	40.6	
		C	0.000	00	0	0	0	0		C	-0.213	-0.568	2286.7	35.1	
									Bus17	A	-2.167	-4.335	22366.8	44.7	
										B	-0.245	-0.551	2293.1	40.6	
										C	-0.213	-0.568	2286.7	35.1	
Bus19	0.480	A	0.217	-666	0	0	0	0	Bus17	A	0.000	0.000	0.0	0.0	
		B	0.263	1783	0	0	0	0		B	0.000	0.000	0.0	0.0	
		C	0.265	57.0	0	0	0	0		C	0.000	0.000	0.0	0.0	
									Bus20	A	0.000	0.000	0.0	0.0	
		B	0.000	0.0	0	0	0	0		B	0.000	0.000	0.0	0.0	
		C	0.000	0.0	0	0	0	0		C	0.000	0.000	0.0	0.0	
Bus20	0.480	A	0.217	-66.6	0	0	0	0	Bus18	A	0.000	0.000	0.0	0.0	
		B	0.263	178.3	0	0	0	0		B	0.000	0.000	0.0	0.0	
		C	0.265	57.0	0	0	0	0		C	0.000	0.000	0.0	0.0	
									Bus19	A	0.000	0.000	0.0	0.0	
		B	0.000	0.0	0	0	0	0		B	0.000	0.000	0.0	0.0	
		C	0.000	0.0	0	0	0	0		C	0.000	0.000	0.0	0.0	
Bus21	13.800	A	7.593	-31.6	0	0	0	0	Bus 5	A	0.216	-3.580	472.3	6.0	
		B	7.790	-151.9	0	0	0	0		B	-0.235	-0.590	81.5	37.0	
		C	7.659	87.0	0	0	0	0		C	-2.690	-2.416	472.1	74.4	
									Bus18	A	-0.216	3.580	472.3	6.0	
		B	0.000	0.0	0	0	0	0		B	0.235	0.590	81.5	37.0	
		C	0.000	0.0	0	0	0	0		C	2.690	2.416	472.1	74.4	

* Indicates a voltage regulated bus (voltage controlled or swing type machine connected to it)

# Indicates a bus with a load mismatch of more than 0.1 MVA

CASE 4

Alert-Basic Summary Report

	% Alert Settings	
	Critical	Marginal
Loading		
Bus	100.0	95.0
Cable	100.0	95.0
Reactor	100.0	95.0
Line	100.0	95.0
Transformer	100.0	95.0
Panel	100.0	95.0
Protective Device	100.0	95.0
Generator	100.0	95.0
Bus Voltage		
OverVoltage	105.0	102.0
UnderVoltage	95.0	98.0
Generator Excitation		
OverExcited (Q Max.)	100.0	95.0
UnderExcited (Q Min.)	100.0	

Alert-Advanced Summary Report

	% Alert Settings	
	Critical	Marginal
Bus Voltage		
Line Voltage Unbalanced Rate (LVUR)	100.0	100.0
Voltage Unbalanced Factor (VUF) Neg. Seq.	7.8	2.7
Voltage Unbalanced Factor (VUF) Zero Seq.	6.3	3.4
Branch Current		
Line Current Unbalanced Rate (LIUR)	150.0	150.0
Current Unbalanced Factor (IUF) Neg. Seq.	74.0	3.7
Current Unbalanced Factor (IUF) Zero Seq.	74.8	2.0

Critical Report

Device ID	Type	Condition	Rating/Limit	Unit	Operating A	Operating B	Operating C	%Op. A	%Op. B	%Op. C
Bus1	Bus	UnderVoltage	230.000	kV	119.511	132.791	132.791	90.0	100.0	100.0
Bus2	Bus	UnderVoltage	230.000	kV	119.292	132.534	132.379	89.8	99.8	99.7
Bus3	Bus	UnderVoltage	230.000	kV	119.292	132.534	132.379	89.8	99.8	99.7
Bus4	Bus	UnderVoltage	13.800	kV	7.214	7.401	7.615	90.5	92.9	95.6
Bus 5	Bus	UnderVoltage	13.800	kV	7.214	7.401	7.615	90.5	92.9	95.6
Bus6	Bus	UnderVoltage	0.120	kV	0.064	0.062	0.065	91.8	89.1	94.0
Bus7	Bus	UnderVoltage	13.800	kV	7.213	7.400	7.614	90.5	92.9	95.6
Bus8	Bus	UnderVoltage	0.120	kV	0.064	0.062	0.065	91.8	89.1	94.0
Bus9	Bus	UnderVoltage	13.800	kV	7.213	7.400	7.614	90.5	92.9	95.6
Bus10	Bus	UnderVoltage	13.800	kV	7.214	7.400	7.614	90.5	92.9	95.6
Bus11	Bus	UnderVoltage	4.160	kV	2.202	2.142	2.246	91.7	89.2	93.5
Bus12	Bus	UnderVoltage	4.160	kV	2.202	2.142	2.246	91.7	89.2	93.5
Bus13	Bus	UnderVoltage	4.160	kV	2.201	2.142	2.245	91.7	89.2	93.5
Bus14	Bus	UnderVoltage	4.160	kV	2.201	2.142	2.245	91.7	89.2	93.5
Bus15	Bus	UnderVoltage	13.800	kV	7.214	7.400	7.614	90.5	92.9	95.6
Bus16	Bus	UnderVoltage	13.800	kV	7.214	7.401	7.614	90.5	92.9	95.6
Bus17	Bus	UnderVoltage	0.480	kV	0.211	0.246	0.260	76.1	88.6	93.7
Bus17	Bus	VUF 2 (Neg. Seq.)	0.413	kV	0.032	0.000	0.000	7.8	0.0	0.0

Bus18	Bus	Under Voltage	0.480	kV	0.211	0.246	0.260	76.1	88.6	93.7
Bus18	Bus	VUF 2 (Neg. Seq.)	0.413	kV	0.032	0.000	0.000	7.8	0.0	0.0
Bus18	Bus	VUF 0 (Zero Seq.)	0.238	kV	0.015	0.000	0.000	6.4	0.0	0.0
Bus19	Bus	Under Voltage	0.480	kV	0.211	0.246	0.260	76.1	88.6	93.7
Bus19	Bus	VUF 2 (Neg. Seq.)	0.413	kV	0.032	0.000	0.000	7.8	0.0	0.0
Bus19	Bus	VUF 0 (Zero Seq.)	0.238	kV	0.015	0.000	0.000	6.4	0.0	0.0
Bus20	Bus	Under Voltage	0.480	kV	0.211	0.246	0.260	76.1	88.6	93.7
Bus20	Bus	VUF 2 (Neg. Seq.)	0.413	kV	0.032	0.000	0.000	7.8	0.0	0.0
Bus20	Bus	VUF 0 (Zero Seq.)	0.238	kV	0.015	0.000	0.000	6.4	0.0	0.0
Bus21	Bus	Under Voltage	13.800	kV	7.214	7.401	7.614	90.5	92.9	95.6
Cable8-	Cable	IUF 2 (Neg. Seq.)	316.748	Amp	234.534	234.534	234.534	74.0	74.0	74.0
Cable11	Cable	IUF 2 (Neg. Seq.)	316.748	Amp	234.534	234.534	234.534	74.0	74.0	74.0
T7	2W XFMR	Overload	7.500	MVA	4.780	0.578	0.598	191.2	23.1	23.9
T7	2W XFMR	IUF 2 (Neg. Seq.)	9106.521	Amp	6742.859	6742.859	6742.859	74.0	74.0	74.0
T7	2W XFMR	IUF 0 (Zero Seq.)	9106.521	Amp	6819.611	6819.611	6819.611	74.9	74.9	74.9
T8	2W XFMR	Overload	7.500	MVA	4.780	0.578	0.598	191.2	23.1	23.9
T8	2W XFMR	IUF 2 (Neg. Seq.)	9106.521	Amp	6742.859	6742.859	6742.859	74.0	74.0	74.0
T8	2W XFMR	IUF 0 (Zero Seq.)	9106.521	Amp	6819.611	6819.611	6819.611	74.9	74.9	74.9
Cable23	Cable	Overload	233.810	Amp	185.608	248.215	214.366	79.4	106.2	91.7

Marginal Report

Device ID	Type	Condition	Rating/Limit	Unit	Operating A	Operating B	Operating C	%Op. A	%Op. B	%Op. C
Bus1	Bus	VUF 2 (Neg. Seq.)	222.313	kV	7.667	0.000	0.000	3.4	0.0	0.0
Bus1	Bus	VUF 0 (Zero Seq.)	128.364	kV	4.426	0.000	0.000	3.4	0.0	0.0
Bus2	Bus	VUF 2 (Neg. Seq.)	221.821	kV	7.533	0.000	0.000	3.4	0.0	0.0
Bus2	Bus	VUF 0 (Zero Seq.)	128.068	kV	4.428	0.000	0.000	3.5	0.0	0.0
Bus3	Bus	VUF 2 (Neg. Seq.)	221.821	kV	7.533	0.000	0.000	3.4	0.0	0.0
Bus3	Bus	VUF 0 (Zero Seq.)	128.068	kV	4.428	0.000	0.000	3.5	0.0	0.0
Bus4	Bus	VUF 2 (Neg. Seq.)	12.812	kV	0.402	0.000	0.000	3.1	0.0	0.0
Bus 5	Bus	VUF 2 (Neg. Seq.)	12.812	kV	0.402	0.000	0.000	3.1	0.0	0.0
Bus6	Bus	VUF 2 (Neg. Seq.)	0.110	kV	0.003	0.000	0.000	3.1	0.0	0.0
Bus7	Bus	VUF 2 (Neg. Seq.)	12.830	kV	0.402	0.000	0.000	3.1	0.0	0.0
Bus8	Bus	VUF 2 (Neg. Seq.)	0.110	kV	0.003	0.000	0.000	3.1	0.0	0.0
Bus9	Bus	VUF 2 (Neg. Seq.)	12.830	kV	0.402	0.000	0.000	3.1	0.0	0.0
Bus10	Bus	VUF 2 (Neg. Seq.)	12.830	kV	0.402	0.000	0.000	3.1	0.0	0.0
Bus11	Bus	VUF 2 (Neg. Seq.)	3.804	kV	0.104	0.000	0.000	2.7	0.0	0.0
Bus12	Bus	VUF 2 (Neg. Seq.)	3.804	kV	0.104	0.000	0.000	2.7	0.0	0.0
Bus13	Bus	VUF 2 (Neg. Seq.)	3.803	kV	0.104	0.000	0.000	2.7	0.0	0.0
Bus14	Bus	VUF 2 (Neg. Seq.)	3.803	kV	0.104	0.000	0.000	2.7	0.0	0.0
Bus15	Bus	VUF 2 (Neg. Seq.)	12.830	kV	0.402	0.000	0.000	3.1	0.0	0.0
Bus16	Bus	VUF 2 (Neg. Seq.)	12.831	kV	0.402	0.000	0.000	3.1	0.0	0.0
Bus21	Bus	VUF 2 (Neg. Seq.)	12.831	kV	0.402	0.000	0.000	3.1	0.0	0.0
Line 1	Line	IUF 2 (Neg. Seq.)	39.720	Amp	13.707	13.707	13.707	34.5	34.5	34.5
Line 2	Line	IUF 2 (Neg. Seq.)	39.720	Amp	13.707	13.707	13.707	34.5	34.5	34.5
Cable1	Cable	IUF 2 (Neg. Seq.)	214.498	Amp	33.575	33.575	33.575	15.7	15.7	15.7
Cable2-	Cable	IUF 2 (Neg. Seq.)	214.455	Amp	36.702	36.702	36.702	17.1	17.1	17.1
Cable3	Cable	IUF 2 (Neg. Seq.)	168.957	Amp	21.441	21.441	21.441	12.7	12.7	12.7
Cable5	Cable	IUF 2 (Neg. Seq.)	560.422	Amp	71.119	71.119	71.119	12.7	12.7	12.7
Cable6-	Cable	IUF 2 (Neg. Seq.)	560.422	Amp	71.119	71.119	71.119	12.7	12.7	12.7
Cable7	Cable	IUF 2 (Neg. Seq.)	168.968	Amp	21.443	21.443	21.443	12.7	12.7	12.7
T1	2W XFMR	IUF 2 (Neg. Seq.)	43.859	Amp	13.707	13.707	13.707	31.3	31.3	31.3
T2	2W XFMR	IUF 2 (Neg. Seq.)	43.859	Amp	13.707	13.707	13.707	31.3	31.3	31.3
T3	2W XFMR	IUF 2 (Neg. Seq.)	93.875	Amp	3.547	3.547	3.547	3.8	3.8	3.8
T4	2W XFMR	IUF 2 (Neg. Seq.)	93.875	Amp	3.547	3.547	3.547	3.8	3.8	3.8
T5	2W XFMR	IUF 2 (Neg. Seq.)	560.482	Amp	71.127	71.127	71.127	12.7	12.7	12.7
T6	2W XFMR	IUF 2 (Neg. Seq.)	560.519	Amp	71.132	71.132	71.132	12.7	12.7	12.7
Cable17	Cable	IUF 2 (Neg. Seq.)	214.498	Amp	33.575	33.575	33.575	15.7	15.7	15.7
Cable23	Cable	IUF 2 (Neg. Seq.)	214.455	Amp	36.702	36.702	36.702	17.1	17.1	17.1
Cable12	Cable	IUF 2 (Neg. Seq.)	125.558	Amp	13.629	13.629	13.629	10.9	10.9	10.9
Cable8	Cable	IUF 2 (Neg. Seq.)	436.576	Amp	57.529	57.529	57.529	13.2	13.2	13.2
Cable19	Cable	IUF 2 (Neg. Seq.)	125.558	Amp	13.629	13.629	13.629	10.9	10.9	10.9
Cable21	Cable	IUF 2 (Neg. Seq.)	436.576	Amp	57.529	57.529	57.529	13.2	13.2	13.2

UNBALANCED LOAD FLOW REPORT

Bus			Voltage		Generation		Load		Load Flow						XFMR
ID	kV	Phase	kV	Ang.	MW	Mvar	MW	Mvar	ID	Phase	MW	Mvar	Amp	% PF	% Tap
* Bus1	230.000	A	119.511	0.0	4.736	4.223	0	0	Bus2	A	2.368	2.112	26.5	74.6	
		B	132.791	-120.0	11.536	4.152	0	0		B	5.768	2.076	46.2	94.1	
		C	132.791	120.0	8.772	9.801	0	0		C	4.386	4.900	49.5	66.7	
									Bus3	A	2.368	2.112	26.5	74.6	
		B	0.000	0.0	0	0	0	0		B	5.768	2.076	46.2	94.1	
		C	0.000	0.0	0	0	0	0		C	4.386	4.900	49.5	66.7	
Bus2	230.000	A	119.292	-0.1	0	0	0	0	Bus1	A	-2.366	-2.837	31.0	64.0	
		B	132.534	-120.1	0	0	0	0		B	-5.773	-2.943	48.9	89.1	
		C	132.379	119.9	0	0	0	0		C	-4.370	-5.763	54.6	60.4	
									Bus4	A	2.366	2.837	31.0	64.0	
		B	0.000	0.0	0	0	0	0		B	5.773	2.943	48.9	89.1	
		C	0.000	0.0	0	0	0	0		C	4.370	5.763	54.6	60.4	
									Bus3	A	0.000	0.000	0.0	0.0	
										B	0.000	0.000	0.0	0.0	
										C	0.000	0.000	0.0	0.0	
Bus3	230.000	A	119.292	-0.1	0	0	0	0	Bus1	A	-2.366	-2.837	31.0	64.0	
		B	132.534	-120.1	0	0	0	0		B	-5.773	-2.943	48.9	89.1	
		C	132.379	119.9	0	0	0	0		C	-4.370	-5.763	54.6	60.4	
									Bus 5	A	2.366	2.837	31.0	64.0	
		B	0.000	0.0	0	0	0	0		B	5.773	2.943	48.9	89.1	
		C	0.000	0.0	0	0	0	0		C	4.370	5.763	54.6	60.4	
									Bus2	A	0.000	0.000	0.0	0.0	
										B	0.000	0.000	0.0	0.0	
										C	0.000	0.000	0.0	0.0	
Bus4	13.800	A	7.214	-31.3	0	0	0	0	Bus7	A	1.312	0.338	187.8	96.8	
		B	7.401	-150.5	0	0	0	0		B	1.709	0.611	245.2	94.2	
		C	7.615	86.9	0	0	0	0		C	1.423	0.803	214.5	87.1	
									Bus10	A	1.021	0.370	150.6	94.0	
		B	0.000	0.0	0	0	0	0		B	1.276	0.550	187.7	91.8	
		C	0.000	0.0	0	0	0	0		C	1.110	0.675	170.7	85.4	
									Bus16	A	-0.204	3.442	477.9	5.9	
										B	0.215	0.570	82.3	35.3	
										C	2.657	2.515	480.5	72.6	
									Bus2	A	-2.738	-4.358	713.4	53.2	
										B	-3.869	-1.969	586.5	89.1	
										C	-5.867	-4.260	952.2	80.9	
									Bus6	A	0.621	0.201	90.5	95.1	
										B	0.667	0.217	94.7	95.1	
										C	0.695	0.239	96.5	94.6	

Bus			Voltage		Generation		Load		Load Flow						XFMR
ID	kV	Phase	kV	Ang.	MW	Mvar	MW	Mvar	ID	Phase	MW	Mvar	Amp	% PF	% Tap
									Bus 5	A	-0.012	0.007	1.9	87.4	
										B	0.002	0.022	2.9	9.7	
										C	-0.018	0.028	4.4	53.7	
Bus 5	13.800	A	7.214	-31.3	0	0	0	0	Bus9	A	1.301	0.318	185.6	97.1	
		B	7.401	-150.5	0	0	0	0		B	1.732	0.612	248.2	94.3	
		C	7.615	86.9	0	0	0	0		C	1.410	0.822	214.4	86.4	
									Bus15	A	1.008	0.404	150.6	92.8	
		B	0.000	0.0	0	0	0	0		B	1.257	0.592	187.7	90.5	
		C	0.000	0.0	0	0	0	0		C	1.087	0.712	170.7	83.7	
									Bus21	A	-0.204	3.442	477.9	5.9	
										B	0.215	0.570	82.3	35.3	
										C	2.657	2.515	480.5	72.6	
									Bus3	A	-2.738	-4.358	713.4	53.2	
										B	-3.869	-1.969	586.5	89.1	
										C	-5.867	-4.260	952.2	80.9	
									Bus8	A	0.621	0.201	90.5	95.1	
										B	0.667	0.217	94.7	95.1	
										C	0.695	0.239	96.5	94.6	

									Bus4	A	0.012	-0.007	1.9	87.4	
										B	-0.002	-0.022	2.9	9.7	
										C	0.018	-0.028	4.4	53.7	
Bus6	0.120	A	0.064	-64.2	0	0	0.653	0.194	Bus4	A	-0.653	-0.194	10709.8	95.9	
		B	0.062	176.4	0	0	0.625	0.173		B	-0.625	-0.173	10502.1	96.4	
		C	0.065	56.5	0	0	0.698	0.207		C	-0.698	-0.207	11186.8	95.9	
Bus7	13.800	A	7.213	-33.3	0	0	1.311	0.338	Bus4	A	-1.311	-0.338	187.8	96.8	
		B	7.400	-156.5	0	0	1.709	0.611		B	-1.709	-0.611	245.2	94.2	
		C	7.614	86.9	0	0	1.423	0.803		C	-1.423	-0.803	214.5	87.1	
Bus8	0.120	A	0.064	-64.2	0	0	0.653	0.194	Bus 5	A	-0.653	-0.194	10709.8	95.9	
		B	0.062	176.4	0	0	0.625	0.173		B	-0.625	-0.173	10502.1	96.4	
		C	0.065	56.5	0	0	0.698	0.207		C	-0.698	-0.207	11186.8	95.9	
Bus9	13.800	A	7.213	-33.3	0	0	1.301	0.317	Bus 5	A	-1.301	-0.317	185.6	97.1	
		B	7.400	-156.5	0	0	1.732	0.612		B	-1.732	-0.612	248.2	94.3	
		C	7.614	86.9	0	0	1.410	0.822		C	-1.410	-0.822	214.4	86.4	
Bus10	13.800	A	7.214	-33.3	0	0	0	0	Bus4	A	-1.021	-0.370	150.6	94.0	
		B	7.400	-156.5	0	0	0	0		B	-1.275	-0.550	187.7	91.8	
		C	7.614	86.9	0	0	0	0		C	-1.110	-0.675	170.7	85.4	
									Bus11	A	1.021	0.370	150.6	94.0	
		B	0.000	0.0	0	0	0	0		B	1.275	0.550	187.7	91.8	
		C	0.000	0.0	0	0	0	0		C	1.110	0.675	170.7	85.4	
Bus11	4.160	A	2.202	-61.6	0	0	0	0	Bus13	A	0.985	0.495	500.7	89.4	
		B	2.142	176.6	0	0	0	0		B	1.152	0.363	563.8	95.4	
		C	2.246	56.8	0	0	0	0		C	1.235	0.659	623.5	88.2	

Bus			Voltage		Generation		Load		Load Flow						XFMR
ID	kV	Phase	kV	Ang.	MW	Mvar	MW	Mvar	ID	Phase	MW	Mvar	Amp	% PF	% Tap
									Bus10	A	-0.993	-0.479	500.8	90.1	
		B	0.000	0.0	0	0	0	0		B	-1.158	-0.344	563.8	95.9	
		C	0.000	0.0	0	0	0	0		C	-1.246	-0.639	623.6	89.0	
									Bus12	A	0.008	-0.017	8.4	44.7	
										B	0.006	-0.019	9.4	29.9	
										C	0.011	-0.021	10.4	46.9	
Bus12	4.160	A	2.202	-61.6	0	0	0	0	Bus14	A	0.985	0.495	500.7	89.4	
		B	2.142	176.6	0	0	0	0		B	1.152	0.363	563.8	95.4	
		C	2.246	56.8	0	0	0	0		C	1.235	0.659	623.5	88.2	
									Bus15	A	-0.977	-0.512	500.8	88.6	
		B	0.000	0.0	0	0	0	0		B	-1.146	-0.382	563.9	94.9	
		C	0.000	0.0	0	0	0	0		C	-1.224	-0.680	623.6	87.4	
									Bus11	A	-0.008	0.017	8.4	44.7	
										B	-0.006	0.019	9.4	29.9	
										C	-0.011	0.021	10.4	46.9	
Bus13	4.160	A	2.201	-61.6	0	0	0.985	0.495	Bus11	A	-0.985	-0.495	500.7	89.4	
		B	2.142	176.6	0	0	1.152	0.363		B	-1.152	-0.363	563.8	95.4	
		C	2.245	56.8	0	0	1.235	0.659		C	-1.235	-0.659	623.5	88.2	
									Bus14	A	0.000	0.000	0.0	0.0	
		B	0.000	0.0	0	0	0	0		B	0.000	0.000	0.0	0.0	
		C	0.000	0.0	0	0	0	0		C	0.000	0.000	0.0	0.0	

Bus14	4.160	A	2.201	-61.6	0	0	0.985	0.495	Bus12	A	-0.985	-0.495	500.7	89.4	
		B	2.142	178.6	0	0	1.152	0.363		B	-1.152	-0.363	563.8	95.4	
		C	2.245	58.8	0	0	1.235	0.659		C	-1.235	-0.659	623.5	88.2	
									Bus13	A	0.000	0.000	0.0	0.0	
		B	0.000	0.0	0	0	0	0		B	0.000	0.000	0.0	0.0	
		C	0.000	0.0	0	0	0	0		C	0.000	0.000	0.0	0.0	
Bus15	13.800	A	7.214	-33.3	0	0	0	0	Bus 5	A	-1.008	-0.404	150.6	92.8	
		B	7.400	-150.5	0	0	0	0		B	-1.256	-0.592	187.7	90.5	
		C	7.614	86.9	0	0	0	0		C	-1.087	-0.712	170.7	83.7	
									Bus12	A	1.008	0.404	150.6	92.8	
		B	0.000	0.0	0	0	0	0		B	1.256	0.592	187.7	90.5	
		C	0.000	0.0	0	0	0	0		C	1.087	0.712	170.7	83.7	
Bus16	13.800	A	7.214	-33.3	0	0	0	0	Bus4	A	0.204	-3.441	477.9	5.9	
		B	7.401	-150.5	0	0	0	0		B	-0.215	-0.570	82.3	35.3	
		C	7.614	86.9	0	0	0	0		C	-2.657	-2.515	480.5	72.6	
									Bus17	A	-0.204	3.441	477.9	5.9	
		B	0.000	0.0	0	0	0	0		B	0.215	0.570	82.3	35.3	
		C	0.000	0.0	0	0	0	0		C	2.657	2.515	480.5	72.6	
Bus17	0.480	A	0.211	-61.3	0	0	0	0	Bus19	A	0.000	0.000	0.0	0.0	
		B	0.246	178.2	0	0	0	0		B	0.000	0.000	0.0	0.0	
		C	0.260	58.4	0	0	0	0		C	0.000	0.000	0.0	0.0	

Bus			Voltage		Generation		Load		Load Flow						XFMR
ID	kV	Phase	kV	Ang.	MW	Mvar	MW	Mvar	ID	Phase	MW	Mvar	Amp	% PF	% Tap
									Bus16	A	-2.138	-4.275	22668.6	44.7	
		B	0.000	0.0	0	0	0	0		B	-0.235	-0.528	2352.0	40.6	
		C	0.000	0.0	0	0	0	0		C	-0.210	-0.560	2303.9	35.1	
									Bus18	A	2.138	4.275	22668.6	44.7	
										B	0.235	0.528	2352.0	40.6	
										C	0.210	0.560	2303.9	35.1	
Bus18	0.480	A	0.211	-61.3	0	0	4.275	8.551	Bus20	A	0.000	0.000	0.0	0.0	
		B	0.246	178.2	0	0	0.469	1.056		B	0.000	0.000	0.0	0.0	
		C	0.260	58.4	0	0	0.420	1.120		C	0.000	0.000	0.0	0.0	
									Bus21	A	-2.138	-4.275	22668.6	44.7	
		B	0.000	0.0	0	0	0	0		B	-0.235	-0.528	2352.0	40.6	
		C	0.000	0.0	0	0	0	0		C	-0.210	-0.560	2303.9	35.1	
									Bus17	A	-2.138	-4.275	22668.6	44.7	
										B	-0.235	-0.528	2352.0	40.6	
										C	-0.210	-0.560	2303.9	35.1	
Bus19	0.480	A	0.211	-61.3	0	0	0	0	Bus17	A	0.000	0.000	0.0	0.0	
		B	0.246	178.2	0	0	0	0		B	0.000	0.000	0.0	0.0	
		C	0.260	58.4	0	0	0	0		C	0.000	0.000	0.0	0.0	
									Bus20	A	0.000	0.000	0.0	0.0	
		B	0.000	0.0	0	0	0	0		B	0.000	0.000	0.0	0.0	
		C	0.000	0.0	0	0	0	0		C	0.000	0.000	0.0	0.0	
Bus20	0.480	A	0.211	-68.3	0	0	0	0	Bus18	A	0.000	0.000	0.0	0.0	
		B	0.246	178.2	0	0	0	0		B	0.000	0.000	0.0	0.0	
		C	0.260	58.4	0	0	0	0		C	0.000	0.000	0.0	0.0	
									Bus19	A	0.000	0.000	0.0	0.0	
		B	0.000	0.0	0	0	0	0		B	0.000	0.000	0.0	0.0	
		C	0.000	0.0	0	0	0	0		C	0.000	0.000	0.0	0.0	
Bus21	13.800	A	7.214	-33.3	0	0	0	0	Bus 5	A	0.204	-3.441	477.9	5.9	
		B	7.401	-150.5	0	0	0	0		B	-0.215	-0.570	82.3	35.3	
		C	7.614	86.9	0	0	0	0		C	-2.657	-2.515	480.5	72.6	
									Bus18	A	-0.204	3.441	477.9	5.9	
		B	0.000	0.0	0	0	0	0		B	0.215	0.570	82.3	35.3	
		C	0.000	0.0	0	0	0	0		C	2.657	2.515	480.5	72.6	

* Indicates a voltage regulated bus (voltage controlled or swing type machine connected to it)

# Indicates a bus with a load mismatch of more than 0.1 MVA

Bus Loading Summary Report

Bus			Bus Load						
ID	kV	Rated Amp	Phase	MW	Mvar	MVA	% PF	Amp	% Loading
Bus1	230.000		A	4.736	4.223	6.345	74.6	53.1	
			B	11.536	4.152	12.261	94.1	92.3	
			C	8.772	9.801	13.153	66.7	99.0	
Bus2	230.000		A	2.366	2.817	3.694	64.0	31.0	
			B	5.773	2.943	6.480	89.1	48.9	
			C	4.370	5.763	7.232	60.4	54.6	
Bus3	230.000		A	2.366	2.817	3.694	64.0	31.0	
			B	5.773	2.943	6.480	89.1	48.9	
			C	4.370	5.763	7.232	60.4	54.6	
Bus4	13.800		A	2.954	4.358	5.265	56.1	729.8	
			B	3.869	1.969	4.341	89.1	586.5	
			C	5.885	4.260	7.265	81.0	954.1	
Bus 5	13.800		A	2.942	4.365	5.264	55.9	729.6	
			B	3.871	1.990	4.352	88.9	588.1	
			C	5.867	4.288	7.267	80.7	954.3	
Bus6	0.120		A	0.653	0.194	0.681	95.9	10709.8	
			B	0.625	0.173	0.648	96.4	10502.1	
			C	0.698	0.207	0.728	95.9	11186.8	
Bus7	13.800		A	1.311	0.318	1.354	96.8	187.8	
			B	1.709	0.611	1.815	94.2	245.2	
			C	1.423	0.803	1.634	87.1	214.5	
Bus8	0.120		A	0.653	0.194	0.681	95.9	10709.8	
			B	0.625	0.173	0.648	96.4	10502.1	
			C	0.698	0.207	0.728	95.9	11186.8	
Bus9	13.800		A	1.301	0.317	1.339	97.1	185.6	
			B	1.732	0.612	1.837	94.3	248.2	
			C	1.410	0.822	1.632	86.4	214.4	
Bus10	13.800		A	1.021	0.370	1.086	94.0	150.6	
			B	1.275	0.550	1.389	91.8	187.7	
			C	1.110	0.675	1.299	85.4	170.7	
Bus11	4.160		A	0.993	0.495	1.110	89.5	504.1	
			B	1.158	0.363	1.213	95.4	566.5	
			C	1.246	0.659	1.410	88.4	627.9	
Bus12	4.160		A	0.985	0.512	1.110	88.7	504.2	
			B	1.152	0.382	1.214	94.9	566.6	
			C	1.235	0.680	1.410	87.6	627.9	
Bus13	4.160		A	0.985	0.495	1.102	89.4	500.7	
			B	1.152	0.363	1.208	95.4	563.8	
			C	1.235	0.659	1.400	88.2	623.5	
Bus14	4.160		A	0.985	0.495	1.102	89.4	500.7	
			B	1.152	0.363	1.208	95.4	563.8	
			C	1.235	0.659	1.400	88.2	623.5	

Bus			Bus Load						
ID	kV	Rated Amp	Phase	MW	Mvar	MVA	% PF	Amp	% Loading
Bus15	13.800		A	1.008	0.484	1.086	92.8	150.6	
			B	1.256	0.592	1.389	90.5	187.7	
			C	1.087	0.712	1.299	83.7	170.7	
Bus16	13.800		A	0.204	3.441	3.447	5.9	477.9	
			B	0.215	0.570	0.609	35.3	82.3	
			C	2.657	2.515	3.659	72.6	480.5	
Bus17	0.480		A	2.138	4.275	4.780	44.7	22668.6	
			B	0.235	0.528	0.578	40.6	2352.0	
			C	0.210	0.560	0.598	35.1	2303.9	
Bus18	0.480		A	4.275	8.551	9.560	44.7	45337.2	
			B	0.469	1.056	1.155	40.6	4703.9	
			C	0.420	1.120	1.196	35.1	4607.8	
Bus19	0.480		A	0	0	0	0	0	
			B	0	0	0	0	0	
			C	0	0	0	0	0	
Bus20	0.480		A	0	0	0	0	0	
			B	0	0	0	0	0	
			C	0	0	0	0	0	
Bus21	13.800		A	0.204	3.441	3.447	5.9	477.9	
			B	0.215	0.570	0.609	35.3	82.3	
			C	2.657	2.515	3.659	72.6	480.5	

* Indicates operating load of a bus exceeds the bus critical limit (100.00 % times the continuous rating).

# Indicates operating load of a bus exceeds the bus marginal limit (95.00 % times the continuous rating).

APPENDIX C. SYNTHESIS DESIGN OF REACTANCE BALANCING COMPENSATOR

Chapter 4 of Dr. Czarnecki unpublished data

Admittance of Shunt Reactance Compensator. When a reactance one-port is implemented as a shunt compensator, then such a compensator has to have specified susceptances for some supply voltage harmonic. When a load is to be compensated for harmonics of the order n from a set N, then the compensator susceptances $B_C(\omega)$ for $\omega = n\omega_1$ have to be equal to B_{Cn}. The general form of admittance $Y_C(s)$, specified by the number of POLEs and ZEROs, has to be found for that purpose. To find the number of POLEs and ZEROs, a constantly increasing susceptance $B_C(\omega)$, which for specified harmonic orders n assumes values B_{Cn}, has to be drafted. After that, POLEs and/or ZEROs at zero and infinity have to be added in such a way that $Y_C(s)$ could be a Reactance function. This enables to express the compensator admittance in the form

$$Y_C(s) = f(s)\frac{(s^2+z_1^2)...(s^2+z_n^2)}{(s^2+p_1^2)...(s^2+p_m^2)}, \quad \text{with } f(s) = \begin{cases} As \\ \dfrac{A}{s} \end{cases} \quad \text{and } A > 0.$$

Illustration 3. Let as assume that a reactance compensator has to compensate a load for the voltage fundamental harmonic and the third and the fifth order harmonics, which requires that compensator susceptances are B_{C1} = 2 S, B_{C3}= 1 S and B_{C5}. = – 0.8 S. A draft of the compensator susceptance $B_C(\omega)$ which can have such values is shown in Fig. 4.12.

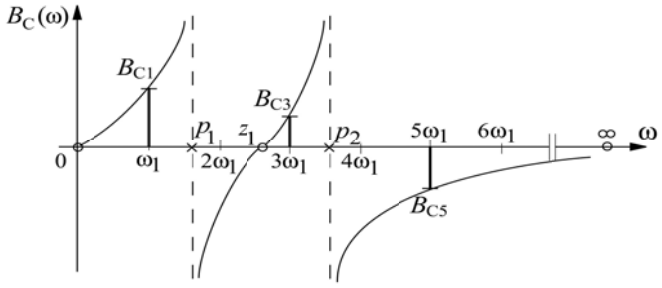

Figure 4.12. Draft of susceptance with given values of B_{C1}, B_{C3} and B_{C5}

Admittance of such a compensator has to have one ZERO and two POLES with ZEROs at zero and infinity, meaning it has to have the form

$$Y_C(s) = As\frac{(s^2+z_1^2)}{(s^2+p_1^2)(s^2+p_2^2)}.$$

It is specified by four unknown parameters: A, z_1, p_1 and p_2. There are, however, only three equations for their calculation, meaning the B_{C1}, B_{C3} and B_{C5} for Thus, one of unknown

parameters has to be chosen at the designer discretion with, of course, some limitations imposed by the plot of $B_C(\omega)$, shown in Fig. 4.12. To simplify calculations, the fundamental frequency ω_1 is usually normalized by assumption that ω_1 = 1 rd/s.

Let the ZERO z_1 is selected as a known parameter, for example, $z_1 = 2\omega_1 = 2$. Thus, three equations for $s = j1$, $s = j3$ and $s = j5$ have to be solved for parameters A, p_1, p_2 calculation, namely

$$A(j1)\frac{(-1+2^2)}{(-1+p_1^2)(-1+p_2^2)} = jB_{C1},$$

$$A(j3)\frac{(-9+2^2)}{(-9+p_1^2)(-9+p_2^2)} = jB_{C3},$$

$$A(j5)\frac{(-25+2^2)}{(-25+p_1^2)(-25+p_2^2)} = jB_{C5}.$$

They can be simplified, with $p_1^2 \to x$, $p_2^2 \to y$, to

$$A\frac{3}{(x-1)(y-1)} = 2,$$

$$3A\frac{-5}{(x-9)(y-9)} = 1,$$

$$5A\frac{-21}{(x-25)(y-25)} = -0.8.$$

This set of equations has a solution: $A = 2.162$, $p_1 = 1.125$, $p_2 = 3.632$. Thus, the admit-tance of the compensator has the form

$$Y_C(s) = 2.162s\frac{(s^2+4)}{(s^2+1.266)(s^2+13.192)}.$$

Reactance One-Port Structures. One of main features that differentiate the circuit synthesis from the circuit analysis is a possibility of existence of equivalent solutions of the same synthesis problem. In particular, one-ports of different structure with different parame-ters can have the same admittance or impedance.

There are four basic procedures of developing the reactance one-port structure when its admittance is known. These are two ***Foster procedures*** and two ***Cauer procedures***.

The one-port admittance $Y(s)$ can be developed in elementary fractions as follows

$$Y(s) = f(s)\frac{(s^2+z_1^2)...(s^2+z_n^2)}{(s^2+p_1^2)...(s^2+p_m^2)} = a_0\frac{1}{s} + a_\infty s + \sum_{r=1}^{m}\frac{a_r s}{s^2+p_r^2},$$

with

$$a_0 = \lim_{s\to 0}\{sY(s)\},$$

$$a_\infty = \lim_{s\to\infty}\{\frac{1}{s}Y(s)\},$$

$$a_r = \lim_{s^2\to -p_r^2}\{\frac{s^2+p_r^2}{s}Y(s)\}.$$

The fractions in this decomposition stand for admittances of LC branches connected in parallel, as shown in Fig. 4.13. Such a procedure is referred to as the ***Foster First Procedure***. In this

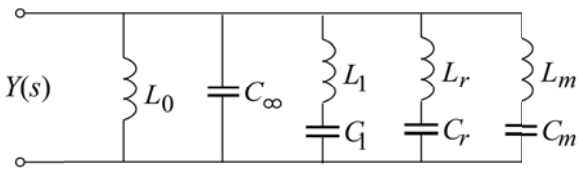

Figure 4.13. Reactance one-port with Foster First structure

structure

$$L_0 = \frac{1}{a_0}, \quad C_\infty = a_\infty, \quad L_r = \frac{1}{a_r}, \quad C_r = \frac{a_r}{p_r^2}.$$

Illustration 4. The admittance of the compensator found in Illustration 3 can be decomposed into elementary fractions as follows

$$Y_C(s) = 2.162\, s \frac{(s^2+4)}{(s^2+1.266)(s^2+13.192)} = a_0 \frac{1}{s} + a_\infty\, s + \frac{a_1 s}{s^2+1.266} + \frac{a_2 s}{s^2+13.192},$$

with

$$a_0 = \lim_{s\to 0}\{s\, Y_C(s)\} = 0, \quad a_\infty = \lim_{s\to\infty}\{\frac{1}{s} Y_C(s)\} = 0,$$

$$a_1 = \lim_{s^2\to -1.266}\{\frac{s^2+1.266}{s} Y_C(s)\} = 2.162 \frac{(-1.266+4)}{(-1.266+13.192)} = 0.495,$$

$$a_2 = \lim_{s^2\to -13.192}\{\frac{s^2+13.192}{s} Y_C(s)\} = 2.162 \frac{(-13.192+4)}{(-13.192+1.266)} = 1.667.$$

Thus, the compensator has the structure shown in Fig. 4.14. Observe that inductance $L_0 = 1/a_0$ is infinite, meaning it is simply an open branch.

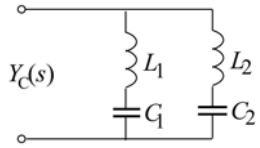

Figure 4.14. Compensator Foster First structure

The remaining parameters are

$$L_1 = \frac{1}{a_1} = \frac{1}{0.495} = 2.02\,\text{H},$$

$$C_1 = \frac{a_1}{p_1^2} = \frac{0.495}{1.266} = 0.391\,\text{F},$$

$$L_2 = \frac{1}{a_2} = \frac{1}{1.667} = 0.60\,\text{H},$$

$$C_2 = \frac{a_2}{p_2^2} = \frac{1.667}{13.192} = 0.126\,\text{F}.$$

These values are surprisingly high. Observe however, that the compensator admittance $Y_C(s)$ and parameters of the compensator were calculated, for the sake of computation simplification, under the assumption that the fundamental angular frequency of the supply voltage is $\omega_1 = 1$ rd/s. Such an assumption is referenced to as the frequency ***normalization***. Moreover, often the level of admittance is normalized as well. It can be assumed for example, that $B_{C1} = 1$ S. Thus, the parameters of the compensator shown in Fig. 4.14 are parameters of a normalized compensator.

The admittance $Y_D(s)$ of a ***de-normalized*** compensator are related to admittance of the normalized compensator by the relation

$$Y_D(s) = kY(\frac{s}{\omega_1}) .$$

Using the Foster decomposition, we can find the LC parameters of a de-normalized compensator as follows

$$Y_D(s) = kY(\frac{s}{\omega_1}) = k\,(a_0\frac{1}{\frac{s}{\omega_1}} + a_\infty\frac{s}{\omega_1} + \sum_{r=1}^{m}\frac{a_r\frac{s}{\omega_1}}{(\frac{s}{\omega_1})^2 + p_r^2}) =$$

$$= (k\omega_1 a_0)\frac{1}{s} + \frac{ka_\infty}{\omega_1}a_\infty\, s + \sum_{r=1}^{m}\frac{(k\omega_1 a_r)\,s}{s^2 + (\omega_1 p_r)^2}.$$

Thus, de-normalization requires that the circuit parameters are recalculated,

$$L_{D0} = \frac{1}{k\omega_1 a_0} = \frac{L_0}{k\omega_1}, \quad C_{D\infty} = \frac{ka_\infty}{\omega_1} = \frac{k}{\omega_1}C_\infty, \quad L_{Dr} = \frac{1}{k\omega_1 a_r} = \frac{L_r}{k\omega_1}, \quad C_{Dr} = \frac{k\omega_1 a_r}{(\omega_1 p_r)^2} = \frac{k}{\omega_1}C_r .$$

Observe that the compensator inductances and capacitances decline with the voltage angular frequency, ω_1. For example, for $f = 60$ Hz, meaning $\omega_1 = 377$ rd/s, and assuming that the admittance level is preserved, meaning $k = 1$, the parameters of the compensator shown in Fig. 4.14 are

$$L_{D1} = 5.36 \text{ mH}, \quad C_{D1} = 0.846 \text{ mF}, \quad L_{D2} = 1.59 \text{ mH}, \quad C_{D2} = 0.334 \text{ mF}.$$

Instead of decomposing the admittance into elementary fractions, its inversion, meaning the impedance can be decomposed in such a fractions, namely

$$Z(s) = \frac{1}{Y(s)} = \frac{1}{f(s)}\frac{(s^2 + p_1^2)\ldots(s^2 + p_m^2)}{(s^2 + z_1^2)\ldots(s^2 + z_n^2)} = b_0\frac{1}{s} + b_\infty\, s + \sum_{r=1}^{n}\frac{b_r s}{s^2 + z_r^2} ,$$

with

$$b_0 = \lim_{s\to 0}\{s\frac{1}{Y(s)}\} ,$$

$$b_\infty = \lim_{s\to\infty}\{\frac{1}{s}\frac{1}{Y(s)}\} ,$$

$$b_r = \lim_{s^2\to -z_r^2}\{\frac{s^2 + z_r^2}{s}\frac{1}{Y(s)}\} .$$

The fractions in this decomposition stand for impedances of LC links connected in series, as shown in Fig. 4.15. Such a procedure is referred to as the ***Foster Second Procedure***.

In this structure

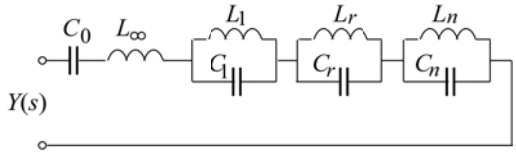

Figure 4.15. Reactance one-port with Foster Second structure

$$C_0 = \frac{1}{b_0}, \quad L_\infty = b_\infty, \quad C_r = \frac{1}{b_r}, \quad L_r = \frac{b_r}{z_r^2}.$$

Illustration 5. The admittance of the compensator found in Illustration 3 can be decomposed according to the Foster Second Procedure into elementary fractions as follows

$$Z_C(s) = \frac{1}{Y_C(s)} = \frac{1}{2.162\,s}\frac{(s^2+1.266)(s^2+13.192)}{(s^2+4)} = b_0\frac{1}{s} + b_\infty\, s + \frac{b_1 s}{s^2+4},$$

with

$$b_0 = \lim_{s\to 0}\{s\frac{1}{Y_C(s)}\} = \frac{1}{2.162}\frac{(1.266)(13.192)}{4} = 1.93,$$

$$b_\infty = \lim_{s\to\infty}\{\frac{1}{s}\frac{1}{Y(s)}\} = \lim_{s\to\infty}\{\frac{1}{2.162\,s^2}\frac{(s^2+1.266)(s^2+13.192)}{(s^2+4)}\} = 0.462,$$

$$b_1 = \lim_{s^2\to -z_1^2}\{\frac{s^2+z_1^2}{s}\frac{1}{Y(s)}\} = \frac{(-4+1.266)(-4+13.192)}{2.162\,(-4)} = 2.90.$$

The compensator structure obtained in the Foster Second Procedure is shown in Fig. 4.16.

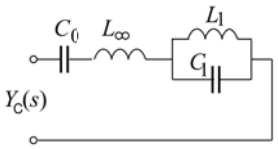

Figure 4.16. Compensator with Foster Second structure

Its parameters are equal to

$$C_0 = \frac{1}{b_0} = 0.518 \text{ F}, \quad L_\infty = b_\infty = 0.462 \text{ H},$$

$$C_1 = \frac{1}{b_1} = 0.345 \text{ F}, \quad L_1 = \frac{b_1}{z_1^2} = 0.725 \text{ H}.$$

If the one-port admittance Y(s) has a POLE at infinity, meaning the numerator polynomial is of higher degree than denominator, then division of the numerator by denominator removes this POLE and consequently, the remainder has ZERO at infinity. Inversion of the remainder has the POLE at infinity which can be removed again by division of the remainder numerator by its denominator.

Sequential division of inverted remainders enables presentation of the reactance admittance in a form of the following stairs-like fraction

$$Y(s) = \frac{a_n s^n + a_{n-2} s^{n-2} + ...}{b_m s^m + b_{m-2} s^{m-2} + ...} = d_1 s + \cfrac{1}{d_2 s + \cfrac{1}{d_3 s + \cfrac{1}{d_4 s + ...}}}$$

This decomposition ends up in a finite number of steps with real, positive coefficients. Such a fraction specifies admittance of an LC one-port with a ladder structure, shown in Fig. 4.17 with parameters,

$$C_1 = d_1,\ L_2 = d_2,\ C_3 = d_3,\ L_4 = d_4,\ ..$$

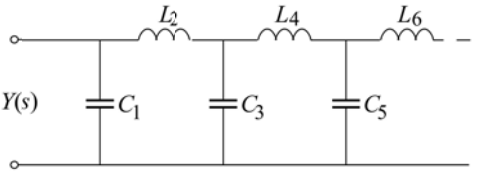

Figure 4.17. Reactance one-port with Cauer First structure

When admittance $Y(s)$ does not have a POLE at infinity, then its inversion has such a POLE. Decomposition of admittance $Y(s)$ into a stars-like fraction begins in such a case from inversion of $Y(s)$. In effect, this fraction will not have the element $d_1 s$ and the branch with capacitance C_1.

Such a procedure is referred to as the ***Cauer First procedure***. Observe, that in the case of the Foster First structure, branches were tuned to specific POLEs frequencies. In the case of the Foster Second structure, links were tuned to specific ZEROs frequencies. The Cauer procedure results in a one-port with the ladder structure. There are no branches or links tuned to specific POLEs or ZEROs frequencies. All circuit LC elements contribute to natural frequencies.

Illustration 6. The admittance of the compensator found in Illustration 3 can be rearranged as follows,

$$Y_C(s) = 2.162\, s \frac{(s^2 + 4)}{(s^2 + 1.266)(s^2 + 13.192)} = \frac{2.162 s^3 + 8.648 s}{s^4 + 14.458 s^2 + 16.701},$$

and decomposed according to the Cauer First Procedure into stirs-like fraction

$$Y_C(s) = \frac{2.162 s^3 + 8.648 s}{s^4 + 14.458 s^2 + 16.701} = \cfrac{1}{0.462 s + \cfrac{1}{0.207 s + \cfrac{1}{2.01 s + \cfrac{1}{0.311}}}},$$

thus, because the coefficient $d_1 = 0$, the compensator does not have the first shunt capacitive branch with the capacitance C_1. Its structure is shown in Fig. 4.18. The parameters are:

$$L_2 = 0.462 \text{ H},\ C_3 = 0.207 \text{ F},$$

$$L_4 = 2.01 \text{ H},\quad C_5 = 0.311 \text{ F}.$$

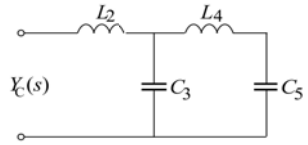

Figure 4.18. Compensator with Cauer First structure

Let us assume that denominator of a reactance function $Y(s)$ is an odd polynomial. The polynomials can be rearranged in such a way that the power of s increases, namely

$$Y(s) = \frac{a_0 + a_2 s^2 + a_4 s^4 + ...}{b_1 s + b_3 s^3 + a_5 s^5 + ...}.$$

It means that the admittance has a POLE at zero. When the odd polynomial is in the numerator of $Y(s)$, then this polynomial is a denominator of the inversion, $1/Y(s)$, thus this inversion has a POLE at zero.

Division of the even polynomial of the numerator by the odd polynomial of denominator removes the POLE at zero, meaning that the remainder has ZERO at zero. The inversion of the remainder has the POLE at zero again and this POLE can be removed again.

Continuation of divisions that remove the POLE at zero results in expression the function in a form of a following stairs-like fraction:

$$Y(s) = \frac{a_0 + a_2 s^2 + a_4 s^4 + ...}{b_1 s + b_3 s^3 + a_5 s^5 + ...} = \frac{1}{d_1 s} + \cfrac{1}{\cfrac{1}{d_2 s} + \cfrac{1}{\cfrac{1}{d_3 s} + \cfrac{1}{\cfrac{1}{d_4 s} + ...}}}.$$

Such decomposition ends up in a finite number of steps with real, positive coefficients d_1, d, d_3, …d_N. Such a stairs-like fraction is the impedance of a reactance one-port with the ladder structure shown in Fig. 4.19. The parameters of such a one-port are

$$L_1 = d_1,\ C_2 = d_2,\ L_3 = d_3,\ C_4 = d_4, \ldots$$

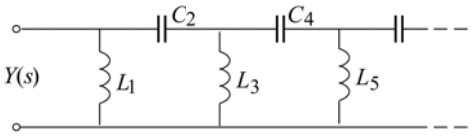

Figure 4.19. Reactance one-port with Cauer Second structure

When the odd polynomial is in the numerator, then the first term in this frac, the inductor does not have inductor L_1.Such procedure is referred to as ***Cauer Second p***rocedure. Simi-larly as in the case of the Cauer First procedure, there are no branches or links tuned to specific POLEs or ZEROs frequencies. All circuit LC elements contribute to natural frequencies.

Illustration 7. The admittance of the compensator found in Illustration 3 can be rearranged as follows,

$$Y_C(s) = 2.162 s \frac{(s^2 + 4)}{(s^2 + 1.266)(s^2 + 13.192)} = \frac{8.648 s + 2.162 s^3}{16.701 + 14.458 s^2 + s^4},$$

and decomposed according to the Cauer Second procedure into stirs-like fraction of the form

$$Y_C(s) = \frac{8.648s + 2.162s^3}{16.701 + 14.458s^2 + s^4} = = \cfrac{1}{\cfrac{1}{0.519s} + \cfrac{1}{\cfrac{1}{1.19s} + \cfrac{1}{\cfrac{1}{0.128s} + \cfrac{1}{\cfrac{1}{0.757s}}}}},$$

The compensator structure is shown in Fig. 4.20. Its LC parameters are equal to

$$C_2 = 0.519 \text{ F}, \quad L_3 = 1.19 \text{ H},$$

$$C_4 = 0.128 \text{ F}, \quad L_5 = 0.757 \text{ H},$$

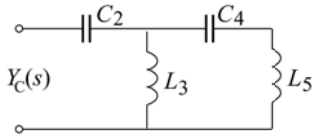

Figure 4.20. Compensator with Cauer Second structure

Compensators obtained as a result of these four procedures are, of course, entirely equivalent as to their admittance $Y_C(s)$. They differ, however, as to number of features, such as the total inductance, capacitance, power rating of compensator components, grounding, capabilities of tuning and so on. These are, moreover, not the only four structures. In the process of synthesis procedures can be changed to different ones, which changes the compensator structure. The more advanced issues are not presented in this Chapter, however. The reader is provided here with only some basic ideas on the reactive compensator synthesis.

APPENDIX D. SWITCHING COMPENSATOR DESIGN DETAILS

Chapter 17 of Dr. Czarnecki unpublished data

The unbalanced component of the fundamental harmonic of the compensator current $\boldsymbol{j}_{1u}(t)$ is equal to

$$\boldsymbol{j}_{1u}(t) = -\,\boldsymbol{i}_{1u}(t) = -\sqrt{2}\,\mathrm{Re}\{\boldsymbol{A}\,\boldsymbol{U}^{\#}e^{j\omega_1 t}\}\,,$$

where $\boldsymbol{A} = Ae^{j\psi}$ denotes the unbalance admittance of the load. Assuming that

$$u_{\mathrm{R}} = \sqrt{2}\,U_{\mathrm{R}}\cos(\omega_1 t+\alpha)\,,$$

the unbalanced current in line R compensator is

$$j_{1uR} = -\sqrt{2}\,AU_{\mathrm{R}}\cos(\omega_1 t+\alpha+\psi)\,,$$

while in phase S

$$j_{1uS} = -\sqrt{2}\,AU_{\mathrm{R}}\cos(\omega_1 t+\alpha+\psi+120^0)\,,$$

The unbalanced component has the following component in α, β coordinates

$$\boldsymbol{j}_{1u}^{\mathrm{C}}(t) = \begin{bmatrix} j_{1u\alpha}(t) \\ j_{1u\beta}(t) \end{bmatrix} = \mathsf{C}\begin{bmatrix} j_{1uR}(t) \\ j_{1uS}(t) \end{bmatrix} = -\sqrt{2}\,AU_{\mathrm{R}}\begin{bmatrix} \sqrt{3/2}, & 0 \\ 1/\sqrt{2}, & \sqrt{2} \end{bmatrix}\begin{bmatrix} \cos(\omega_1 t+\alpha+\psi) \\ \cos(\omega_1 t+\alpha+\psi+120^0) \end{bmatrix} =$$

$$= -\sqrt{3}\,AU_{\mathrm{R}}\begin{bmatrix} \cos(\omega_1 t+\alpha+\psi) \\ -\sin(\omega_1 t+\alpha+\psi) \end{bmatrix}\mathrm{V}.$$

The Clarke Vector of the unbalance current is equal to

$$\begin{aligned} \boldsymbol{J}_{1u}^{\mathrm{C}}(t) = j_{1u\alpha}(t) + j\,j_{1u\beta}(t) &= -\sqrt{3}\,AU_{\mathrm{R}}\,[\cos(\omega_1 t+\alpha+\psi) - j\sin(\omega_1 t+\alpha+\psi)] = \\ &= -\sqrt{3}\,A\,U_{\mathrm{R}}\,e^{-j(\omega_1 t+\alpha+\psi)} = -\boldsymbol{A}\,\boldsymbol{U}^{\mathrm{C}}\,e^{-j\omega_1 t} = \boldsymbol{J}_{1u}^{\mathrm{C}}\,e^{-j\omega_1 t} \end{aligned} \tag{17.20}$$

Thus, it rotates on the complex plane in the opposite direction to the Clarke Vector of the supply voltage. The Clarke Vector of the voltage drop on the inductor is

$$\Delta\boldsymbol{U}_{1u}^{\mathrm{C}}(t) = L\frac{d}{dt}\boldsymbol{J}_{1u}^{\mathrm{C}}(t) = L\frac{d}{dt}\{\boldsymbol{J}_{1u}^{\mathrm{C}}\,e^{-j\omega_1 t}\} = -j\,\omega_1 L\,\boldsymbol{J}_{1u}^{\mathrm{C}}\,e^{-j\omega_1 t}\,. \tag{17.21}$$

Orientation of all these vectors is shown in Fig. 17.7.

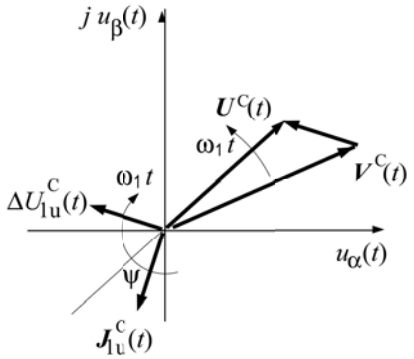

Figure 17.7. Clarke Vector of the voltage drop at inductor *L* caused unbalanced current

Due to rotation of vectors $\boldsymbol{U}^{\mathrm{C}}(t)$ and $\Delta\boldsymbol{U}^{\mathrm{C}}(t)$ in the opposite direction, there are instant of time when the length of the vector $\boldsymbol{V}^{\mathrm{C}}(t)$ is the sum of vectors $\boldsymbol{U}^{\mathrm{C}}(t)$ and $\Delta\boldsymbol{U}^{\mathrm{C}}(t)$ length and there are instants of time when it is their difference. Trajectory of the Clark Vector

$$\boldsymbol{V}^{\mathrm{C}}(t) = \boldsymbol{U}^{\mathrm{C}}\, e^{j\omega_1 t} - \Delta\boldsymbol{U}^{\mathrm{C}}\, e^{-j\omega_1 t}\,, \tag{17.22}$$

is an ellipse on the complex plane, as shown in Fig. 17.8.

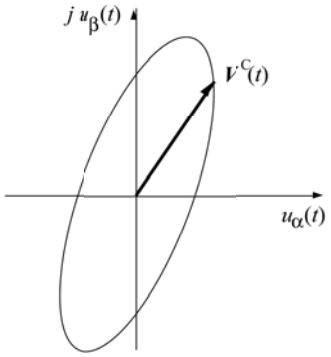

Figure 17.8. Clarke Vector of the inverter voltage at compensation of unbalanced current

Inverter switching modes. The PWM inverter enables control of the compensator line current by controlling the voltage on the inverter output terminals.

Since the sum of the compensator currents has to be equal to zero at each instant of time, only two compensator line currents, say $j_{\mathrm{R}}(t)$ and $j_{\mathrm{S}}(t)$, have to be controlled. The third current cannot be other than $j_{\mathrm{T}}(t) = -\,[j_{\mathrm{R}}(t) + j_{\mathrm{S}}(t)]$. This is fulfilled independently on whether there is an inductor in the T line or not, as shown in Fig. 17.13. Although it is commonly used, it is not needed for normal compensator operation.

To control these two line currents of the compensator, two line-to-line output voltages of the compensator have to be controlled. These could be voltages, referenced to the same common point, say voltages v_{RT} and v_{ST}.

The Clarke transform in the form presented by formula (17.10) is specified for phase-to-zero quantities. Its form for phase-to-phase quantities is therefore needed.

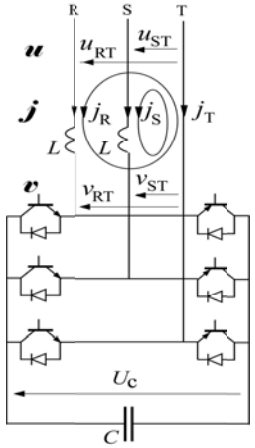

Figure 17.13. Switching compensator with only two line inductors

Since

$$v_{RT} = v_R - v_T = v_R - (-v_R - v_S) = 2v_R + v_S,$$
$$v_{ST} = v_S - v_T = v_S - (-v_R - v_S) = 2v_S + v_R, \tag{17.32}$$

line-to-zero voltages v_R and v_S can be expressed in terms of line-to-line voltages v_{RT} and v_{ST}, namely

$$v_R = \frac{1}{3}(2v_{RT} - v_{ST}),$$
$$v_S = \frac{1}{3}(2v_{ST} - v_{RT}), \tag{17.33}$$

hence, the voltage $\boldsymbol{v}$ in Clarke coordinates,

$$\boldsymbol{v}^C(t) = \begin{bmatrix} v_\alpha(t) \\ v_\beta(t) \end{bmatrix} = C \begin{bmatrix} v_R \\ v_S \end{bmatrix} = \frac{1}{3} \begin{bmatrix} \sqrt{3/2}, & 0 \\ 1/\sqrt{2}, & \sqrt{2} \end{bmatrix} \begin{bmatrix} 2v_{RT} - v_{ST} \\ 2v_{ST} - v_{RT} \end{bmatrix},$$

can be rearranged to the form

$$\boldsymbol{v}^C(t) = \begin{bmatrix} v_\alpha(t) \\ v_\beta(t) \end{bmatrix} = \begin{bmatrix} \sqrt{2/3}, & -1/\sqrt{6} \\ 0, & 1/\sqrt{2} \end{bmatrix} \begin{bmatrix} v_{RT}(t) \\ v_{ST}(t) \end{bmatrix} \equiv D \begin{bmatrix} v_{RT}(t) \\ v_{ST}(t) \end{bmatrix}. \tag{17.34}$$

A Two-Level inverter is built of six power transistor switches, with a diode that provides a current path for current of the opposite direction that can flow through the transistor. A pair of such switches with symbols of components is shown in Fig. 17.14.

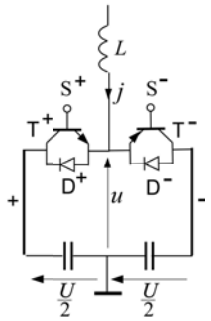

Figure 17.14. Pair of switches

Control of the inverter requires that there is full control over ON-OFF switching. Transistors enable such full control, but only for one direction of the current, marked by the emitter arrow. Diodes, however, are not controlled devices. One might have a doubt whether switches shown in Fig. 17.14 provide full ON-OFF control of a bidirectional current in the compensator output lines. Therefore, a detailed analysis of such a switch would be desirable.

Symbols T^+ and T^- as well as D+ and D^- denote transistors and diodes connected to the positive (+) and negative (–) dc bars of the inverter. Symbols S^+ and S^- denote switching signals of transistors, with logical values 1 (transistor in ON state) and 0 (transistor in OFF state).

To avoid a short circuit of the capacitor, the switches have to be controlled such that both of them cannot be in the ON state at the same time, meaning the logic product of control signals has to be equal to zero

$$S^+ \cdot S^- \equiv 0.$$

The change of the value of switching signals, S^+ and S^-, and the change of direction of the output current i, creates six different combinations of the switch conditions, thus it operates in one of six different modes. These combinations are shown in Fig. 17.15.

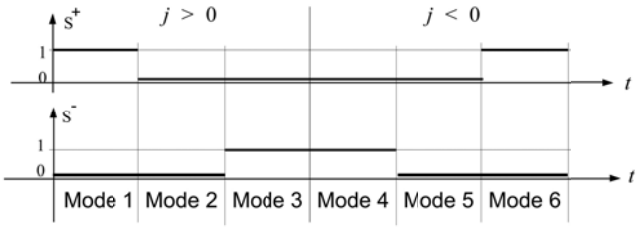

Figure 17.15. Combinations of switching signal values and the sign of output current

Observe that to avoid situations that, due to transients, both switches are in the ON state, there have to be intervals of time, where both switching signals have zero value, thus Mode 2 and Mode 5 are needed. Operation of the switch in particular modes is shown in Fig. 17.16.

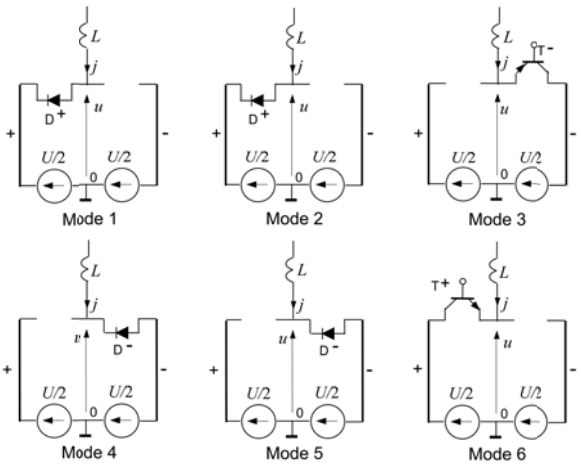

Figure 17.16. Modes of inverter switches operations

The purpose of the switch is connecting, according to the value of the switching signal, the output line of the inverter to the positive or negative dc bus.

Current paths in Fig. 17.16 show that at positive output current j, the output line is connected to the negative bus before switching signal S^- is equal to 1, meaning in Mode 2. When this current is negative, the output line is connected to the positive dc bus before S^+ is equal to 1, meaning in Mode 5. Thus, in Modes 2 and 5 the output line is not connected to the dc buses according to the switching signal values. Therefore, these two modes, necessary for avoiding switching hazard, should be as short as possible. Sequential switching of the inverter switches changes the state of the inverter and the voltage at the node $u(t)$ as shown in Fig. 17.17.

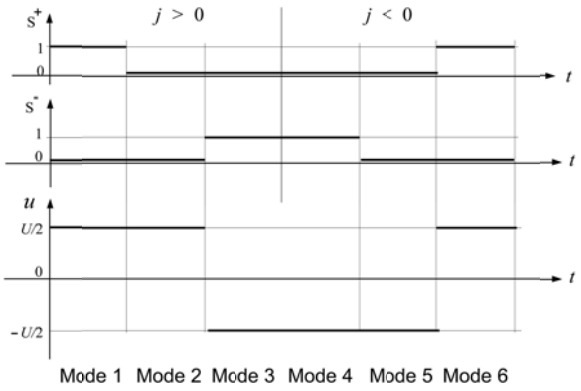

Figure 17.17. Switch states and the output voltage

The logical state of transistors which connect terminals R, S and T to the positive dc voltage bus specifies the ***state of the inverter*** in a binary or in a decimal number. According to Fig. 17.18 with sequential switching of only one switch, the inverter progresses through the sequence: State 4 >> State 6 >> State 2 >> State 3 >> State 1 >> state 5 >> State 4…..

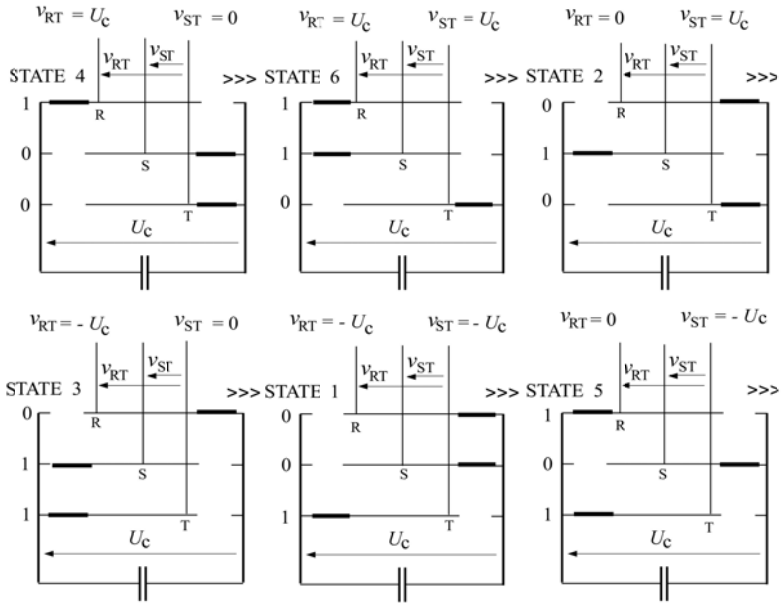

Figure 17.18. Inverter states

To produce zero voltage at the inverter output terminals, all switches connected to the positive dc bus have to be in ON or OFF states, as shown in Fig. 17.19. This creates two additional states of the inverter. Because the inverter output lines are short-circuited in these two state, they can be referred to as ***short-circuit states***. One of these states can be reached with only one transistor switched ON at any instant of the switching sequence.

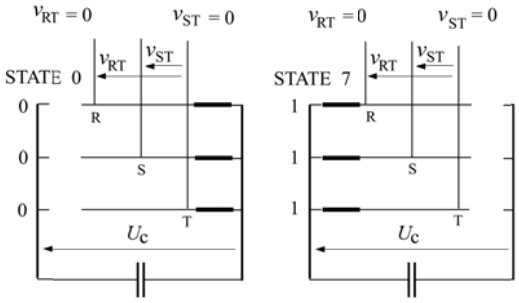

Figure 17.19. Short circuit states

The inverter output voltage $\boldsymbol{v}$ can have only seven values $\boldsymbol{v}_s$, where index s denotes the state decimal number, $\boldsymbol{v}_0$, $\boldsymbol{v}_1$, $\boldsymbol{v}_2$, $\boldsymbol{v}_3$, $\boldsymbol{v}_4$, $\boldsymbol{v}_5$, $\boldsymbol{v}_6$. The voltage in state 7, is equal to that in state 0, i.e., $\boldsymbol{v}_7 = \boldsymbol{v}_0 = \mathbf{0}$. The entries of vectors $\boldsymbol{v}_s$ in the line-to-line voltage form, meaning values of voltages v_{RT} and v_{ST}, are compiled in Figs. 17.18 and 17.19, respectively.

Clarke Vector of inverter voltage. Since the output voltage of the inverter can have only seven discrete values, the Clarke Vector of this voltage, denoted generally by $\boldsymbol{V}^C(t)$, can have only seven constant values

$$\boldsymbol{V}_s^C = V_s^C e^{j\phi_s} = [1, j]\boldsymbol{v}_s^C = [1, j]D\begin{bmatrix} v_{RT} \\ v_{ST} \end{bmatrix}_s = [1, j]\begin{bmatrix} \sqrt{2/3}, & -1/\sqrt{6} \\ 0, & 1/\sqrt{2} \end{bmatrix}\begin{bmatrix} v_{RT} \\ v_{ST} \end{bmatrix}_s . \qquad (17.35)$$

With this general expression, for sequential states of the inverter, we obtain

$$\boldsymbol{V}_1^C = [1, j]\begin{bmatrix} \sqrt{2/3}, & -1/\sqrt{6} \\ 0, & 1/\sqrt{2} \end{bmatrix}\begin{bmatrix} -U_c \\ -U_c \end{bmatrix} = \sqrt{\frac{2}{3}}U_c e^{-j120^0},$$

$$\boldsymbol{V}_2^C = [1, j]\begin{bmatrix} \sqrt{2/3}, & -1/\sqrt{6} \\ 0, & 1/\sqrt{2} \end{bmatrix}\begin{bmatrix} 0 \\ U_c \end{bmatrix} = \sqrt{\frac{2}{3}}U_c e^{j120^0},$$

$$\boldsymbol{V}_3^C = [1, j]\begin{bmatrix} \sqrt{2/3}, & -1/\sqrt{6} \\ 0, & 1/\sqrt{2} \end{bmatrix}\begin{bmatrix} -U_c \\ 0 \end{bmatrix} = \sqrt{\frac{2}{3}}U_c e^{j180^0},$$

$$\boldsymbol{V}_4^C = [1, j]\begin{bmatrix} \sqrt{2/3}, & -1/\sqrt{6} \\ 0, & 1/\sqrt{2} \end{bmatrix}\begin{bmatrix} U_c \\ 0 \end{bmatrix} = \sqrt{\frac{2}{3}}U_c,$$

$$\boldsymbol{V}_5^C = [1, j]\begin{bmatrix} \sqrt{2/3}, & -1/\sqrt{6} \\ 0, & 1/\sqrt{2} \end{bmatrix}\begin{bmatrix} 0 \\ -U_c \end{bmatrix} = \sqrt{\frac{2}{3}}U_c e^{-j60^0},$$

$$\boldsymbol{V}_6^C = [1, j]\begin{bmatrix} \sqrt{2/3}, & -1/\sqrt{6} \\ 0, & 1/\sqrt{2} \end{bmatrix}\begin{bmatrix} U_c \\ U_c \end{bmatrix} = \sqrt{\frac{2}{3}}U_c e^{j60^0}.$$

Thus, Clarke Vectors of the inverter output voltage $\boldsymbol{v}$ in particular states s have the same module

$$V_s^C = V^C = \sqrt{\frac{2}{3}}U_C = \text{const.},$$

with different angle ϕ_s which is an integer multiple of 60^0.

Since the length of the Clarke Vector cannot be lower than the minimum value specified by formula (17.31), the capacitor voltage cannot be lower than

$$U_{\mathrm{C}} \geq \sqrt{\frac{3}{2}}\, V_{\min}^{\mathrm{C}} = \sqrt{\frac{3}{2}}\{U^{\mathrm{C}} + \omega_1 L\,[(B_{1\mathrm{e}} + A)U^{\mathrm{C}} + \sum_{n\in N} n\, I_n^{\mathrm{C}}\} \tag{17.36}$$

The remaining two Clarke Vectors $\boldsymbol{V}_0^{\mathrm{C}} = \boldsymbol{V}_7^{\mathrm{C}} = \mathbf{0}$. Clarke Vectors of the inverter possible values of the output voltage $\boldsymbol{v}$ are shown in Fig. 17.20. These values change with the angle ϕ_{s} sequential increases from 0 to 360^0 with only one switch change from the OFF to the ON state between adjacent sectors.

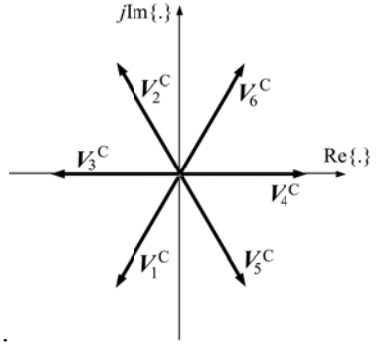

Figure 17.20. Clarke Vectors of the inverter output voltage $\boldsymbol{v}$.

Clarke Vectors $\boldsymbol{V}_s^{\mathrm{C}}$ of the inverter output voltage in particular states s divide the complex plane into six polar zones, Z_0, Z_1, Z_2, Z_3, Z_4 and Z_5, with the same polar angle of 60^0, as shown in Fig. 17.21.

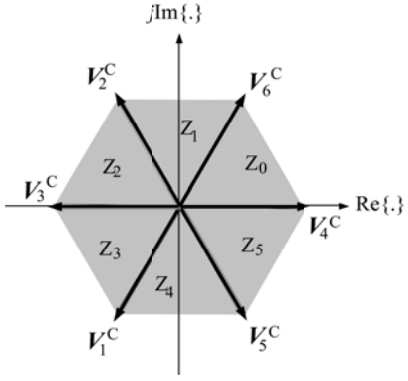

Figure 17.21. Zones of the complex plane of inverter voltage Clarke Vectors.

The zones are confined by Clarke Vectors of inverter states. For example, zone Z_0 is confined by vectors $\boldsymbol{V}_4^{\mathrm{C}}$ and $\boldsymbol{V}_6^{\mathrm{C}}$. Zone Z_4 is confined by vectors $\boldsymbol{V}_1^{\mathrm{C}}$ and $\boldsymbol{V}_5^{\mathrm{C}}$, and so on. The vector with the lower angle ϕ_{s} will be referred to as a ***right border*** of the zone and denoted with index "*n*", while the vector with higher ϕ_{s} will be referred to as the ***left border*** of the zone and denoted with index "m". For example, for zone Z_5, the borders are: $\boldsymbol{V}_n^{\mathrm{C}} = \boldsymbol{V}_5^{\mathrm{C}}$ and $\boldsymbol{V}_m^{\mathrm{C}} = \boldsymbol{V}_4^{\mathrm{C}}$.

Instant values of Clark Vector. The compensator control is not continuous, but discrete. The reference signal is calculated for sequential instants, kT_{s}. All calculations are performed on data sampled at the instant $(k-1)T_{\mathrm{s}}$, applied at instant kT_{s}, and effect can be observed at instant $(k+1)T_{\mathrm{s}}$. Taking into account that there is usually several hundred samples per single period T, let us neglect here, for simplification, the delay between data acquisition and control effects, i.e., let us assume that all happens at the same instant of time kT_{s}.

The needed Clarke Vector of inverter output voltage at instant kT_{s} is

$$\boldsymbol{V}^{\mathrm{C}}(k) \equiv V^{\mathrm{C}}(k)e^{j\Theta(k)} = \boldsymbol{U}^{\mathrm{C}}(k) - (R + L\frac{\Delta}{T_{\mathrm{s}}})\boldsymbol{J}_{\mathrm{r}}^{\mathrm{C}}(k), \tag{17.37}$$

where

$$\boldsymbol{U}^{\mathrm{C}}(k) \equiv u_{\alpha}(k) + i\,u_{\beta}(k) = [1, i]\,\boldsymbol{u}^{\mathrm{C}}(k) = [1, i]\,D\begin{bmatrix} u_{\mathrm{RT}}(k) \\ u_{\mathrm{ST}}(k) \end{bmatrix},$$

$$\boldsymbol{J}_{\mathrm{r}}^{\mathrm{C}}(k) \equiv j_{\mathrm{r}\alpha}(k) + i\,j_{\mathrm{r}\beta}(k) = [1, i]\,\boldsymbol{j}_{\mathrm{r}}^{\mathrm{C}}(k) = [1, i]\,C\begin{bmatrix} j_{\mathrm{rR}}(k) \\ j_{\mathrm{rS}}(k) \end{bmatrix}.$$

Observe that the symbol $i \equiv \sqrt{-1}$ was used to avoid confusion in the last formulae instead of j, which also denotes the compensator line current. This vector is located in one of six zones $Z_0,\ldots Z_5$, as illustrated in Fig. 17.22.

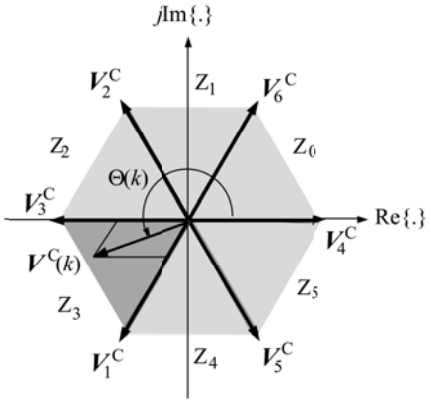

Figure 17.22. Example of Clarke Vector of inverter voltage at instant kT_{s}, located in zone Z_3

The zone number has to be identified because the needed voltage can be obtained only as a linear form of voltages that confines that zone, namely

$$\boldsymbol{V}^{\mathrm{C}}(k) = a_m \boldsymbol{V}_{\mathrm{m}}^{\mathrm{C}} + a_n \boldsymbol{V}_n^{\mathrm{C}}. \tag{17.38}$$

Coefficients of this form, a_{m} and a_n, are duty factors of switches, meaning the ratio of time τ_m in state m and time τ_n in state n to the sampling period, T_{s}, namely

$$\tau_m = a_m T_{\mathrm{s}}, \qquad \tau_n = a_n T_{\mathrm{s}}, \tag{17.39}$$

Since usually $\tau_m + \tau_n < T_{\mathrm{s}}$, for the remaining part of the sampling period T_{s}

$$\tau_0 = T_{\mathrm{s}} - (\tau_m + \tau_n), \tag{17.40}$$

the inverter should not contribute to the output voltage, meaning it should be in a short-circuit state, i.e., in state 0 or in state 7. The duty factor of the inverter in the short-circuit state is

$$a_0 \equiv \frac{\tau_0}{T_{\mathrm{s}}} = 1 - (a_m + a_n). \tag{17.41}$$

Since zones Z_0, Z_1, $\ldots Z_5$ are confined by different vectors, the calculation of duty factors a_m and a_n in these zones would result in a different formula. This could be avoided if the Clarke Vector of the inverter voltage needed at instant kT_{s}, originally located in zone Z_{s}, specified by formula

$$s(k) = \mathrm{int}\{\frac{\Theta(k)}{60}\}, \tag{17.42}$$

is rotated to zone Z_0 confined by vectors

$$A \rightarrow \boldsymbol{V}_4^{\mathrm{C}}, \qquad Ae^{j60^0} \rightarrow \boldsymbol{V}_6^{\mathrm{C}},$$

shown in Fig. 17.23.

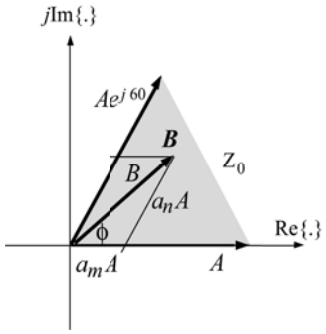

Figure 17.23. Zone Z_0 with rotated Clarke Vector ***B*** of the needed inverter voltage

After duty factors a_m and a_n are calculated for zone Z_0, they specify the linear form of the Clarke Vector in the original zone Z_s. The Clark Vector of the inverter voltage rotated to zone Z_0 has the value

$$\boldsymbol{B} \rightarrow Be^{j\phi} = V^{\mathrm{C}}(k)e^{j[\Theta(k)]\mathrm{mod}(60)}, \tag{17.43}$$

i.e., $B \rightarrow V^{\mathrm{C}}(k)$ and $\phi \rightarrow [\Theta(k)]$ mod(60). These three vectors have to satisfy the relationship

$$Be^{j\phi} = a_n\, Ae^{j60^0} + a_m\, A,$$

which can be presented in the rectangular form

$$B\cos\phi + jB\sin\phi = a_nA\cos 60^0 + ja_nA\sin 60^0 + a_mA,$$

$$B\cos\phi + jB\sin\phi = a_nA\frac{1}{2} + ja_nA\frac{\sqrt{3}}{2} + a_mA.$$

From equations for the real and the imaginary part, formulae for duty factor can be found:

$$a_n = \frac{2}{\sqrt{3}}\frac{B}{A}\sin\phi, \tag{17.44}$$

$$a_m = \frac{B}{A}\cos\phi - \frac{a_n}{2} = \frac{B}{A}(\cos\phi - \frac{1}{\sqrt{3}}\sin\phi). \tag{17.45}$$

Indeed, let us assume that $\phi = 0$, then $a_n = 0$, while $a_m = B/A$, meaning the inverter required output voltage is obtained entirely by the inverter in state 4. Now, let us assume that $\phi = 60^0$, than $a_n = B/A$, while $a_m = 0$, meaning the inverter output voltage is obtained entirely by the inverter in state 5. When $\phi = 30^0$ then

$$a_n = a_m = \frac{1}{\sqrt{3}}\frac{B}{A},$$

meaning the inverter should be in state 4 and 5 for the same interval of time.

Illustration 2. The Clarke Vector of the inverter voltage $\boldsymbol{v}(k)$ at some instant of time should be equal to $\boldsymbol{V}^{\mathrm{C}}(k) = 250\, e^{j200\mathrm{deg}}$ [V]. Which state of the inverter can provide this voltage and how long it should stay in these states if the capacitor voltage is $U_{\mathrm{C}} = 500$ [V] and the switching frequency $f_s = 18$ [kHz].

The Clarke Vector at this instant of time is in sector

$$s(k) = \mathrm{int}\{\frac{\Theta(k)}{60^0}\} = \mathrm{int}\{\frac{200^0}{60^0}\} = 3,$$

confined by vectors $\boldsymbol{V}_3^{\mathrm{C}}$ and $\boldsymbol{V}_1^{\mathrm{C}}$. States 3 and 1, which provide voltages $\boldsymbol{v}_3$ and $\boldsymbol{v}_1$ as well as state 0 are shown in Fig.17.24.

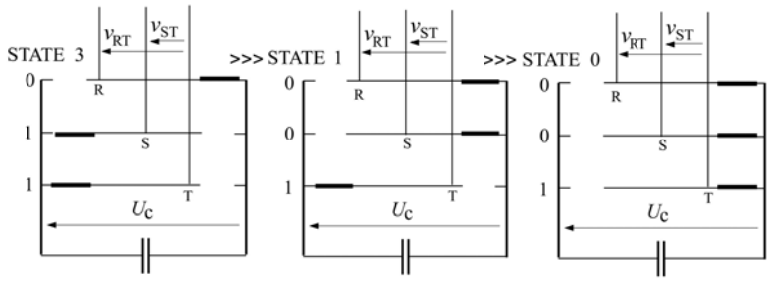

Figure 17.24. Inverter states in Illustration 1

Vector $\boldsymbol{V}^{\mathrm{C}}(k)$ rotated to sector zero is equal to

$$\boldsymbol{B} \square Be^{j\phi} = V^{\mathrm{C}}(k)e^{j[\Theta(k)]\mathrm{mod}(60)} = 250e^{j20^0}\ [\mathrm{V}],$$

while

$$A = \sqrt{\frac{2}{3}}U_{\mathrm{C}} = \sqrt{\frac{2}{3}}500 = 408\ [\mathrm{V}].$$

Duty factors a_{m} and a_{n} are equal to

$$a_n = \frac{2}{\sqrt{3}}\frac{B}{A}\sin\phi = \frac{2}{\sqrt{3}}\frac{250}{408}\sin(20^0) = 0.24,$$

$$a_m = \frac{B}{A}(\cos\phi - \frac{1}{\sqrt{3}}\sin\phi) = \frac{250}{408}(\cos 20^0 - \frac{1}{\sqrt{3}}\sin 20^0) = 0.45.$$

Duty factor in the zero state is

$$a_0 = 1 - (a_m + a_n) = 1 - (0.45 + 0.24) = 0.31.$$

Since the sampling period $T_{\mathrm{s}} = 1/f_{\mathrm{s}} = 1/18 \text{ x } 10^3 = 55$ [μs], thus the inverter should be in state 3 over time interval

$$\tau_{\mathrm{m}} = a_{\mathrm{m}}T_{\mathrm{s}} = 0.45 \text{ x } 55 = 24.7\ [\mu\mathrm{s}],$$

in state 1 over the interval

$$\tau_{\mathrm{n}} = a_{\mathrm{n}}T_{\mathrm{s}} = 0.24 \text{ x } 55 = 13.3\ [\mu\mathrm{s}],$$

and in state 0 over the interval

$$\tau_0 = a_0T_{\mathrm{s}} = 0.31 \text{ x } 55 = 17.0\ [\mu\mathrm{s}].$$

VITA

Isaac Plummer was born in Mandeville, Jamaica. He received his Diploma in Electronic and Telecommunication from the University of Technology Jamaica in 1996. He then worked as a telecommunication technician at AT&T until he returned to school at the Electrical and Computer Engineering Department at Louisiana State University in 2000. He later received his Bachelor of Science in electrical engineering in 2003. He then worked at PCS2000 as an intern, CDConsulting as a commissioning engineer, Kajola-Kristada Ltd, as an electrical maintenance manager and is now currently working at PCS 2000 as a part-time electrical engineer. He is now a candidate for the degree of Master of Science in Electrical Engineering in the Electrical and Computer Engineering Department at Louisiana State University.